

AN ABSTRACT OF THE THESIS OF

Richard L. Nafshun for the degree of Doctor of Philosophy in Chemistry presented on August 9, 1996. Title: The Synthesis and Characterization of Novel Materials for Use in Secondary Lithium-Ion Batteries.

Redacted for Privacy

Abstract approved: _____

Michael M. Lerner

Poly(ethylene oxide) (PEO), $(\text{CH}_2\text{CH}_2\text{O})_n$, is utilized as a polymer host for polymer electrolytes containing lithium salts. The polymer electrolytes $\text{PEO}_x\text{LiSO}_3\text{CF}_2\text{SF}_6$, and $\text{PEO}_x\text{LiSO}_3\text{CFHSF}_6$, (where x reflects the mole ratio of etheric oxygens in PEO to lithium) are synthesized and characterized by impedance spectroscopy, differential scanning calorimetry (DSC), and thermal gravimetric analysis (TGA). The $\text{PEO}_x\text{LiSO}_3\text{CF}_2\text{SF}_6$ complexes show significantly suppressed crystallinity. The $\text{PEO}_4\text{LiSO}_3\text{CF}_2\text{SF}_6$ complex has a bulk ionic conductivity (σ) near $10^{-5} (\Omega \text{ cm})^{-1}$ at 30 °C, comparable to conductivities obtained with PEO complexes of other known plasticizing salts. The role of the anion in plasticizing is discussed by considering the common features of known plasticizers. Unlike the $\text{PEO}_x\text{LiSO}_3\text{CF}_2\text{SF}_6$ complexes, a plasticizing effect for the $\text{PEO}_x\text{LiSO}_3\text{CFHSF}_6$ complexes is absent. This observation is discussed in terms of hydrogen bonding between $\text{SF}_6\text{CFHSO}_3^-$ anions.

The polymer electrolytes $\text{PEO}_x[\text{LiSO}_3(\text{CF}_2)_n\text{SO}_3\text{Li}]$ where $n = 1$ to 4 , and $\text{PEO}_x[\text{LiSO}_3\text{CF}_2\text{CF}_2\text{OCF}_2\text{CF}_2\text{SO}_3\text{Li}]$ are synthesized and characterized by impedance spectroscopy. The $\text{PEO}_{64}\text{LiSO}_3\text{CF}_2\text{CF}_2\text{OCF}_2\text{CF}_2\text{SO}_3\text{Li}$ complex was found to have the highest conductivity: σ is near $5 \times 10^{-6} (\Omega \text{ cm})^{-1}$ at 100°C .

The polymer electrolytes $\text{PEO}_x\text{LiCH}(\text{SO}_2\text{CF}_3)_2$ are synthesized and characterized by impedance spectroscopy, DSC, TGA, and cyclic voltammetry. The complexes show ionic conductivities as high as, or higher than, those derived from other plasticizing salts, with σ reaching $10^{-4} (\Omega \text{ cm})^{-1}$ at 30°C .

The electrical and thermal properties of ternary solutions containing PEO, $\text{LiN}(\text{SO}_2\text{CF}_3)_2$, and $\text{LiSO}_3\text{C}_8\text{F}_{17}$ are described. For the equimolar concentration of salts, $\text{PEO}_x[\text{LiN}(\text{SO}_2\text{CF}_3)_2]_y[\text{LiSO}_3\text{C}_8\text{F}_{17}]_z$ ($y = z = 1$), a conductivity maximum of $10^{-4} (\Omega \text{ cm})^{-1}$ at 30°C occurs at $x = 16$. The compositional range $\text{PEO}_{16}[\text{LiN}(\text{SO}_2\text{CF}_3)_2]_y[\text{LiSO}_3\text{C}_8\text{F}_{17}]_z$, ($y = 2 - z$) is fully evaluated and a conductivity maximum of $2.5 \times 10^{-3} (\Omega \text{ cm})^{-1}$ at 80°C occurs at $y = 1.75$. Thermal data indicate decreasing melting transition temperatures, and increasing glass transition temperatures, as y increases from 0 to 2 .

**The Synthesis and Characterization of Novel Materials for Use in
Secondary Lithium-Ion Batteries**

by

Richard L. Nafshun

A THESIS

submitted to

Oregon State University

in partial fulfillment of

the requirement of the

degree of

Doctor of Philosophy

Completed August 9, 1996

Commencement June 1997

Doctor of Philosophy thesis of Richard L. Nafshun presented on August 9, 1996

APPROVED:

Redacted for Privacy

Major Professor, representing Chemistry

Redacted for Privacy

Chair of Department of Chemistry

Redacted for Privacy

Dean of Graduate School

I understand that my thesis will become part of the permanent collection of Oregon State University libraries. My signature below authorizes release of my thesis to any reader upon request.

Redacted for Privacy

Richard L. Nafshun, Author

ACKNOWLEDGMENT

I would like to thank Dr. Michael Lerner for his support and guidance in my research, my teaching, my presentations, and the preparation of this thesis. He has served as a role model; I will reflect on his effective teaching during Chemistry 462, his presentations, his professional rapport with associates and students, and his investigative insight. I would like to thank my research associates, Dr. Victor Koch, Dr. Christopher Oriakhi, Dr. Steven Sloop, Dr. John Lemmon, Dr. Zhengwei Zhang, and Jinghe Wu. I have learned a great deal from my colleagues and have many fond memories of the MML Group. I have had the pleasure of working with and learning from Dr. Michael Schuyler, Dr. Christine Pastorek, Dr. James Krueger, Dr. Carroll DeKock, Dr. Glenn Evans, Dr. Douglas Keszler, and Dr. Phil Watson. I have received support from Mrs. Joey Carson, Mr. Dean Johnson, Mr. Dean Link, and the Chemistry Staff during the last four years. I thank Kenneth Vandenberghe for being a good friend (and for moving and storing my stuff several times). I wish to thank my wife, Amy, for her love and support during the past 13 years. The greatest day of my life was June 10, 1983. I thank my parents, my brother and sister, and my mother-in-law, Dorothy, for their continued support.

CONTRIBUTION OF AUTHORS

Dr. Michael Lerner was involved in the analysis and writing of each manuscript.

Dr. Gary Gard was involved in the analysis and writing of Chapters 2,3,4, and 5. Nicolas Hamel, Paul Nixon, Steven Ullrich, Nelson Holcomb, and Gary Gard synthesized and collected NMR, IR and Mass Spec data for the salts $\text{LiSO}_3\text{CF}_2\text{SF}_3$, $\text{LiSO}_3\text{CFHSF}_5$, $(\text{CF}_2)_n(\text{SO}_2\text{OLi})_2$, for $n = 1$ to 4, $\text{LiCH}(\text{SO}_2\text{CF}_3)_2$, and $\text{O}(\text{CF}_2\text{CF}_2\text{SO}_3\text{Li})_2$.

TABLE OF CONTENTS

	<u>Page</u>
1. Introduction	1
1.1 General Introduction	1
1.2 Introduction to Polymer Electrolytes	4
1.2.1 Motivation	4
1.2.2 The Solubility of Lithium Salts in Polymers	5
1.2.3 Polymer Hosts	6
1.2.4 Homopolymer Hosts	7
1.2.4.1 Poly(ethylene oxide) (PEO)	7
1.2.4.2 Poly(propylene oxide)	8
1.2.4.3 Poly(ethylenimine) (PEI)	8
1.2.5 Poly[(oxymethylene)oligo(oxyethylene)]	10
1.2.6 Poly(bis[methoxyethoxyethoxy]phosphazene)	10
1.2.7 Liquid Plasticizers	11
1.2.8 The Transport of Lithium Cations in Poly(ethylene oxide)	12
1.2.9 Platicizing Salts	16
1.3 General Apparatus and Procedures	19
1.3.1 Handling of Air Sensitive Materials	19
1.3.2 Solvent and Reagent Purification	20
1.3.3 Film Casting	21
1.4 Characterization Techniques	22
1.4.1 Impedance Spectroscopy	22
1.4.1.1 Introduction	22
1.4.1.2 dc Methods	22
1.4.1.3 ac Methods	27
1.4.1.4 Cell Impedance	28
1.4.1.5 Alternating Current Response to Several Simple Circuits	31

TABLE OF CONTENTS (Continued)

	<u>Page</u>
1.4.1.6 Alternating Current Response to a Polymer Electrolyte Cell	34
1.4.2 Cyclic Voltammetry	40
1.4.3 Differential Scanning Calorimetry	40
1.4.4 Thermal Gravimetric Analysis	41
1.5 References	42
2. Ion Conductivity and Scanning Calorimetry of Poly(ethylene oxide) Complexes of the Plasticizing Salt $\text{LiSO}_3\text{CF}_2\text{SF}_5$	48
2.1 Abstract	49
2.2 Introduction	50
2.3 Experimental	51
2.4 Results and Discussion	52
2.5 References	59
3. Lithium Salts of SF_5 alkylsulfonic Acids: Synthesis, Characterization, and Conductivity	60
3.1 Abstract	61
3.2 Introduction	62
3.3 Experimental	63
3.3.1 Materials	63
3.3.2 General Methods	63
3.3.3 Synthesis of $\text{SF}_5\text{CFHSO}_3\text{Li}$ (1)	64
3.3.4 Preparation of $\text{PEO}_x\text{LiSO}_3\text{CFHSF}_5$ (3)	65
3.3.5 Characterization of $\text{PEO}_x\text{LiSO}_3\text{CFHSF}_5$	66
3.3.6 Synthesis of $\text{SF}_5\text{CF}_2\text{SO}_3\text{Li}$ (2)	66

TABLE OF CONTENTS (Continued)

	<u>Page</u>
3.4 Results and Discussion	67
3.5 Acknowledgments	75
3.6 References	76
 4. Lithium Salts of Bis(Perfluoroalkyl)sulfonic Acids: Synthesis, Characterization and Conductivity Studies	 78
4.1 Abstract	79
4.2 Introduction	80
4.3 Experimental	81
4.3.1 Materials	81
4.3.2 General Procedures	81
4.3.3 Synthesis of $\text{CF}_2(\text{SO}_2\text{OLi})_2 \cdot 3/2\text{H}_2\text{O}$ (1)	83
4.3.4 Synthesis of $(\text{CF}_2\text{SO}_2\text{OLi})_2 \cdot 2\text{H}_2\text{O}$ (2)	84
4.3.5 Synthesis of $\text{CF}_2(\text{CF}_2\text{SO}_2\text{OLi})_2 \cdot 2\text{H}_2\text{O}$ (3)	84
4.3.6 Synthesis of $(\text{CF}_2\text{CF}_2\text{SOLi})_2 \cdot 3/2\text{H}_2\text{O}$ (4)	85
4.3.7 Synthesis of $\text{O}(\text{CF}_2\text{CF}_2\text{SO}_2\text{OLi})_2$ (5)	86
4.3.8 Electrochemical Analysis of Polymer Complexes	87
4.3.8.1 Preparation of $\text{PEO}_x(\text{LiSO}_3\text{CF}_2\text{CF}_2)_2\text{O}$	87
4.3.8.2 Characterization of $\text{PEO}_x(\text{LiSO}_3\text{CF}_2\text{CF}_2)_2\text{O}$	88
4.3.8.3 Electrochemical Work With Other Salts	88
4.4 Results and Discussion	88
4.5 Acknowledgments	97
4.6 References	98
 5. Synthesis of $\text{LiCH}(\text{SO}_2\text{CF}_3)_2$ and Ionic Conductivity of Polyether-Salt Complexes	 100
5.1 Abstract	101
5.2 Introduction	102

TABLE OF CONTENTS (Continued)

	<u>Page</u>
5.3 Experimental	103
5.3.1 Preparation of $\text{LiCH}(\text{SO}_2\text{CF}_3)_2$	103
5.3.2 Characterization of $\text{LiCH}(\text{SO}_2\text{CF}_3)_2$	104
5.3.3 Preparation of $\text{PEO}_x\text{LiCH}(\text{SO}_2\text{CF}_3)_2$	104
5.3.4 Characterization of $\text{PEO}_x\text{LiCH}(\text{SO}_2\text{CF}_3)_2$	104
5.4 Results and Discussion	105
5.5 Acknowledgments	116
5.6 References	117
6. Conductivity in the Poly(ethylene oxide) Mixed Salt Complexes $\text{PEO}_x[\text{LiN}(\text{SO}_2\text{CF}_3)_2]_y[\text{LiSO}_3\text{C}_8\text{F}_{17}]_z$	118
6.1 Abstract	119
6.2 Introduction	120
6.3 Experimental	121
6.3.1 Preparation of $\text{PEO}_x[\text{LiN}(\text{SO}_2\text{CF}_3)_2]_y[\text{LiSO}_3\text{C}_8\text{F}_{17}]_z$	121
6.3.2 Characterization of $\text{PEO}_x[\text{LiN}(\text{SO}_2\text{CF}_3)_2]_y[\text{LiSO}_3\text{C}_8\text{F}_{17}]_z$	121
6.4 Results and Discussion	122
6.5 References	128
7. Summary	129
Bibliography	131

TABLE OF CONTENTS (Continued)

	Page
Appendices	139
Appendix A A QuickBASIC 4.5 Program to Control the Instrumentation to Measure the Electrical Properties of a Cell	140
Appendix B A QuickBASIC 4.5 Program to Control a EG&G Princeton Applied Research 362 Scanning Potentiostat for Modified Galvanostatic Intermittent Titration Technique Measurements .	149
Appendix C A QuickBASIC 4.5 Program to Control a EG&G Princeton Applied Research 362 Scanning Potentiostat for Cyclic Voltammetry Measurements	178

LIST OF FIGURES

Figure	Page
1.1 Branched poly(ethyleneimine)	9
1.2 $\log \sigma$ vs. $1000/T$ for the polymer electrolyte $\text{PEO}_{32}\text{LiCH}(\text{SO}_2\text{CF}_3)_2$	15
1.3 $\log \sigma$ vs. $1000/T$ for the polymer electrolyte $\text{PEO}_{16}\text{LiCH}(\text{SO}_2\text{CF}_3)_2$	17
1.4 A representation of the symmetrical direct current cell with two non-blocking electrodes	23
1.5 The equivalent circuit for the symmetrical direct current cell with two non-blocking electrodes	25
1.6 The equivalent circuit for the symmetrical direct current cell with two non-blocking electrodes and a voltage probe	26
1.7 A representation of the sinusoidal voltage and current, at a given frequency . .	29
1.8 A representation of the impedance, Z , of a cell. $ Z \sin \theta$ is the y component, $ Z \cos \theta$ is the x component; or Z' is the real component, and Z'' is the y component	30
1.9 Representation of (a) a resistor, R , and (b) a capacitor, C , in the complex impedance plane	32
1.10 (a) Representation of a resistor, R , and a capacitor, C , in series in the complex impedance plane. (b) Representation of a resistor, R , and a capacitor, C , in parallel in the complex impedance plane	33
1.11 A complex impedance representation for the polymer electrolyte $(\text{PEO})_4\text{LiCH}(\text{SO}_2\text{CF}_3)_2$	35
1.12 An equivalent circuit representing the ac response to the polymer electrolyte cell	36
1.13 An equivalent circuit representing the ac response to the polymer electrolyte cell with the inclusion of a constant-phase element	39

LIST OF FIGURES (Continued)

Figure	Page
2.1 Arrhenius plots of impedance data for $\text{PEO}_x\text{LiSO}_3\text{CF}_2\text{SF}_5$ between -40 and 100 °C; (*) $x = 16$, (■) $x = 8$, (▲) $x = 4$, and (□) $x = 2$	53
2.2 Differential scanning calorimetry traces for $\text{PEO}_x\text{LiSO}_3\text{CF}_2\text{SF}_5$ complexes. Samples were run at 10 °C / min under an inert atmosphere . . .	54
3.1 DSC and TGA traces for $\text{LiSO}_3\text{CHFSF}_5$	69
3.2 DSC and TGA traces for $\text{LiSO}_3\text{CF}_2\text{SF}_5$	69
3.3 DSC traces for $\text{PEO}_x\text{LiSO}_3\text{CHFSF}_5$ complexes	73
3.4 Arrhenius plots for the $\text{PEO}_x\text{LiSO}_3\text{CHFSF}_5$ complexes	74
4.1 TGA and DSC traces for $\text{LiSO}_3\text{CF}_2\text{CF}_2\text{OCF}_2\text{CF}_2\text{SO}_3\text{Li}$	90
4.2 Arrhenius plots for $\text{CH}_2\text{CH}_2\text{O}:\text{Li}::8:1$ complexes of	95
4.3 Arrhenius plots for PEO complexes with $\text{LiSO}_3\text{CF}_2\text{CF}_2\text{OCF}_2\text{CF}_2\text{SO}_3\text{Li}$ at $\text{CH}_2\text{CH}_2\text{O}:\text{Li}$ mole ratios of 64:1, 32:1, and 16:1	96
5.1 DSC and TGA traces for $\text{LiCH}(\text{SO}_2\text{CF}_3)_2$	107
5.2 TGA trace for $\text{PEO}_8\text{LiCH}(\text{SO}_2\text{CF}_3)_2$	108
5.3 Arrhenius plots for $\text{PEO}_x\text{LiCH}(\text{SO}_2\text{CF}_3)_2$ complexes	109
5.4 Log σ versus x for $\text{PEO}_x\text{LiCH}(\text{SO}_2\text{CF}_3)_2$ complexes at 30, 50, and °80	112
5.5 DSC traces for $\text{PEO}_x\text{LiCH}(\text{SO}_2\text{CF}_3)_2$ complexes	113
5.6 Cyclic voltammogram for $\text{PEO}_{16}\text{LiCH}(\text{SO}_2\text{CF}_3)_2$ thin film at 20 mV/s	115
6.1 log σ versus x for the complexes $\text{PEO}_x[\text{LiN}(\text{SO}_2\text{CF}_3)_2]_1[\text{LiSO}_3\text{C}_8\text{F}_{17}]_1$	123

LIST OF FIGURES (Continued)

Figure	Page
6.2 $\log \sigma$ versus y for the complexes $\text{PEO}_{16}[\text{LiN}(\text{SO}_2\text{CF}_3)_2]_y[\text{LiSO}_3\text{C}_8\text{F}_{17}]_{1-y}$	124
6.3 T_m versus y for the complexes $\text{PEO}_{16}[\text{LiN}(\text{SO}_2\text{CF}_3)_2]_y[\text{LiSO}_3\text{C}_8\text{F}_{17}]_{1-y}$	126
6.4 T_g versus y for the complexes $\text{PEO}_{16}[\text{LiN}(\text{SO}_2\text{CF}_3)_2]_y[\text{LiSO}_3\text{C}_8\text{F}_{17}]_{1-y}$	127

LIST OF TABLES

Table	Page
2.1 Thermal data for $\text{PEO}_x\text{LiSO}_3\text{CF}_2\text{SF}_3$ complexes	55
4.1 ^{19}F NMR Spectra of Dilithium Perfluoroalkyl Sulfonate Salts	92
4.2 ^{13}C NMR Spectra of Dilithium Perfluoroalkyl Sulfonate Salts	93
5.1 A, B, and T_g parameters derived from Arrhenius plots in Figure 5.2	110
5.2 Melting transition temperatures, T_m , and enthalpies, ΔH_m , and glass transition temperatures, T_g , and magnitudes, ΔP_g , for $\text{PEO}_x\text{LiCH}(\text{SO}_2\text{CF}_3)_2$ complexes	114

The Synthesis and Characterization of Novel Materials for Use in Secondary Lithium-Ion Batteries

Chapter 1 INTRODUCTION

1.1 General Introduction

In 1973, Wright and coworkers reported on the conducting properties of poly(ethylene oxide)-salt complexes. In this seminal work, potassium thiocyanate was dissolved in poly(ethylene oxide) (PEO) and it was noted that the electrical conductivity of the complex was very sensitive to temperature and increased markedly as the degree of crystallinity reduced [1]. In 1978, Armand et al highlighted the potential of these materials as a new class of solid electrolytes for energy storage applications [2].

PEO solvates a wide variety of salts [3] and forms complexes with concentrations as high as 16.5 M. The solvated ions can be quite mobile in the polymeric solvent and give rise to significant bulk ionic conductivities. Below its melting transition PEO is semicrystalline, possessing both amorphous and crystalline regions. The melting point (T_m) of the crystalline phase of PEO is $T_m = 65\text{ }^{\circ}\text{C}$, and the glass transition temperature (T_g) of the amorphous phase is about $-60\text{ }^{\circ}\text{C}$. Solid state nuclear magnetic resonance studies, which correlated conductivity with relaxation times, first demonstrated that the high conductivity exhibited by polymer electrolytes was due to the mobility of ions in the amorphous phase alone [4].

Many PEO-based polymer electrolytes exhibit ionic conductivities exceeding $10^{-4} (\Omega \text{ cm})^{-1}$ above the melting point of pure PEO, but much lower ionic conductivities at ambient temperature. Considerable research effort has been aimed at achieving an ionic conductivity of $10^{-4} (\Omega \text{ cm})^{-1}$ at ambient temperature. It is the thin film configuration that allows for these materials, with modest conductivities, to be of practical interest. A $10 \mu\text{m}$ thick polymer electrolyte film, exhibiting a conductivity of $10^{-4} (\Omega \text{ cm})^{-1}$, has a resistance of $10 \Omega / \text{cm}^2$. An electrolyte having a resistance of $10 \Omega / \text{cm}^2$ allows for an appreciable current in batteries constructed of thin, high-area electrodes. These investigations have focused on three materials:

- (1) non-crystalline polymers, such as poly(bis[methoxyethoxyethoxy]phosphazene) [5-13] and poly[(oxymethylene)oligo(oxyethylene)] [14-17];
- (2) gelled electrolytes, which are comprised of a polymer and salt, blended with a low-molecular-weight liquid; [18-24];
- (3) polymer-electrolytes with plasticizing salts, which suppress the crystallization of the complex and elevate the ionic conductivity at ambient temperatures.

The goal of this work has been to prepare and characterize poly(ethylene oxide)-salt complexes which contain new plasticizing lithium salts. The lithium salts $\text{LiSO}_3\text{CF}_2\text{SF}_3$, $\text{LiSO}_3\text{CFHSF}_3$, $\text{LiCH}(\text{SO}_2\text{CF}_3)_2$, and $\text{LiSO}_3\text{CF}_2\text{CF}_2\text{OCF}_2\text{CF}_2\text{SO}_3\text{Li}$ were

synthesized by Gard and coworkers [25], and the lithium salts $\text{LiN}(\text{SO}_2\text{CF}_3)_2$ and $\text{LiSO}_3\text{C}_8\text{F}_{17}$ were obtained from 3M [26]. We have focussed on the thermal and electrical behavior of PEO-based polymer electrolytes. There are additional factors that must be considered before the applications of these materials can be realized. These factors include mechanical properties, toxicity, cost, and interfacial stability.

While the conductivity in amorphous polymers is high, the mechanical properties of these materials are poor [27]. The dimensional stability of these materials may be enhanced by chemical [28-30] or irradiative [31-32] cross linking.

This thesis examines the synthesis and characterization of materials with potential applications as components in secondary, solid-state, high-energy-density, lithium-ion batteries, and is divided into eight sections. The first six sections address polymer electrolytes, and the seventh section summarizes the results. Chapter 1 gives a general introduction of polymer electrolytes along with the basic goals and details of the experimental methods utilized. Because impedance spectroscopy is a specialized characterization technique, a rigorous description of this method is presented in Section 1.4.1. Chapters 2 and 3 describe the synthesis and characterization of the PEO-salt complexes of $\text{LiSO}_3\text{CF}_2\text{SF}_3$ and $\text{LiSO}_3\text{CFHSF}_5$. Chapter 4 describes the synthesis and characterization of PEO-salt complexes containing $\text{LiSO}_3\text{CF}_2\text{CF}_2\text{OCF}_2\text{CF}_2\text{SO}_3\text{Li}$. Chapter 5 describes the synthesis and characterization of PEO-salt complexes containing $\text{LiCH}(\text{SO}_2\text{CF}_3)_2$. Chapter 6 describes the synthesis and characterization of PEO- $\text{LiN}(\text{SO}_2\text{CF}_3)_2$ - $\text{LiSO}_3\text{C}_8\text{F}_{17}$ mixed salt complexes.

1.2 Introduction to Polymer Electrolytes

1.2.1 Motivation

A considerable scientific effort has been dedicated to exploring and understanding the characteristics of polymer electrolytes [33–45]. The motivation has been for the utilization of these materials in all solid-state, high-energy-density secondary power sources. There are several advantages to replacing the liquid electrolytes of conventional batteries with polymer electrolytes [46]:

- (1) Polymers--specifically polyethers--have good kinetic stability toward lithium. This implies long storage life and low interfacial impedance;
- (2) Polymer electrolytes can be utilized in thin films; thus the battery volume and weight devoted to the electrolyte are decreased, and less packaging is required;
- (3) Polymer electrolytes are dimensionally stable, therefore have attractive mechanical properties;
- (4) Polymer electrolytes offer safety; phase changes in sealed cells are eliminated.

1.2.2 The Solubility of Lithium Salts in Polymers

The solvation of lithium salts in PEO occurs by the coordination of lithium cations with the etheric oxygens in the polymer backbone. A favorable free energy for the dissolution of the salt in the crystalline polymer is observed when the solvation energy and the lattice energy of the polymer-salt complex compensate for the loss of lattice energy of the lithium salt and the loss of lattice energy of the polymer. Based in the hard-soft, acid-base principle [47], lithium salts of large anions favor dissolution because of their low lattice energies. A reasonable estimation of the lattice energy of a salt can be obtained from the Kapustinskii equation [48]:

$$\Delta H_L = \frac{120,200vZ^+Z^-}{r_0} \left(1 - \frac{34.5}{r_0}\right) \quad (1.1)$$

where, ΔH_L is the lattice enthalpy (kJ/mol), v is the number of ions per formula unit, Z^+ and Z^- are the ion charges, and r_0 is the sum of the cation and anion radii (pm). Ratner and Shriver have quantitatively investigated the relationship between the salts that form complexes with PEO and their lattice energies [49]. For example, while LiCl ($\Delta H_L = 853$ kJ/mol) and PEO will form a complex, LiF ($\Delta H_L = 1036$ kJ/mol) and PEO will not.

1.2.3 Polymer Hosts

The polymer employed should meet the following criteria:

- (1) contain electron donating atoms, or groups of atoms, to form coordinate bonds with the salt cations;
- (2) have low bond rotation barriers to facilitate segmental motion;
- (3) have a suitable distance between coordinating atoms.

The conductivity of a homogeneous polymer electrolyte at a given temperature may be expressed as:

$$\sigma = \sum n q \mu \quad (1.2)$$

where n is the number of charge carriers, q is the charge on each, and μ is the mobility. At low salt concentrations, the mobility of the ions is unaffected by changes in the salt concentration, and the conductivity will be dependent upon the number of charge carriers.

For example, the conductivities at 30 °C for $\text{PEO}_{16}\text{LiCH}(\text{SO}_2\text{CF}_3)_2$ and

$\text{PEO}_{32}\text{LiCH}(\text{SO}_2\text{CF}_3)_2$ are $1 \times 10^{-4} (\Omega \text{ cm})^{-1}$ and $8 \times 10^{-6} (\Omega \text{ cm})^{-1}$, respectively.

1.2.4 Homopolymer Hosts

1.2.4.1 Poly(ethylene oxide) (PEO)

Lithium salts easily form complexes with PEO [50]. PEO is an aprotic, solvating polymer. Hydrogen bonding is not available for anion solvation, therefore, salts with large anions, having delocalized charge will be most soluble. Much of the early work carried out on polymer electrolytes, and the majority of reports to date concentrate on PEO [51].

Of the polyethers in the series $[-(\text{CH}_2)_m\text{O}]_n$, poly(ethylene oxide) ($m = 2$) will dissolve alkali metal salts, while the others--poly(methylene oxide) $-(\text{CH}_2\text{O})_n$ and poly(trimethylene oxide) $-(\text{CH}_2\text{CH}_2\text{CH}_2\text{O})_n$ for example--will not dissolve these to an appreciable extent [52]. The $-(\text{CH}_2\text{CH}_2\text{O})_n$ chemical repeat unit in poly(ethylene oxide) offers the most favorable spacing for solvating alkali metal salts.

The crystal structure of the polymer electrolyte $\text{PEO}_3\text{LiSO}_3\text{CF}_3$ has been determined [53]. The lithium ions is coordinated by five oxygen atoms--three ether oxygens and one from each of two adjacent CF_3SO_3^- groups. Each CF_3SO_3^- in turn bridges two lithium ions to form chains running parallel to and intertwined with the PEO chain.

1.2.4.2 Poly(propylene oxide)

Poly(propylene oxide) $-\text{[CH}_2\text{CH(CH}_3\text{)O]}_n-$ has been studied as a polymer electrolyte host [54]. Atactic poly(propylene oxide) has the same backbone structure as poly(ethylene oxide), hence, the optimal spacing for the solvation of alkali metal salts. The glass transition temperature (T_g) of PPO is $-70\text{ }^\circ\text{C}$, and the polymer is amorphous at ambient temperature. However, lithium salts are far less soluble in poly(propylene oxide) than in PEO because of the steric hindrance invoked by the methyl group. While low molecular weight poly(propylene oxide) ($M_w \sim 2000$) will dissolve KSCN at ambient temperatures, the salt precipitates out of the polymer above $80\text{ }^\circ\text{C}$ [55]. Poly(propylene oxide)-salt complexes, like PEO-salt complexes, have a negative entropy and enthalpy of dilution, therefore, an inverse temperature-solubility relation.

1.2.4.3 Poly(ethylenimine) (PEI)

Poly(ethylenimine) $-(\text{CH}_2\text{CH}_2\text{NH})_n-$ has been studied as a polymer host [56,57]. PEI can be obtained in either linear (LPEI) or branched (BPEI) form. LPEI is highly crystalline ($T_m = 60\text{ }^\circ\text{C}$) [58], while BPEI is amorphous at ambient temperatures due to the suppression of crystallization. About 25% of the nitrogen atoms in BPEI are primary amines, 50% are secondary amines, and 25% are tertiary amines [59]. The tertiary nitrogen atoms are branching points on the polymer skeleton (Figure 1.1).

The conductivity values observed for BPEI-salt complexes are lower than those

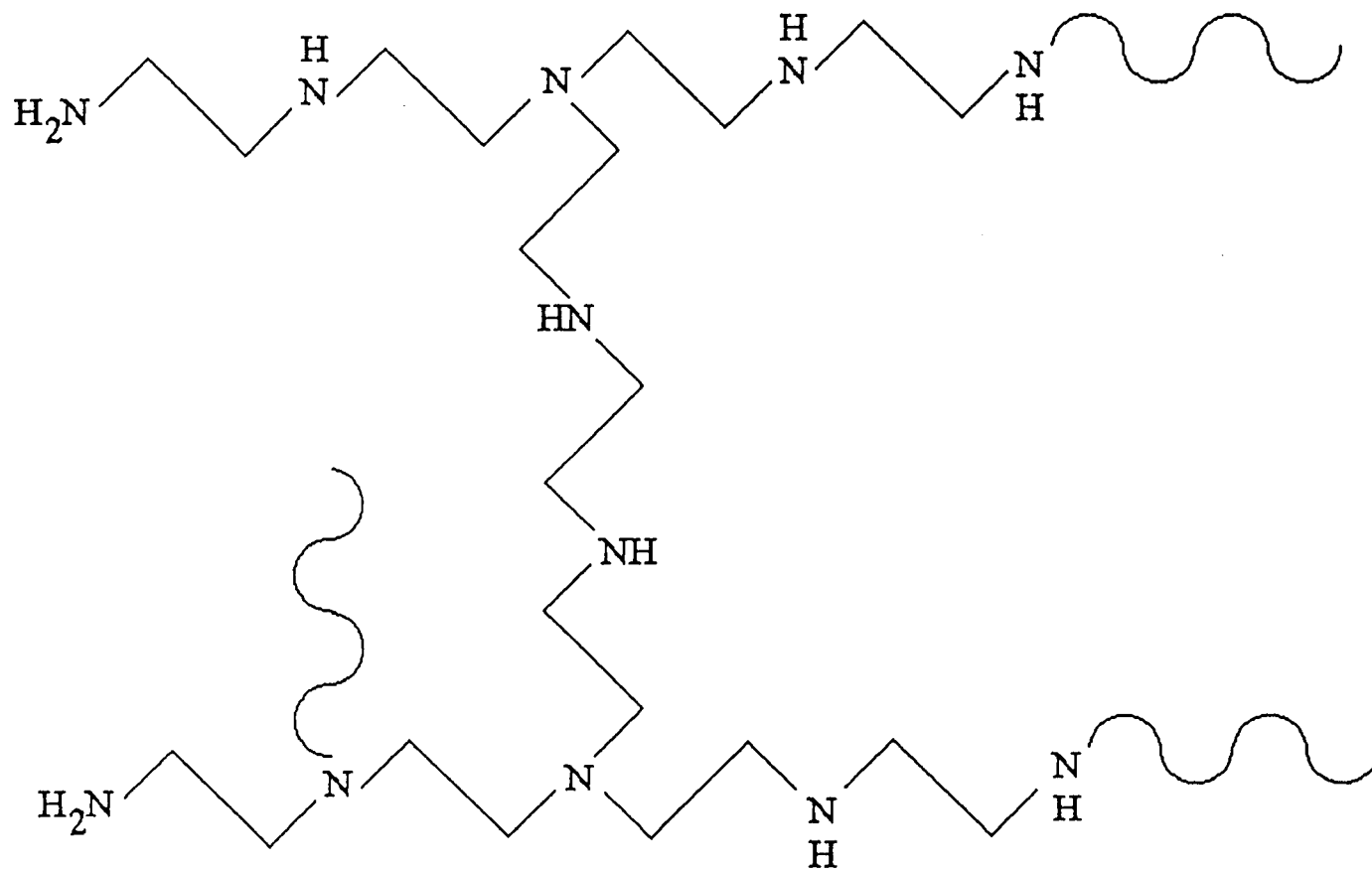


Figure 1.1: Branched poly(ethyleneimine)

reported for the analogous complexes prepared with PEO. For example, at 85 °C, $\text{PEO}_8\text{LiCF}_3\text{SO}_3$ exhibited a conductivity of $5 \times 10^{-5} (\Omega \text{ cm})^{-1}$ and $\text{PEI}_8\text{LiCF}_3\text{SO}_3$ exhibited a conductivity of $9 \times 10^{-7} (\Omega \text{ cm})^{-1}$ [60]. Infrared spectroscopy data reveals significant $\text{N-H} \cdots \text{N}$ hydrogen bonding interactions in pure BPEI and $\text{N-H} \cdots$ anion hydrogen bonding interactions in $\text{BPEI-LiSO}_3\text{CF}_3$ salt complexes [61]. This is responsible for smaller anionic transport numbers and hence lower ionic conductivities compared with poly(ethylene oxide)-salt complexes.

1.2.5 Poly[(oxymethylene)oligo(oxyethylene)]

Poly[(oxymethylene)oligo(oxyethylene)] (PEM) is a linear polymer which is amorphous at ambient temperatures. The reduced crystallinity is a result of incorporating methoxy units into the polyether chain, creating a random copolymer. PEM $\{-[(\text{OCH}_2\text{CH}_2)_m\text{OCH}_2]_n\}$ (where m is between 8 and 10) is conveniently prepared by the oxymethylene linkage of poly(ethylene glycol) [62]. Polymer-salt complexes of PEM have been found to exhibit ionic conductivities on the order of 1-2 orders of magnitude greater than those in comparable PEO complexes at ambient temperature [63].

1.2.6 Poly(bis[methoxyethoxyethoxy]phosphazene)

Poly(bis[methoxyethoxyethoxy]phosphazene) (MEEP) is a linear polymer, consisting of a backbone of alternating phosphorus and nitrogen atoms with two pendants

attached to the phosphorus: $(N=P[OCH_2CH_2OCH_2CH_2OCH_3]_2)_n$. MEEP was synthesized and examined in salt complexes because of the low glass transition temperature of phosphazene polymers; due to the flexible macromolecular backbone [64]. It has been reported that the ionic conductivities of MEEP-salt complexes are 2 - 3 orders of magnitude higher than the PEO-salt complexes near ambient temperature [65].

1.2.7 Liquid Plasticizers

Low molecular weight solvents have been added to polymer electrolytes to increase the ionic conductivity [66,67]. These are not true solid-state electrolytes, for the ionic transport resembles that in a liquid, and the polymer basically acts as a support for the matrix [68]. Batteries constructed of these "gelled electrolytes" require the additional packaging used for batteries constructed with liquid electrolytes. The criteria for a useful liquid plasticizer are:

- (1) a high dielectric constant to increase the salt dissociation;
- (2) miscibility with the polymer-salt complexes;
- (3) low volatility;
- (4) stability toward electrode materials, e.g. lithium metal.

Several liquid plasticizers, such as propylene carbonate (PC), satisfy many of the above constraints, however, relatively high concentrations may be required to achieve

appreciable ionic conductivities at ambient temperature. At high concentrations, these liquids can degrade the mechanical properties of the polymer and decrease electrolyte performance. Kelly et al [70] have studied poly(ethylene glycol) (PEG) $[H(OCH_2CH_2)_nOH]$ as a low molecular weight ($M_w = 200-2000$) plasticizer for $PEO_xLiSO_3CF_3$ complexes. They reported that the conductivity of the $PEO_xLiSO_3CF_3$ complex increased from $3 \times 10^{-7} (\Omega \text{ cm})^{-1}$ to $1 \times 10^{-4} (\Omega \text{ cm})^{-1}$ at 40°C when 65 mole percent PEG was added. The hydroxyl end groups of PEG react with lithium metal, so such a system would not be suitable for batteries.

Low molecular weight, "capped" PEG $[CH_3(OCH_2CH_2)_nOCH_3]$, with the absence of hydroxyl groups, has been investigated as a liquid plasticizer. The conductivities reported for these complexes are similar to the conductivities reported for PEG complexes [71]. The mechanical properties of these materials are, however, poor [68].

1.2.8 The Transport of Lithium Cations in Poly(ethylene oxide)

The mechanism for the transport of ions in a polymer electrolyte has been identified as a combination of the segmental motion of the polymer, and the interpolymer and intrapolymer transition of ions between coordinating sites. This mechanism is similar to that in a liquid, in which the local relaxation processes of the polymer chains assist the migration of lithium ions through the polymer matrix. The macroscopic complex remains immobile during this migration process.

At temperatures below the glass transition temperature (T_g) of the polymer-

electrolyte, there is no segmental motion, and the only dimensional changes in the chain are due to the temporary distortions of the valence bonds. The glass transition temperature corresponds to the onset of the short-range motion of the atoms in the polymer chain. This transition is signified by an abrupt change in the specific volume to accompany the segmental chain motion. This transition may also be detected by differential scanning calorimetry, for the glass transition is an endothermic event.

Since Armand first published conductivity data for polymer electrolytes [72], the Vogel-Tamman-Fulcher (VTF) equation has been utilized to fit conductivity measurements as a function of temperature. A form of the VTF equation [73-75] is given as:

$$\sigma = AT^{-1/2} \exp[-B/(T-T_0)] \quad (1.3)$$

where:

σ	$(\Omega \text{ cm})^{-1}$	is the conductivity;
A	$(\Omega \text{ cm})^{-1} \text{K}^{-1/2}$	is a unique constant for the polymer electrolyte, proportional to the number of charge carriers;
T	(K)	is the temperature;
B	(K)	is a constant which can be related to the apparent activation energy;
T_0	(K)	is the equilibrium glass transition temperature--it is typically about 50 °C lower than the measured T_g for the polymer electrolyte.

The VTF equation is semi-empirical and was first developed to describe the viscosity of supercooled liquids. The VTF equation is similar in form to the Arrhenius equation ($\sigma = AT^{-1}\exp[-E_a/kT]$), however, the distinct curvature given by the VTF equation more accurately describes the temperature dependence of the conductivity.

As this form of the VTF equation suggests, the observed conductivity of a polymer electrolyte increases with temperature. It is the thermal motion that contributes to the relaxation and transport processes. The equilibrium glass transition temperature (T_g) is critical to the conductivity of a polymer electrolyte. Above this temperature, the polymer is rubber like and the thermal energy contributes to the mobility of the polymer chains. The pre-exponential term, A , is proportional to the number of charge carriers. As the number of charge carries increases, the conductivity increases.

Figure 1.2 is a plot of the $\log[\text{conductivity } (\Omega \text{ cm})^{-1}]$ versus $1000/\text{Temperature } (1000/K)$ for the polymer electrolyte $\text{PEO}_{32}\text{LiCH}(\text{SO}_2\text{CF}_3)_2$. (These are often called "Arrhenius Plots" due to the inverse dependence of the temperature.) The data in the range of 50 - 100 °C is presented with a curve, fit to the parameters in the VTF equation. This curve is representative of Arrhenius plots for polymer electrolytes--the negative slope curves downward with a decrease in temperature. This deviation from linearity is expected and due to the dependence on $(T-T_g)^{-1}$ rather than T^{-1} . There is a sudden decrease in the conductivity in the temperature range of 35 - 50 °C. This temperature region corresponds to the melting transition temperature of the polymer electrolyte. This behavior is consistent with the theory that significant ionic conductivity takes place in the amorphous phase of the polymer electrolyte.

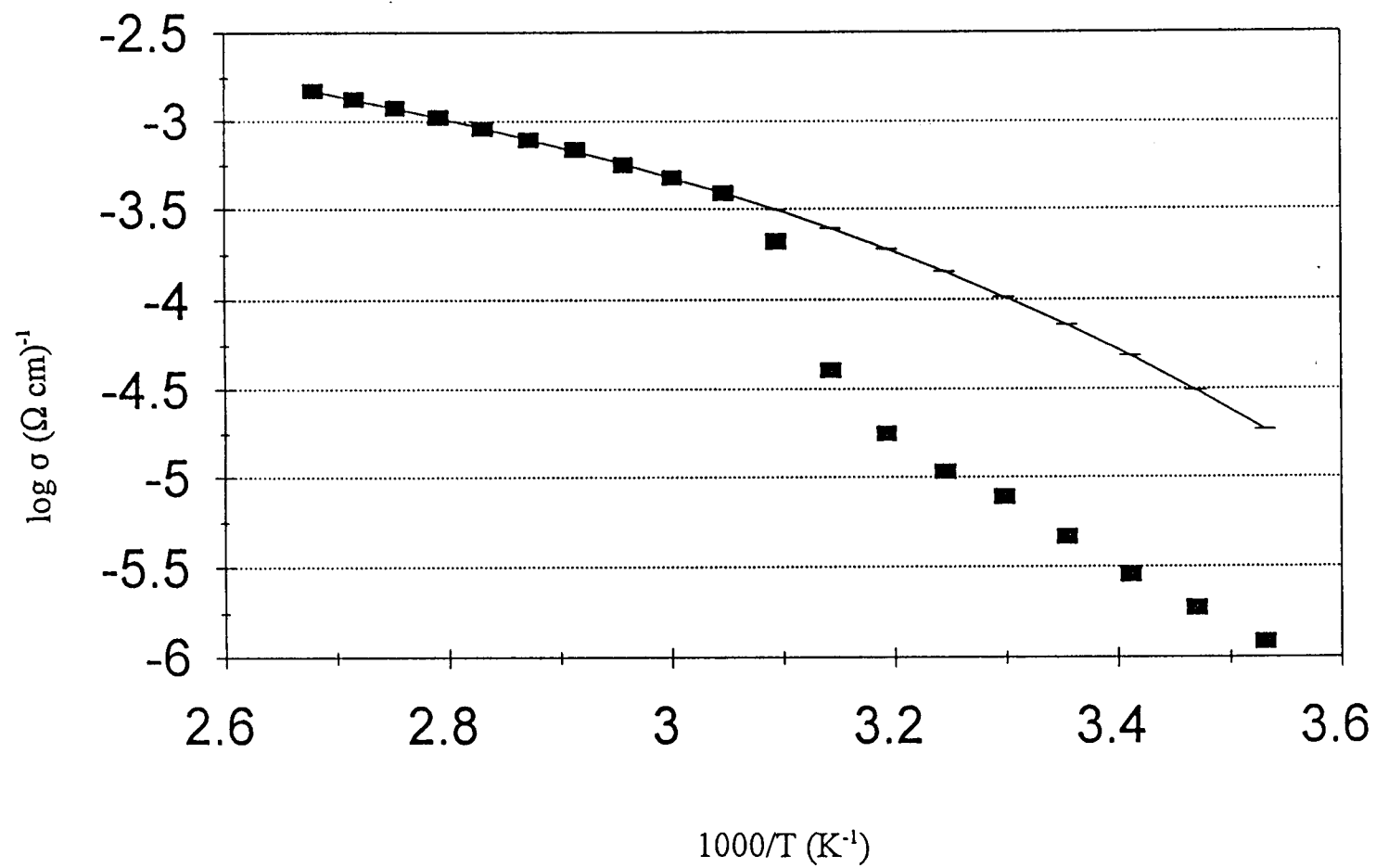


Figure 1.2: $\log \sigma$ vs. $1000/T$ for the polymer electrolyte $\text{PEO}_{32}\text{LiCH}(\text{SO}_2\text{CF}_3)_2$

Figure 1.3 is an Arrhenius plot for the polymer electrolyte $\text{PEO}_{16}\text{LiCH}(\text{SO}_2\text{CF}_3)_2$. The data in the range of 10 - 100 °C is presented with a curve, fit to the parameters in the VTF equation. This curve has a negative slope which curves downward with a decrease in temperature. In this case, there is no dramatic break in the conductivity. As a result, the conductivity at 30 °C is above $10^{-4} (\Omega \text{ cm})^{-1}$. Differential scanning calorimetry data reveal that the magnitude of the principle melting transition for the 16:1 complex is half of that for the 32:1 complex [76]. This indicates that the polymer electrolyte in the 16:1 complex forms less crystalline phase and thus retains a higher ionic conductivity.

1.2.9 Plasticizing Salts

Most PEO-lithium salt complexes have melting transition temperatures (T_m) near 60 °C. For example, $\text{PEO}_8\text{LiSO}_3\text{CF}_3$ exhibits a T_m at 57 °C [77]; $\text{PEO}_8\text{LiClO}_4$ exhibits a T_m at 58 °C [77]; $\text{PEO}_{16}\text{LiNHSO}_2\text{F}$ displays a T_m at 62 °C [78]; and $\text{PEO}_8\text{LiAsF}_6$ exhibits a T_m at 54 °C [79]. These complexes are semi-crystalline at ambient temperature and show conductivities near $10^{-8} (\Omega \text{ cm})^{-1}$ at 30 °C. However, several PEO-lithium salt complexes have been studied which do not exhibit melting transitions or show melting transitions of reduced magnitudes at significantly lower temperatures [80-84]. These complexes exhibit markedly reduced crystallinity at ambient temperature, and display room temperature conductivities in excess of $10^{-5} (\Omega \text{ cm})^{-1}$. Armand called this the "plasticizer" effect [83]. The lithium salts in these complexes contain relatively large anions with delocalized charge. These anions have a major influence on the phase

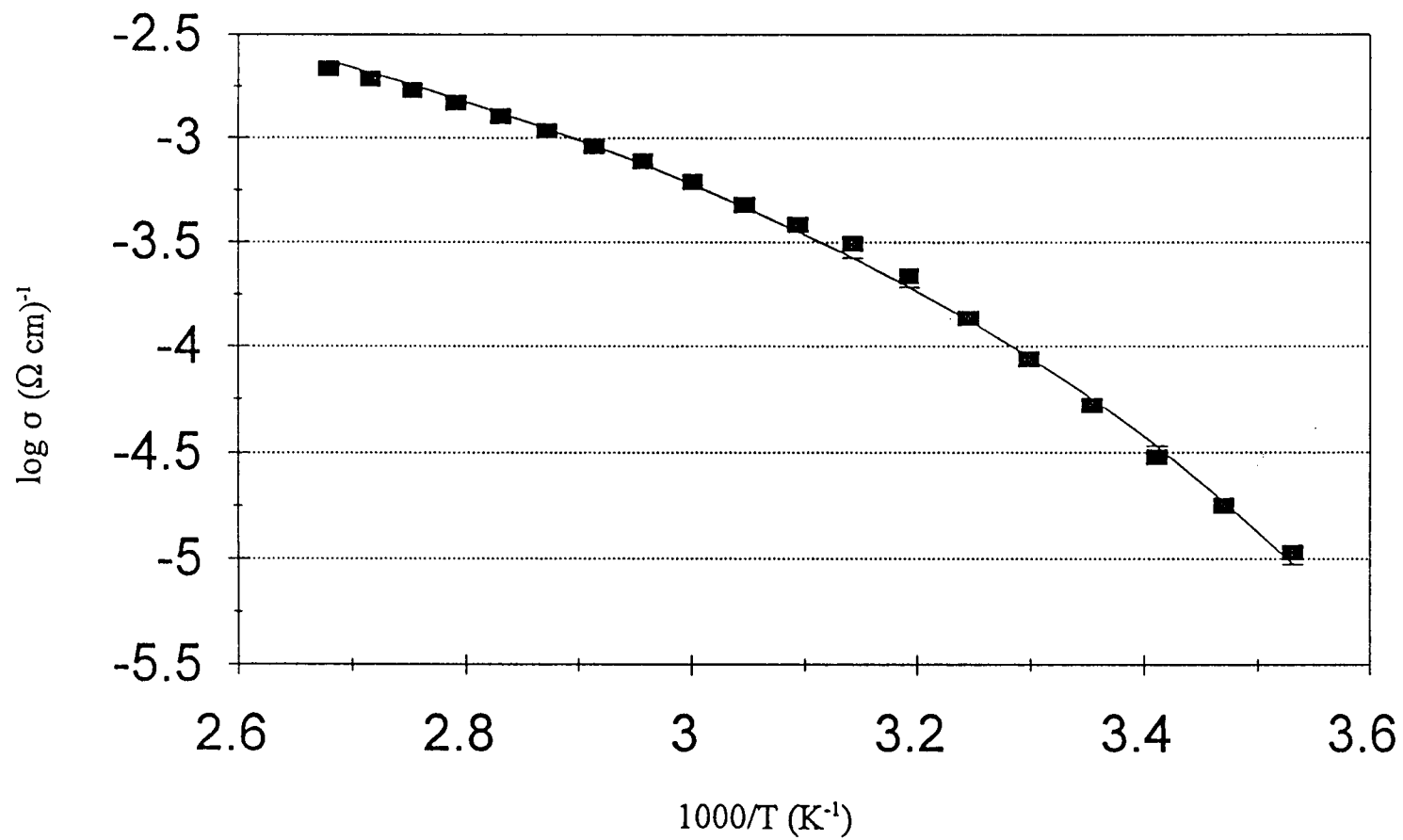


Figure 1.3: $\log \sigma$ vs. $1000/T$ for the polymer electrolyte $\text{PEO}_{16}\text{LiCH}(\text{SO}_2\text{CF}_3)_2$

composition and conductivity of the polymer electrolyte.

In 1989, Armand and coworkers synthesized the lithium salt $\text{LiN}(\text{SO}_2\text{CF}_3)_2$ [lithium bis(trifluoromethylsulfonyl)imide] (LiTFSI) and characterized a series of PEO- $\text{LiN}(\text{SO}_2\text{CF}_3)_2$ complexes [83]. The $\text{PEO}_{10}\text{LiN}(\text{SO}_2\text{CF}_3)_2$ complex exhibits a conductivity of $1 \times 10^{-5} (\Omega \text{ cm})^{-1}$ at 25°C , and the absence of a melting transition near 60°C . Armand suggested that the bulkiness and conformational flexibility of the anion suppressed the crystallization of the complex.

In 1993, in order to increase the "plasticizer" effect of the salt, Armand and coworkers investigated a lithium salt $[\text{LiC}(\text{SO}_2\text{CF}_3)_3]$ (lithium tris(trifluoromethylsulfonyl)methide) (LiTFSM) with enhanced effects [85]. The $\text{PEO}_{10}\text{LiC}(\text{SO}_2\text{CF}_3)_3$ complex exhibits a conductivity of $3 \times 10^{-5} (\Omega \text{ cm})^{-1}$ at 25°C , and the absence of a melting transition near 60°C .

In 1994, Armand and coworkers [81] synthesized and characterized the two bulky lithium salts $\text{C}_6\text{H}_4[\text{RLiC}(\text{SO}_2\text{CF}_3)_2]_2$, where $\text{R} = \text{CO}$ or SO_2 . The $\text{PEO}_8\text{C}_6\text{H}_4[\text{COLiC}(\text{SO}_2\text{CF}_3)_2]_2$ complex exhibits a conductivity near $10^{-4} (\Omega \text{ cm})^{-1}$ at 25°C , and features a reduced endothermic event near 30°C .

In 1995, Gard and coworkers [82] synthesized lithium pentafluorothiometane sulfonate ($\text{LiSO}_3\text{CF}_2\text{SF}_5$) and investigated a series of PEO- $\text{LiSO}_3\text{CF}_2\text{SF}_5$ complexes. The $\text{PEO}_4\text{LiSO}_3\text{CF}_2\text{SF}_5$ complex exhibits a conductivity near $10^{-5} (\Omega \text{ cm})^{-1}$ at 25°C . The plasticizing effect of $\text{LiSO}_3\text{CF}_2\text{SF}_5$ appears to lie in the reduction, but not the complete eliminating of the crystallization of the complex. The $\text{PEO}_4\text{LiSO}_3\text{CF}_2\text{SF}_5$ complex shows a reduction in the magnitude of the melting transition compared with complexes of less salt

content. This behavior differs from that of LiTFSI and LiTFSM complexes, which completely suppress crystallization, and is similar to that of the $C_6H_4[COLiC(SO_2CF_3)_2]_2$ complexes.

A disadvantage of the LiTFSI and LiTFSM salts has been in their preparation. In 1996, Lerner and coworkers [80] investigated the PEO complexes of $LiCH(SO_2CF_3)_2$. The synthesis of $LiCH(SO_2CF_3)_2$ involves a one-step reaction, carried out at room temperature, in aqueous solution, with commercially available reagents. Conductivities are highest for the $PEO_{16}LiCH(SO_2CF_3)_2$ complex, approaching $10^{-4} (\Omega \text{ cm})^{-1}$ at 30 °C. As the salt concentration is increased, the complexes exhibit a decrease in the temperature and the magnitude of the principle melting transition; indicating the plasticizing effect of the salt.

1.3 General Apparatus and Procedures

1.3.1 Handling of Air Sensitive Materials

A glass vacuum line was utilized for the drying of air sensitive materials and samples. A Welch 1402 Duo-Seal vacuum pump was connected to the glass vacuum line and protected by a liquid nitrogen trap. A typical vacuum of 10 millitorr was obtained. Samples were dried in custom drying tubes at temperatures ranging from 30 - 120 °C. The samples were loaded and removed under an inert atmosphere. The drying tube was attached to the vacuum line by a 15-mm O-ring seal. Flow through the side arm was

controlled with a Teflon stopcock.

Materials which required handling in an inert atmosphere were manipulated using standard Schlenck line techniques [86]. Dry argon (99.998%) and helium (99.998%) gases were used from cylinders without further purification. Dry nitrogen (99.999%) gas was obtained from a cylinder and dried by flowing through a column packed with P_2O_5 and $CaSO_4$.

Air sensitive materials were manipulated and stored in a dry box (Vacuum Atmospheres Company, Hawthorne, CA, Model MO-40-2B) containing a dry argon and/or helium atmosphere. The dry box allowed for the loading and removing of samples in an inert atmosphere.

1.3.2 Solvent and Reagent Purification

Acetonitrile (Mallinckrodt, reagent) was dried over molecular sieves (4A), distilled under a dry nitrogen atmosphere over CaH_2 (Aldrich), and transferred into Schlenck flasks purged with dry nitrogen gas. The flasks were then stored in a solvent box (Forma Scientific). Poly(ethylene oxide) (Aldrich, MW = 5×10^6) was dried under vacuum at 30 °C for 48 h to remove residual water. The dried polymer was stored in a dry box. Lithium salts were dried under vacuum to remove residual water and solvents prior to complexation $\{LiSO_3CF_2SF_3, 120\text{ }^\circ C; LiSO_3CFHSF_3, 120\text{ }^\circ C; LiCH(SO_2CF_3)_2, 120\text{ }^\circ C; LiSO_3CF_2CF_2OCF_2CF_2SO_3Li, 120\text{ }^\circ C; LiNHSO_2F, 120\text{ }^\circ C; \text{ and } (CF_2)_n(SO_2OLi)_2 \cdot wH_2O, \text{ where } n = 1 - 4, 120\text{ }^\circ C\}$. The lithium salts $LiN(SO_2CF_3)_2$ (3M) and $LiSO_3C_8F_{17}$ (3M)

were recrystallized from acetonitrile and dried under vacuum at 80 °C for several days.

All purified salts were stored in a dry box.

1.3.3 Film Casting

Thin polymer electrolyte films were cast in a solvent box (Forma Scientific) containing a dry nitrogen atmosphere. The film casting mixture was transferred with a disposable plastic syringe into a glass ring on a Teflon surface. Typical films were 100 μm thick of a 3 cm^2 surface area, cast from 10 mL of a mixture containing about 3-4 g of PEO and the appropriate mass of salt, in 300 mL of acetonitrile. After the film dried, the glass ring was lifted from the Teflon surface. The film remained attached to the glass ring to maintain its conformation.

Thin film electrodes were cast by a similar procedure. The film casting mixture was transferred with a disposable plastic syringe onto a stainless steel cylinder surrounded by a tight-fitting glass ring. After the film dried, the glass ring was slid down the stainless steel cylinder, leaving a uniform film on the stainless steel surface. Typical films were 100 μm thick, having a 1 cm^2 surface area, consisting of 4 mg of the electrode material.

1.4 Characterization Techniques

1.4.1 Impedance Spectroscopy

1.4.1.1 Introduction

Impedance spectroscopy is an alternating current method utilized for the determination of the electrical properties of polymer electrolytes; including the bulk ionic conductivity. Compared to direct current methods, impedance spectroscopy requires sophisticated, and relatively expensive, instrumentation. This section will begin with a description of a simple direct current experiment and a discussion of the advantages of the impedance method. This is followed by a description of an alternating current experiment, a discussion of cell impedance, and a description of data analysis using equivalent circuits.

1.4.1.2 dc Methods

The simplest experiment to examine the electrical properties of a polymer electrolyte is the direct current (dc) measurement of a polymer electrolyte sample placed between two non-blocking electrodes (Figure 1.4). Under a sufficient applied potential, lithium ions in the electrolyte are reduced to Li metal at the cathode (B) and Li metal is oxidized at the anode to release Li^+ into the electrolyte. Lithium ions transport through the electric field in the electrolyte from A to B. We can represent the resistance to lithium

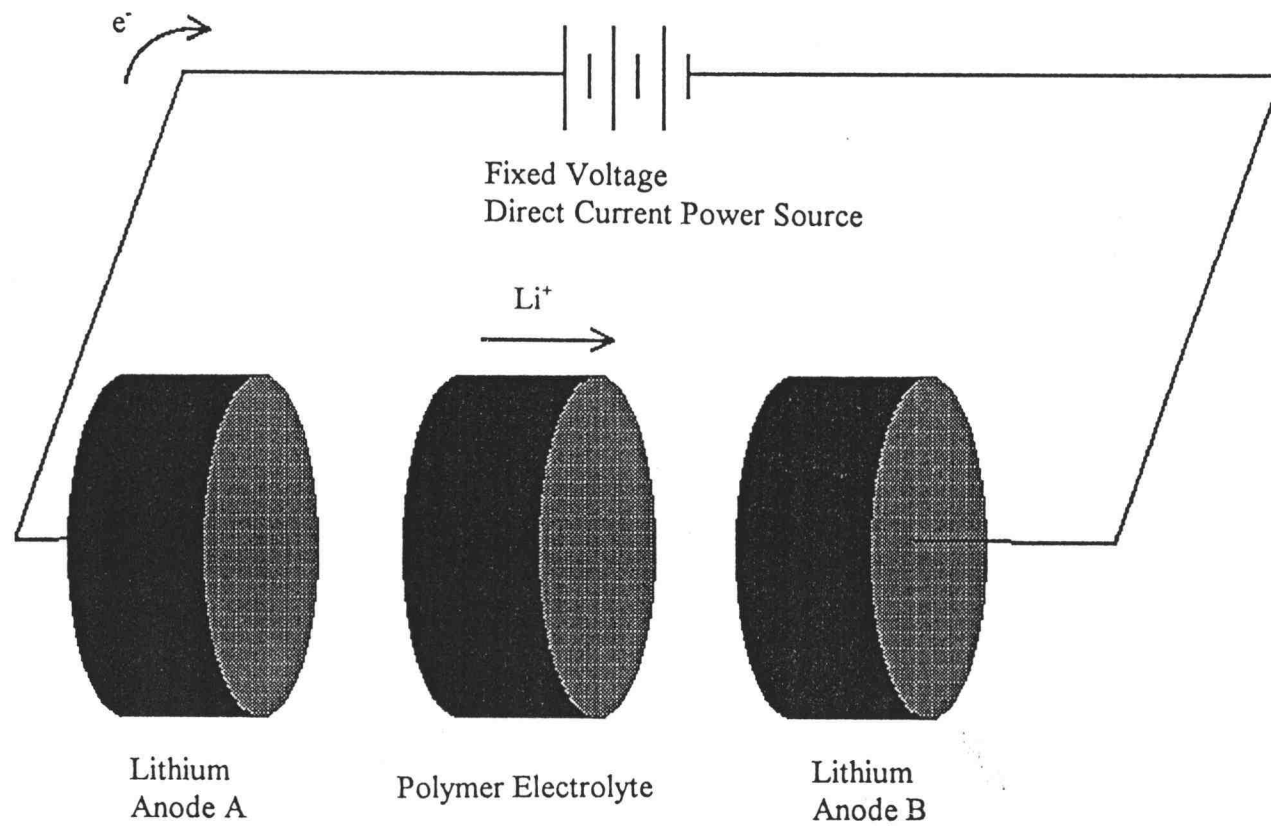


Figure 1.4: A representation of the symmetrical direct current cell with two non-blocking electrodes

ion migration within the polymer electrolyte by a resistor, R_b . This resistance is related to the voltage drop across the electrolyte, V , and the current through the cell, I , $R_b = V/I$. Because this resistance is dependant on the polymer electrolyte dimensions, it is useful to calculate the specific conductivity, σ , where: $\sigma = l/R_b A$; where l is the distance between the lithium metal electrodes, and A is their surface area. Although the resistance through the electrodes and the external circuit are usually negligible, there are also significant resistances associated with the interfaces between the electrodes and the electrolyte. These interfacial resistances to current flow may be represented by resistors, R_{eA} and R_{eB} , as depicted in the equivalent circuit shown in Figure 1.5, and are due to the finite rates of the oxidation and reduction processes as well as formation of an interfacial layer. Ordinarily, polymer electrolyte-lithium metal electrode interfacial resistances are not negligible, and are often greater in magnitude than the bulk resistances observed for the polymer electrolytes [88]. Since dc experiments measure the total resistance, the bulk ionic conductivity cannot be determined separately.

The addition of two non-polarized electrodes--located on the polymer electrolyte, between the two lithium metal electrodes--can lead to the determination of the bulk ionic conductivity of the polymer electrolyte (Figure 1.6). These two electrodes serve as voltage probes, while the original electrodes pass the constant current. These non-polarizing electrodes are often platinum, eliminating the oxidation and reduction reactions at the interfaces, and reducing the interfacial resistance. The bulk resistance, R_b , can be determined from the current through the circuit, I , and the voltage drop across the polymer electrolyte between the voltage probes, V' ; $R_b = V'/I$. The conductivity may be

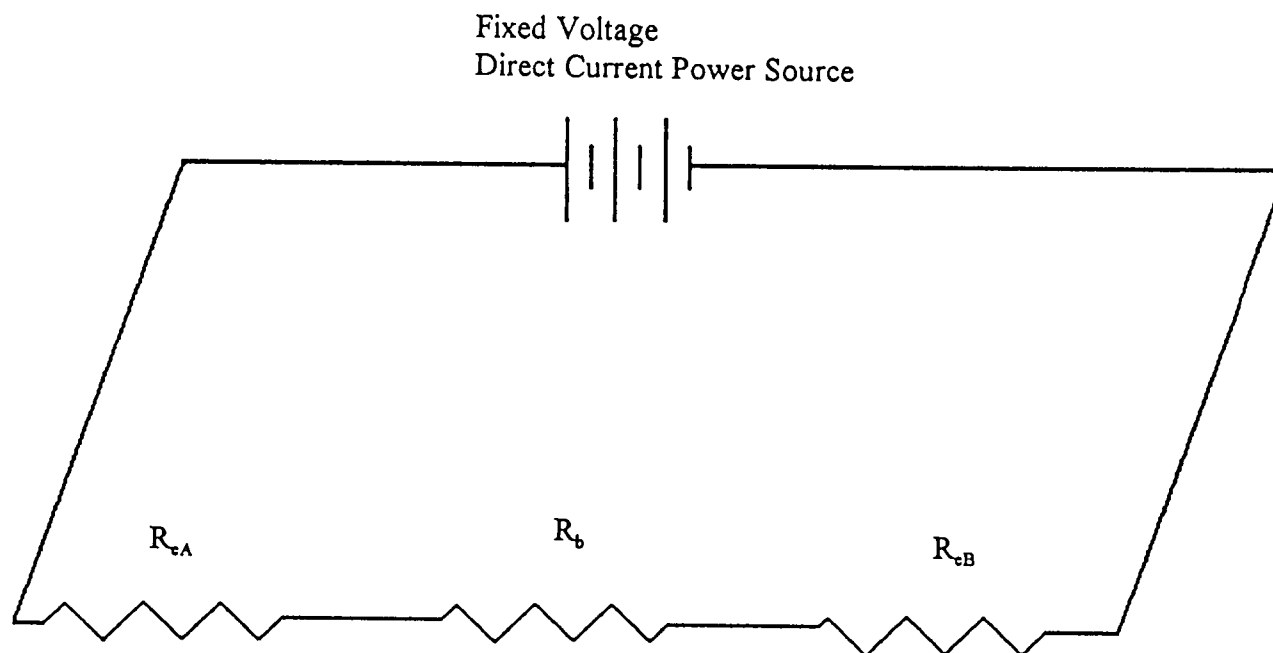


Figure 1.5: The equivalent circuit for the symmetrical direct current cell with two non-blocking electrodes

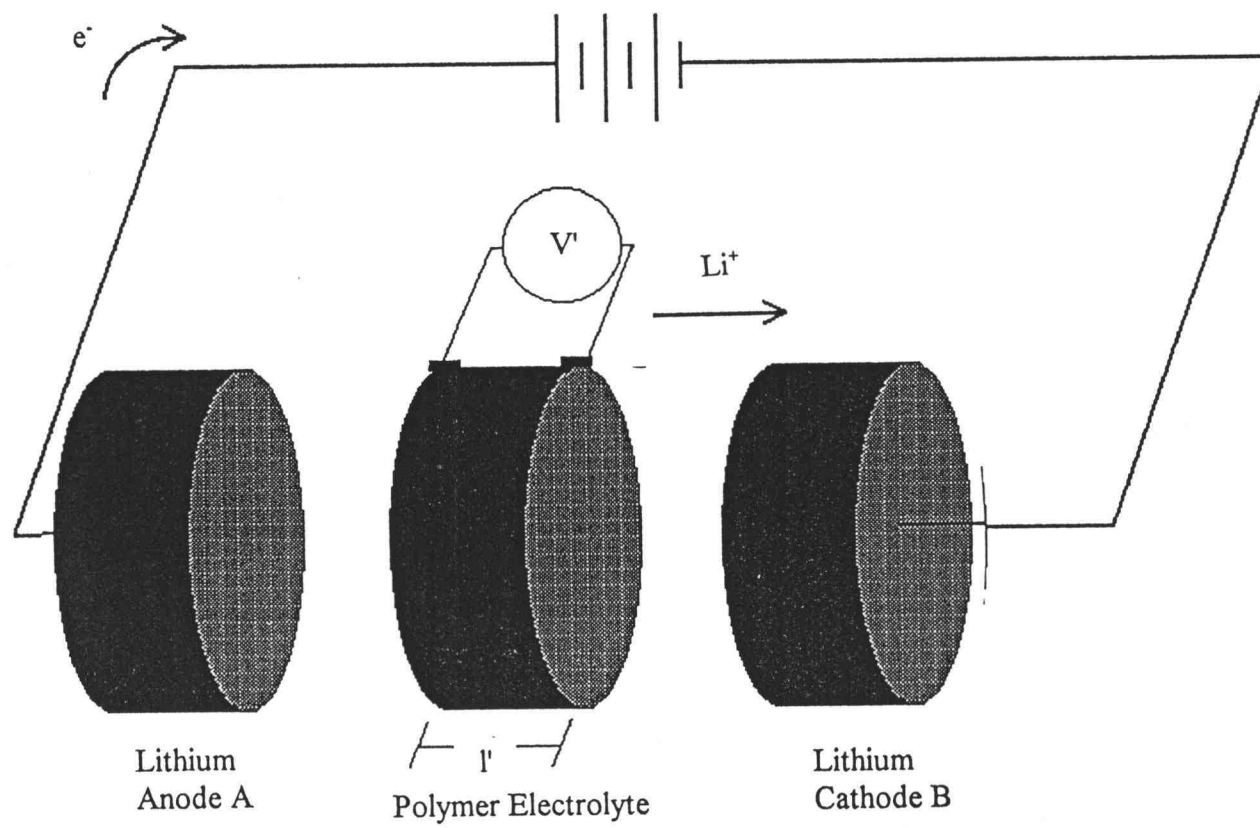


Figure 1.6: The equivalent circuit for the symmetrical direct current cell with two non-blocking electrodes and a voltage probe

calculated using the distance between the voltage probe; $\sigma = l/R_b A$.

The four-terminal direct current cell has two shortcomings. Reliable four-terminal polymer electrolyte cells are difficult to construct. Secondly, a concentration gradient evolves during the dc experiment and the resistance may change over time. It is because of these disadvantages that bulk polymer electrolyte conductivities are generally determined by the non-perturbing alternating current method rather than by dc methods [87].

1.4.1.3 ac Methods

The alternating current (ac) experiment consists of applying a sinusoidal voltage across a cell and monitoring the current response produced through the circuit. Since the ac experiment is non-perturbing--it requires no net change in the local conditions--it allows for multiple experiments and longer experiment times.

In these experiments, bulk ionic conductivities were measured between -40 °C and 100 °C on ½-inch diameter pressed pellets--approximately 1 mm in thickness--in a symmetrical cell with stainless steel blocking electrodes . A Solartron 1260 Impedance/Gain-Phase Analyzer and a Sun EC01 Environmental Chamber under computer control were employed for impedance measurements. Pellets were first annealed at 100 °C for several hours, quenched to -40 °C, then equilibrated for 90 minutes at each measurement temperature.

1.4.1.4 Cell Impedance

In the alternating current (ac) experiment, the current, I , is related to the potential, V , by two parameters. One, the magnitude of the impedance, represents the opposition to the flow of charge, and is the ratio of the maximum potential and the maximum current;

$$|Z| = V_{\max}/I_{\max} \quad (1.4)$$

The second parameter, θ , is the phase difference between the applied potential and the monitored current (Figure 1.7). These two parameters constitute the cell impedance,

$$Z^* = Z \cos \theta \quad (1.5)$$

Both the magnitude of the impedance and the phase angle are functions of the frequency of the applied potential. The cell impedance is a vector quantity which may be represented where the real (Z') and imaginary (Z'') components of the complex number;

$$Z^* = Z' - (\sqrt{-1})Z'' \quad (1.6)$$

are plotted at different frequencies (Figure 1.8). This is referred to as a Cole-Cole plot or a Nyquist diagram.

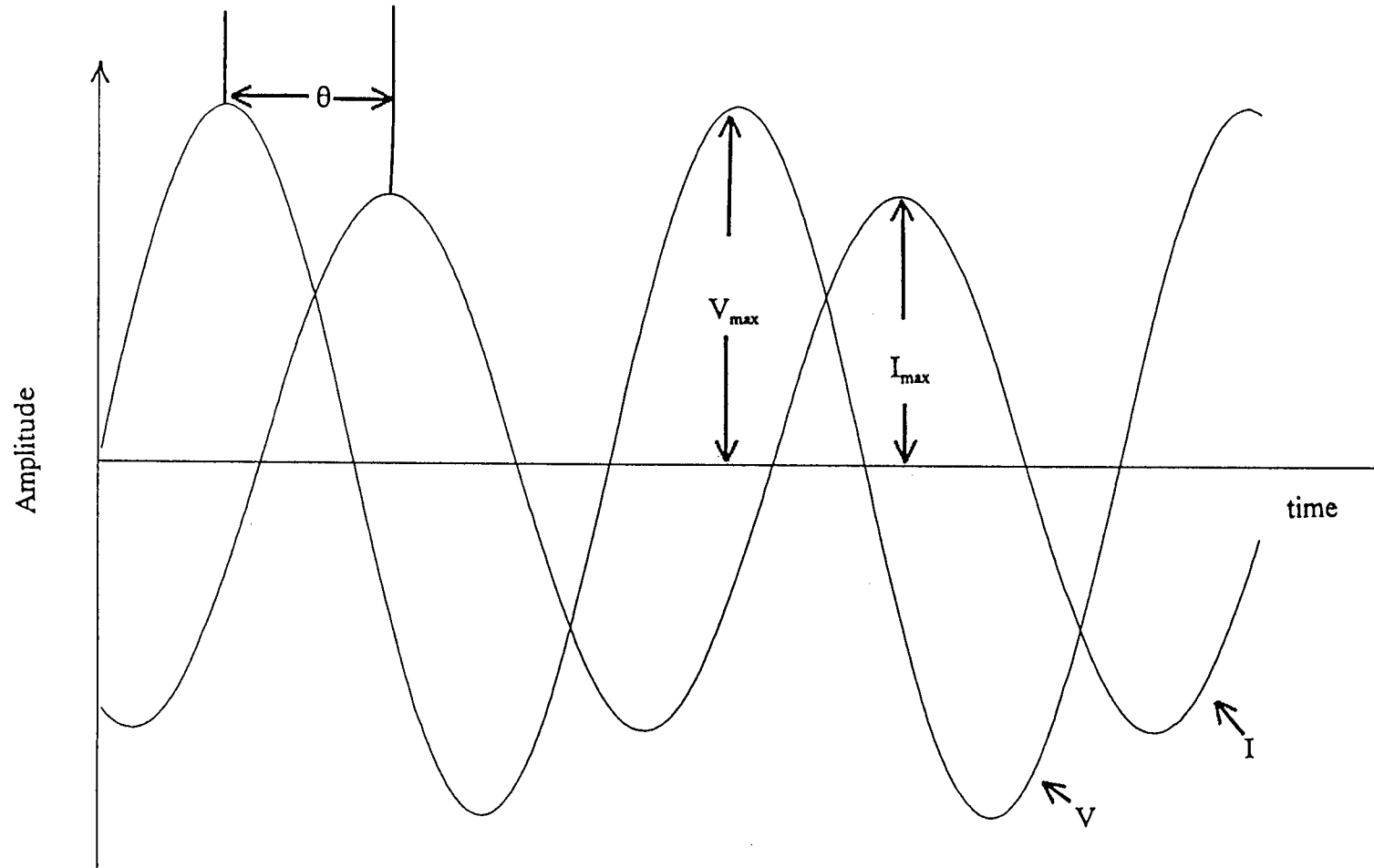


Figure 1.7: A representation of the sinusoidal voltage and current, at a given frequency

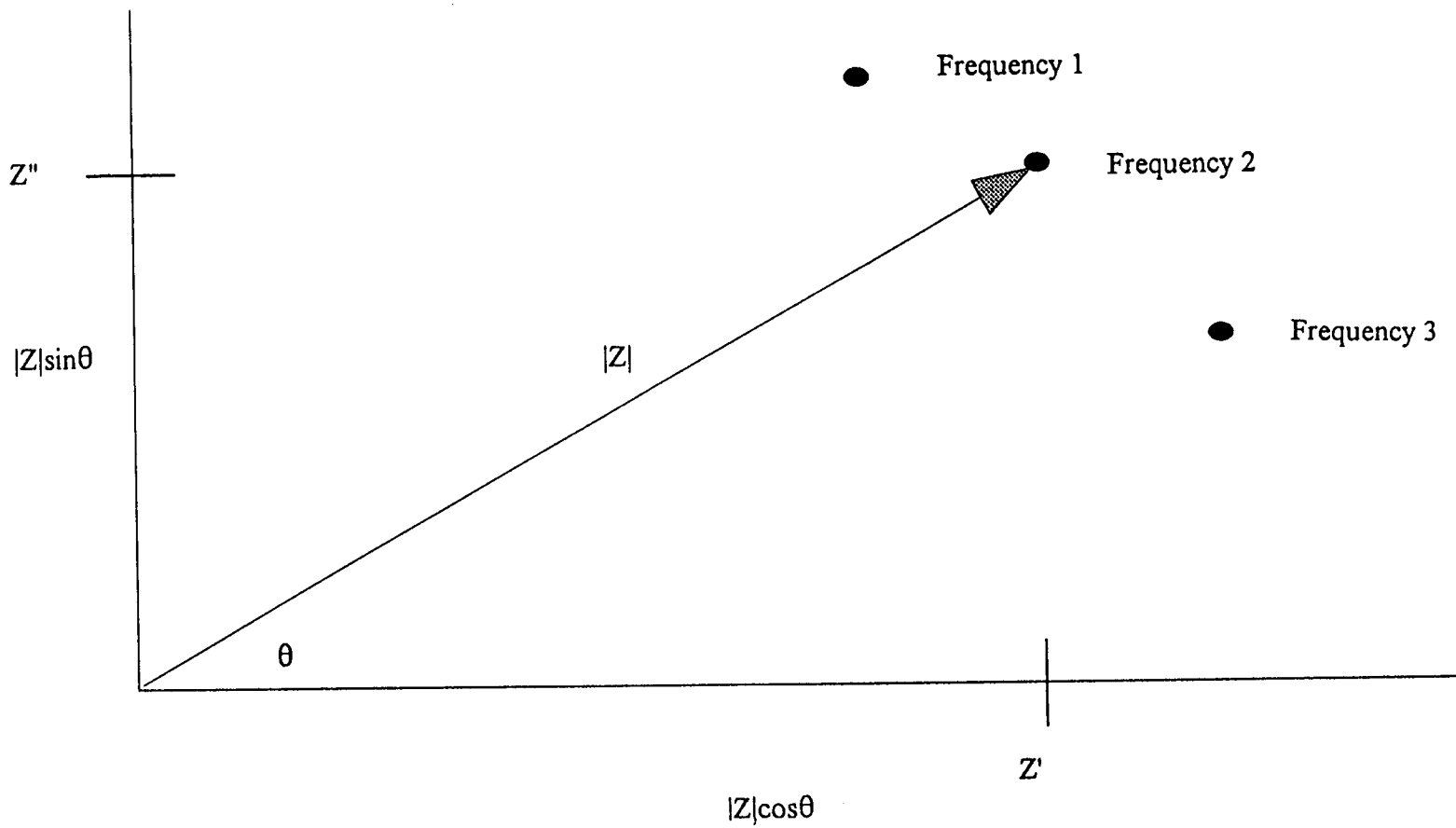


Figure 1.8: A representation of the impedance, Z , of a cell. $|Z| \sin \theta$ is the y component, $|Z| \cos \theta$ is the x component; or Z' is the real component, and Z'' is the y component

1.4.1.5 Alternating Current Response to Several Simple Circuits

It has proven to be of value to evaluate the cell response by using equivalent circuits. The equivalent circuit is constructed from ideal components--particularly resistors and capacitors--which individually represent the fundamental migration and polarization processes occurring in the cell [89]. The ac response to several simple circuits is discussed below and the ac response to a polymer electrolyte cell is discussed in the next section.

The total cell impedance is a complex quantity and is only real when $\theta = 0$ [89]. For an equivalent circuit consisting solely of a resistor, $\theta = 0$, the impedance is frequency independent, and the impedance is simply the resistance ($|Z| = R$)(Figure 1.9a).

For an equivalent circuit consisting of solely of a capacitor, the impedance is frequency dependent. The voltage is out of phase with the current by 90° ; $\theta = -\pi/2$, and

$$|Z| = 1/\omega C \quad (1.7)$$

where ω is the angular frequency, $2\pi f$, and C is the capacitance [87] (Figure 1.9b).

For an equivalent circuit consisting of a resistor and a capacitor in series, the impedance is calculated as the sum of the two components;

$$Z_{\text{Total}}^*(\omega) = Z_1^*(\omega) + Z_2^*(\omega) \quad (1.8)$$

or

$$Z_{\text{Total}}^*(\omega) = R - (\sqrt{-1})/\omega C \quad (1.9)$$

The complex impedance representation (Figure 1.10a) is a vertical line shifted along the real axis by a magnitude of R .

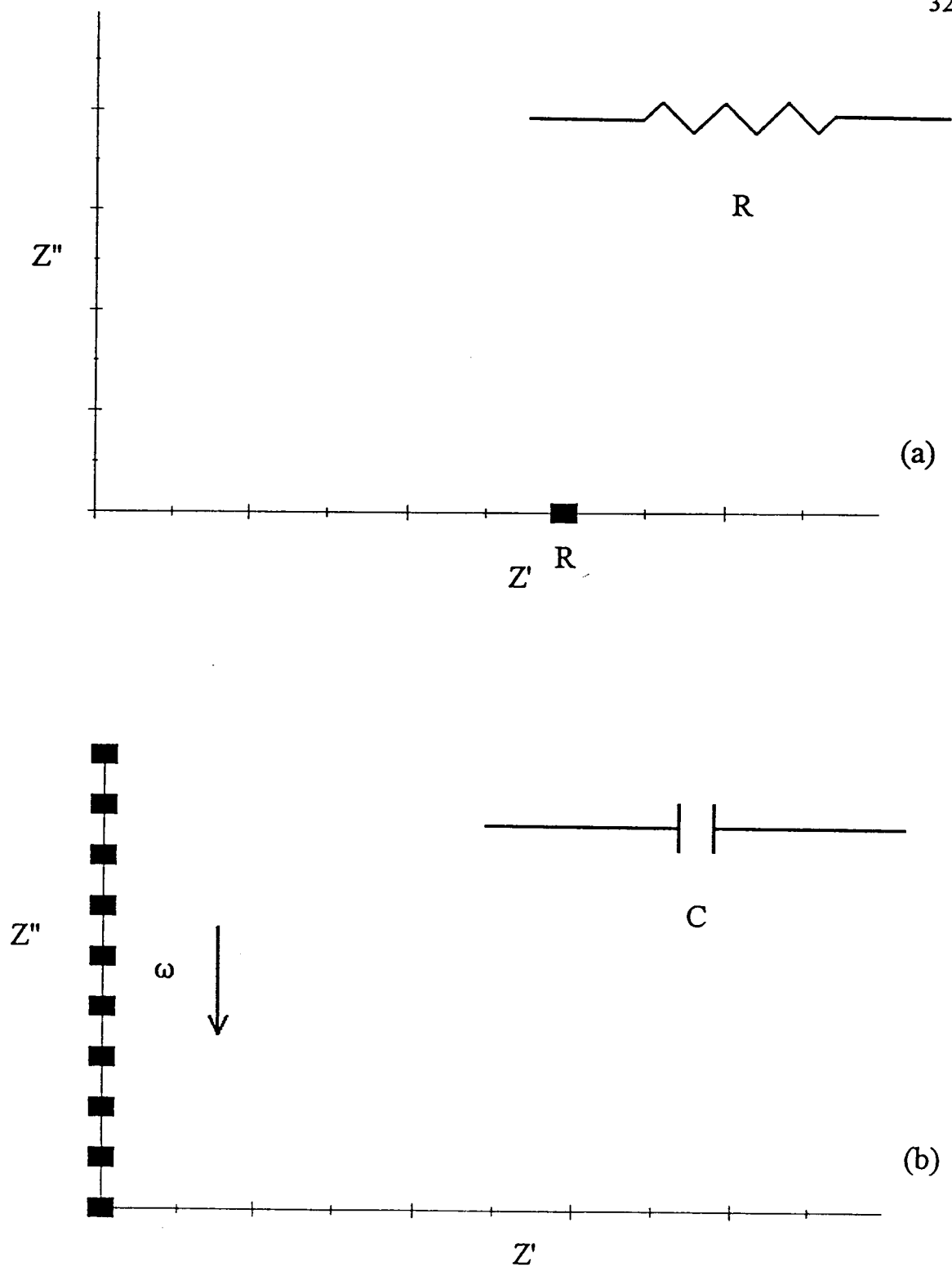


Figure 1.9: Representation of (a) a resistor, R , and (b) a capacitor, C , in the complex impedance plane

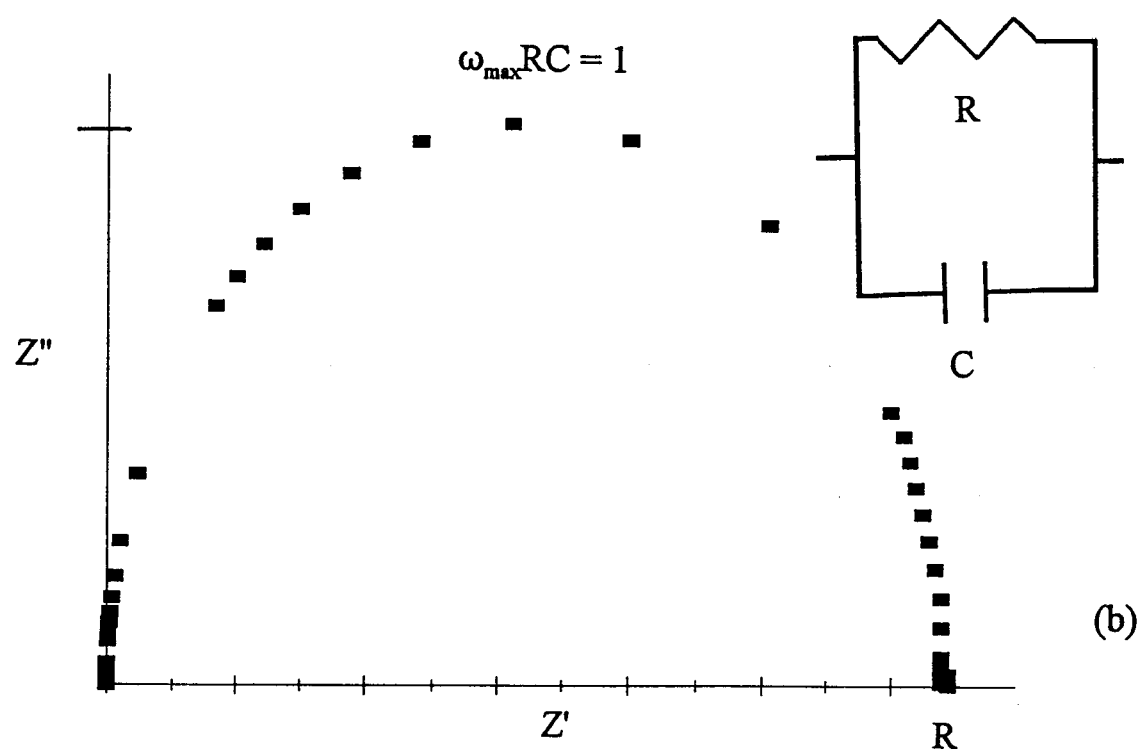
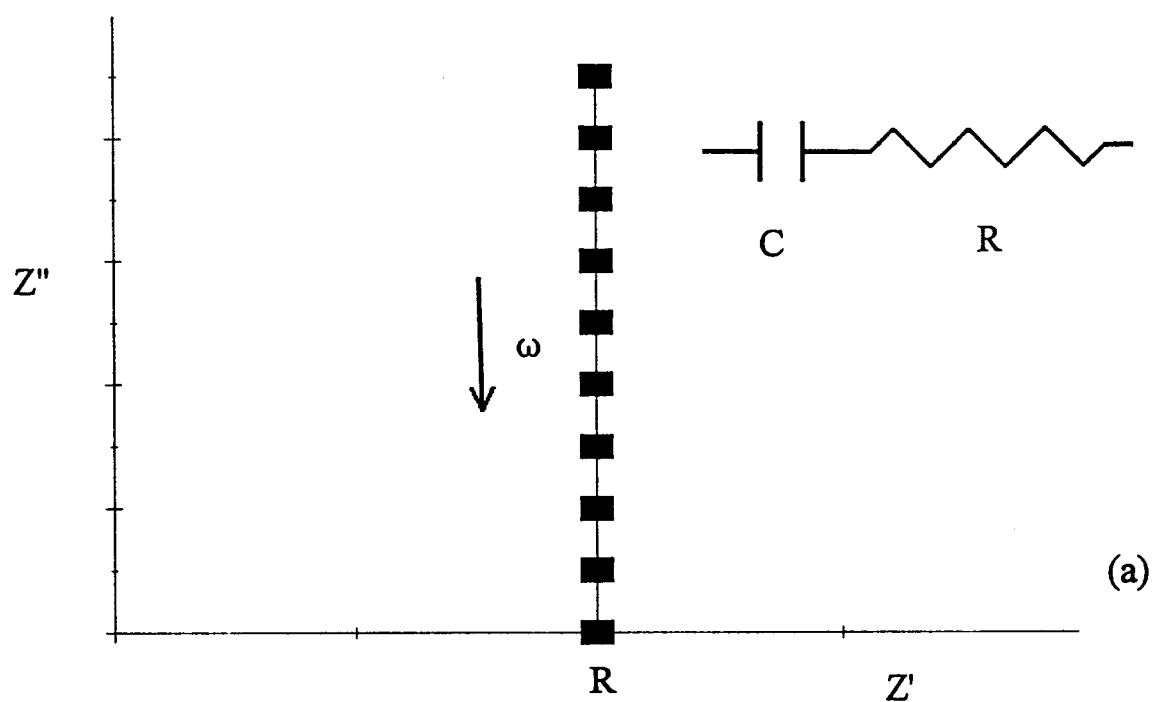


Figure 1.10: (a) Representation of a resistor, R , and a capacitor, C , in series in the complex impedance plane.
 (b) Representation of a resistor, R , and a capacitor, C , in parallel in the complex impedance plane.

For an equivalent circuit consisting of a resistor and a capacitor in a parallel circuit, the impedances of the two components are not simply additive, but

$$Y^*(\omega) = Y_R^*(\omega) + Y_C^*(\omega) \quad (1.10)$$

where the admittance $[Y^*(\omega)]$ is the reciprocal impedance:

$$Y^*(\omega) = 1/Z^*(\omega) \quad (1.11)$$

For a resistor and a capacitor in a parallel circuit:

$$Z_{\text{Total}}^*(\omega) = R[1/\{1+(\omega RC)^2\}] - (\sqrt{-1})R[\omega RC/\{1+(\omega RC)^2\}] \quad (1.12)$$

The complex impedance representation is a semicircle extending along the Z' axis from the origin to R (Figure 1.10b). Furthermore, the maximum of the semicircle corresponds to the point where the impedance of the resistor and the capacitor are equal:

$$R = 1/\omega_{\text{max}}C \quad (1.13)$$

1.4.1.6 Alternating Current Response to a Polymer Electrolyte Cell

A complex impedance representation for the polymer electrolyte $(\text{PEO})_4\text{LiCH}(\text{SO}_2\text{CF}_3)_2$ is shown in Figure 1.11. The cell factor (ℓ/A) is 0.189 cm^{-1} . The experiment was conducted at 65°C and the responses are due to a 10 mV perturbation in the frequency domain of 3 MHz to 5 Hz.

An equivalent circuit representing the ac response to the polymer electrolyte cell is that of a resistor (R_b) and a capacitor (C_b) in a parallel circuit (Figure 1.12).

During the ac experiment, the applied voltage causes the electrodes to become alternately positively and negatively charged. The alternating field produced causes the

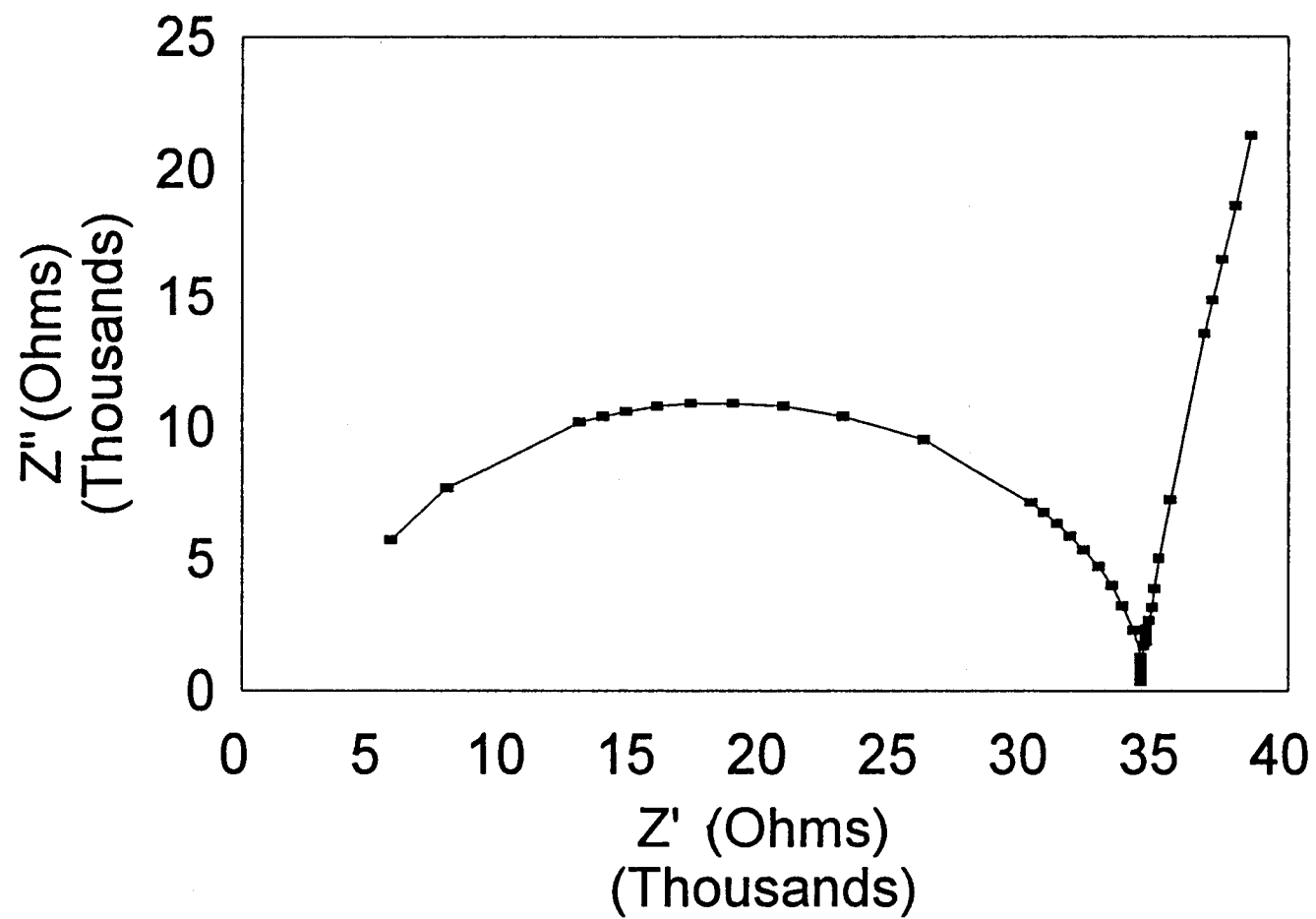


Figure 1.11: A complex impedance representation for the polymer electrolyte $(\text{PEO})_4\text{LiCH}(\text{SO}_2\text{CF}_3)_2$

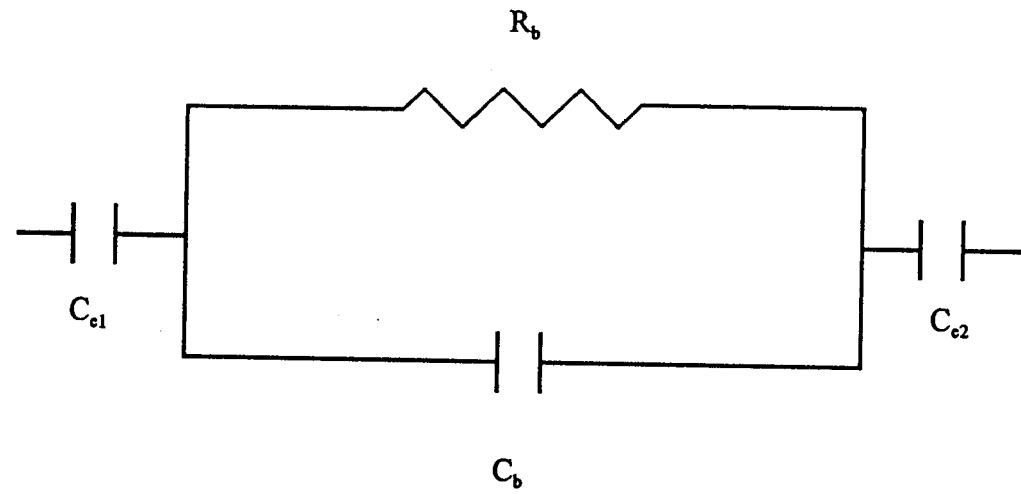


Figure 1.12: An equivalent circuit representing the ac response to the polymer electrolyte cell

lithium ions in the polymer electrolyte to migrate back and forth in phase with the voltage. The resistor, R_b , represents this migration of lithium ion. Simultaneously, the stationary polymer becomes polarized. The capacitor, C_b , represents this dielectric polarization. Due to the accumulation and depletion of lithium ions at the electrodes during cycling, and the equal and opposite charge on the electrodes, the electrode is not unlike a parallel plate capacitor. The two capacitors (C_{e1} and C_{e2}) in series with the parallel circuit describe the electrolyte-electrode as a double layer capacitance. This representation of the electrolyte-electrode interface as a double layer capacitance is a reasonable approximation when the concentration of ions in the electrolyte is high ($\geq 1M$) [91], as is the case for all of the polymer electrolytes examined in this study.

At sufficiently high frequencies, R_b and C_b contribute to the total impedance, whereas the impedance of the electrode capacitance, C_e , is insignificant. Therefore, in this frequency range, the equivalent circuit reduces to the parallel $R_b C_b$ circuit [87]. The bulk resistance, R_b , may be interpreted as the point where the semicircle touches down on the real axis. At lower frequencies (typically less than 1 kHz), C_b makes an insignificant contribution to the total impedance, and the equivalent circuit reduces to R_b and C_e in series, producing a vertical line in the Nyquist diagram at R_b . Often in thin film cells, the vertical line anticipated at low frequencies is inclined to an angle of 45° to the real axis (see Figure 11). This response is due to the classic Warburg impedance [89], which derives from the finite length diffusion process. The diffusion of the electroactive ions is represented by W , the Warburg element, in which the impedance is given by

$$Z_w(\omega) = A\omega^{-1/2} - jA\omega^{-1/2} \quad (1.14)$$

where A is a constant which depends on a number of factors including the diffusion coefficient of the electroactive ions [87].

Although the ideal equivalent circuits described above usually suffice for the evaluation of R_b , the complex impedance representation for a polymer electrolyte cell is generally a semicircle which is flattened and broadened. This effect has been ascribed to a distributed response arising from inhomogeneities in the polymer electrolyte. The salt may not be evenly distributed throughout the polymer, and/or the electrolyte consists of a mixture of crystalline and amorphous regions. This semi-circle depression is described by an equivalent circuit in which the bulk capacitor has been replaced by a constant-phase element (Figure 1.13). The Constant-phase element is an empirical impedance function of the type

$$Z_{CPE}^*(\omega) = 1/[j\omega Q]^n \quad (1.15)$$

where Q is the constant-phase element and n is a measure of the distribution of relaxation times. The constant-phase element is equivalent to a capacitor when $Q = C$ and $n = 1$. With an increase in the distribution of relaxation times, n decreases, and the semi-circle in the complex impedance representation is depressed.

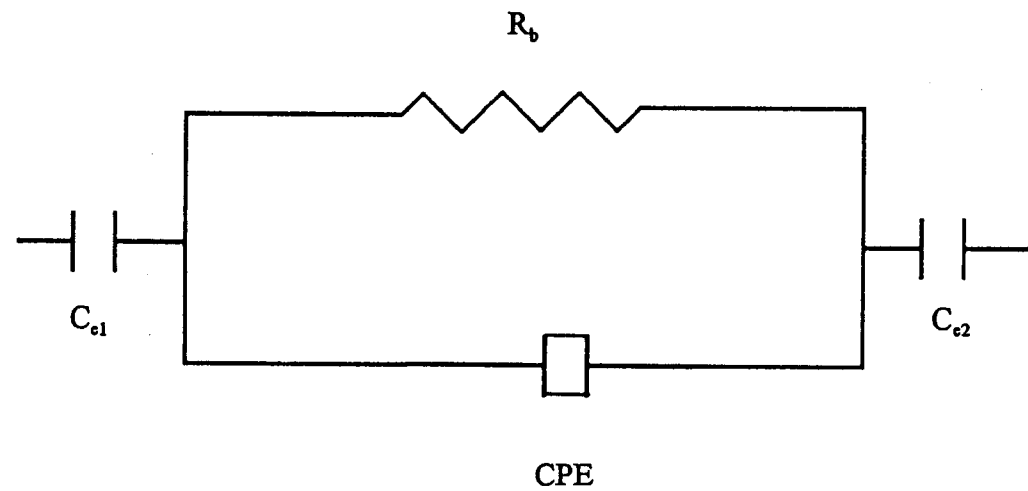


Figure 1.13: An equivalent circuit representing the ac response to the polymer electrolyte cell with the inclusion of a constant-phase element

1.4.2 Cyclic Voltammetry

A three-electrode cell configuration with a lithium metal reference and a thin-film polymer electrolyte was utilized for cyclic voltammetry experiments. Experiments were performed at 20 mV / s between -0.1 and +5.0 V using a computer controlled EG&G Princeton Applied Research Model 362 Scanning Potentiostat. The QuickBASIC 4.5 program written to control the instrumentation is presented in Appendix B.

1.4.3 Differential Scanning Calorimetry

Differential scanning calorimetry (DSC) was performed with 20 - 25 mg samples loaded in hermetically-sealed aluminum pans in a Shimadzu DSC-50. Samples were loaded in a dry box to maintain an inert atmosphere. Salt samples were heated at a rate of 10 °C / min from 20 °C to 450 °C. Polymer electrolyte samples were heated to 100 °C, quenched below -100 °C, then heated at a rate of 10 °C / min from -100 °C to +120 °C.

1.4.4 Thermal Gravimetric Analysis

Thermal gravimetric analysis (TGA) utilized a Shimadzu TGA-50. Samples were loaded into a platinum pan, and heated from 30 °C to 450 °C at a rate of 10 °C / min under a flow of purified nitrogen gas (50 mL / min).

1.5 References

1. D. Fenton, J. Parker, and P. Wright, *Polymer* **14**, 589 (1973).
2. M. Armand, J. Chabagno, and M. Muclot, Second International Meeting on Solid Electrolytes, St. Andrews, Scotland, 20-22 Sept. 1978, Extended Abstract.
3. C. Vincent, *Solid St. Chem.* **17**, 145 (1987).
4. C. Berthier, W. Gorecki, M. Minier, and M. Armand, *Solid State Ionics* **11**, 91 (1983).
5. P. Blonsky, D. Shriver, P. Austin, and H. Allcock, *J. Am. Chem. Soc.* **106**, 6854, (1984).
6. D. Shriver, S. Clancy, P. Blonsky, and L. Hardy, in *Proceedings of the 6th Risø International Symposium on Metallurgy and Materials Science* (F. Poulsen, N. Hessel Andersen, K. Clausen, S. Skaarup, and O. Sørensen, Eds.), Risø National Laboratory, Roskilde (1984).
7. G. Nazri, D. MacArthur, and F. Ogara, *Chem. Mater.* **1**, 370 (1989).
8. S. Greenbaum, K. Adamic, Y. Pak, M. Wintersgill, and J. Fontanella, *Solid State Ionics* **28-30**, 1042 (1988).
9. G. Nazri, D. MacArthur, and F. Ogara, *Polym. Prepr.* **30**, 430 (1989).
10. M. Lerner, L. Lyons, J. Tonge, and D. Shriver, *Polym. Prepr.* **30**, 435 (1989).
11. P. Blonsky, D. Shriver, P. Austin, and H. Allcock, *Solid State Ionics* **18/19**, 258 (1989).
12. H. Allcock, P. Austin, T. Neenan, J. Sisko, P. Blonsky, and D. Shriver, *Macromolecules* **19**, 1508 (1986).
13. J. Tonge, and D. Shriver, *J. Electrochem. Soc.* **134**, 270 (1987).
14. C. Nicholas, D. Wilson, and C. Booth, *Br. Polym. J.* **20**, 289 (1988).
15. J. Lemmon, and M. Lerner, *Macromolecules* **25**, 2907 (1992).

16. M. Wintersgill, J. Fontanella, Y. Pak, S. Greenbaum, A. Al-Mударis, and A. Chadwick, *Polymer* **30**, 1123 (1989).
17. G. Nazri, D. MacArthur, J. O'Gara, and R. Aroca, *Mater. Res. Soc. Symp. Proc.* **210**, 163 (1991).
18. I. Kelly, J. Owen, and B. Steele, *J. Power Sources* **14**, 13 (1985).
19. F. Gray, in *Polymer Electrolyte Reviews-1* (J. MacCallum, and C. Vincent, Eds.), Elsevier, London (1987), p. 139.
20. G. Cameron, M. Ingram, and K. Sarmouk, *Eur. Polym. J.* **26**, 197 (1990).
21. M. Kaplan, E. Rietman, R. Cava, L. Holt, and E. Chandross, *Solid State Ionics* **25**, 37 (1987).
22. M. Kaplan, E. Rietman, and R. Cava, *Polymer* **30**, 504 (1989).
23. J. Weston, and B. Steele, *Solid State Ionics* **7**, 75 (1982).
24. F. Gray, J. MacCallum, and C. Vincent, *Solid State Ionics* **18/19**, 252 (1986).
25. G. Gard, P. Nixon, N. Hamel, S. Ullrich, and N. Holcomb, Department of Chemistry, Portland State University.
26. 3M, Industrial Chemical Products Division, St. Paul, MN.
27. F. Gray, *Solid Polymer Electrolytes*, VCH Publishers, New York, 1991, p.97.
28. J. Tonge, and D. Shriver, *J. Electrochem. Soc.* **134**, 270 (1987).
29. S. Sylla, J. Sanchez, and M. Armand, *Electrochim. Acta* **37**, 1699 (1992).
30. D. Benrabah, J. Sanchez, and M. Armand, *Electrochim. Acta* **37**, 1737 (1992).
31. S. Sloop, M. Lerner, T. Stephens, A. Tipton, D. Paull, and J. Stenger-Smith, *J. Appl. Poly. Sci.* **53**, 1563 (1994).
32. J. MacCallum, M. Smith, and C. Vincent, *Solid State Ionics* **11**, 307 (1984).
33. B. Scrosati, *Mater. Sci. Eng.* **112**, 269 (1992).

34. F. Gray, Solid Polymer Electrolytes, VCH Publishers, New York, 1991.; Polymer Electrolyte Reviews-1; J. MacCallum, and C. Vincent, Eds; Elsevier: New York (1987).
35. L. Dominey, V. Koch, and T. Blacley, *Electrochim. Acta* **37**, 1551 (1992).
36. D. Benrabah, D. Baril, J. Sanchez, M. Armand, and G. Gard, *J. Chem. Soc. Far. Trans.* **89**, 355 (1992).
37. R. Nafshun, M. Lerner, N. Hamel, P. Nixon, and G. Gard, *J. Electrochem. Soc.* **142**, L153 (1995).
38. P. Lightfoot, M. Mehta, and P. Bruce, *Science* **262**, 883 (1993).
39. B. Scrosati (ed.), Applications of Electroactive Polymers, Chapman and Hall, London, 1993.
40. M. Ratner, and D. Shriver, *Chem. Rev.* **88**, 109 (1988).
41. R. Nafshun, M. Lerner, N. Holcomb, P. Nixon, and G. Gard, *J. Electrochem. Soc.* **143**, 1297 (1996).
42. A. Vallee, S. Besner, and J. Prud'homme, *Electrochim. Acta*, **37** 1579 (1992).
43. Polymer Electrolyte Reviews-2; J. MacCallum, and C. Vincent, Eds; Elsevier: New York (1989).
44. J. Lemmon, and M. Lerner, *Macromolecules* **25**, 2907 (1992).
45. S. Sloop, M. Lerner, T. Stephens, A. Tipton, D. Paull, and J. Stenger-Smith, *J. Appl. Poly. Sci.* **53**, 1563 (1994).
46. M. Mendolia, and G. Farrington, *High-Conductivity, Solid Polymeric Electrolytes, in Materials Chemistry: An Emerging Discipline*; L. Interrante, L. Casper, and A. Ellis, Eds; American Chemical Society: Washington, D.C., 1995, p. 107.
47. R. Pearson, *J. Amer. Chem. Soc.* **85**, 3533 (1963).
48. A. F. Kapustinskii, *Quart. Rev. Chem. Soc.* **10**, 283 (1956).
49. M. Ratner, and D. Shriver, *Chem. Rev.* **88**, 109 (1988).

50. M. Armand, in *Polymer Electrolyte Reviews-1*; J. MacCallum, and C. Vincent, Eds; Elsevier: New York (1987).
51. F. Gray, *Solid Polymer Electrolytes*, VCH Publishers, New York, 1991, p. 35.
52. M. Armand, J. Chabagno, and M. Duclot, in *Fast Ion Transport in Solids*; P. Vashista, J. Mundy, and G. Shenoy, Eds; Elsevier North-Holland, Amsterdam, 1979.
53. P. Lightfoot, M. Mehta, P. Bruce, *Science* **262**, 883 (1993).
54. M. Wantanabe, and N. Ogata, in *Polymer Electrolyte Reviews-1*; J. MacCallum, and C. Vincent, Eds; Elsevier: New York (1987), p. 39.
55. J. Sandahl, S. Schantz, L. Torell, and R. Frech, *Proceedings of SSI 87 Garmish FRG*, Sep. 6 - 11, 1987.
56. J. Paul, C. Jegat, and J. Lassegues, *Electrochimica Acta* **37**, 1623 (1992).
57. C. Harris, D. Shiver, and M. Ratner, *Macromolecules* **19**, 987 (1986).
58. B. Rivas, K. Geckeler, in *Advances in Polymer Science*, v. 102, Springer-Verlag, Berlin (1992), p. 173.
59. C. Dick, G. Ham, *J. Macromol. Sci. Chem. A4*, 1301 (1970).
60. R. Nafshun, and M. Lerner, unpublished results.
61. J. Paul, C. Jegat, and J. Lassegues, *Electrochimica Acta* **37**, 1623 (1992).
62. C. Nicholas, D. Wilson, and C. Booth, *Br. Polym. J.* **20**, 289 (1988).
63. J. Lemmon, and M. Lerner, *Macromolecules* **25**, 2907 (1992).
64. P. Blonsky, D. Shriver, P. Austin, and H. Allcock, *J. Am. Chem. Soc.* **106**, 6854 (1984).
65. P. Blonsky, D. Shriver, P. Austin, and H. Allcock, *Solid State Ionics* **18/19**, 258 (1986).
66. G. Cameron, M. Ingram, and K. Sarmouk, *Eur. Polym. J.* **26**, 197 (1990).
67. I. Kelly, J. Owen, and B. Steele, *J. Electroanal. Chem.* **168**, 467 (1984).

68. F. Gray, *Solid Polymer Electrolytes*, VCH Publishers, New York, 1991, p. 108.
69. H. Lee, X. Yang, J. McBreen, Z. Xu, T. Skotheim, and Y. Okamoto, *J. Electrochem. Soc.* **141**, 886 (1994).
70. I. Kelly, J. Owen, and B. Steele, *J. Electroanal. Chem.* **168**, 467 (1984).
71. I. Kelly, J. Owen, and B. Steele, *J. Power Sources* **14**, 13 (1985).
72. M. Armand, J. Chabagno, and M. Duclot, *Fast Ion Transport in Solids*; P. Vashista, J. Mundy, and G. Shenoy, Eds.; Elsevier: New York (1979), p. 131.
73. H. Vogel, *Phys. Z.* **22**, 645 (1921).
74. G. Tamman, and W. Hesse, *Z. Anorg. Allg. Chem.* **156**, 245 (1926).
75. G. Fulcher, *J. Amer. Ceram. Soc.* **8**, 339 (1925).
76. N. Holcomb, P. Nixon, G. Gard, R. Nafshun, and M. Lerner, *J. Electrochem. Soc.* **143**, 1297 (1996).
77. A. Vallee, S. Besner, and J. Prud'homme, *Electrochim. Acta.* **37**, 1579 (1992).
78. R. Nafshun, and M. Lerner, Unpublished results.
79. C. Robitaille, and D. Fauteux, *J. Electrochem. Soc.* **133**, 315 (1986).
80. N. Holcomb, P. Nixon, G. Gard, R. Nafshun, and M. Lerner, *J. Electrochem. Soc.* **143**, 1297 (1996).
81. D. Benrabah, J. Sanchez, D. Deroo, and M. Armand, *Solid State Ionics* **70/71**, 157 (1994).
82. R. Nafshun, M. Lerner, N. Hamel, P. Nixon, and G. Gard, *J. Electrochem. Soc.* **142**, L153 (1995).
83. M. Armand, W. Gorecki, and R. Andreani, in *Proceedings of 2nd International Symposium on Polymer Electrolytes*, B. Scorsati, Ed., **105**, Elsevier, London, p.99.
84. L. Dominey, V. Koch, and T. Blacley, *Electrochim. Acta* **37**, 1551 (1992).

85. D. Benrabah, D. Baril, J. Sanchez, M. Armand, and G. Gard, *J. Chem. Soc. Faraday. Trans.* **89**(2), 355 (1993).
86. D. Shriver, and M. Drezdson, *The Manipulation of Air-Sensitive Compounds*, Second Edition, John Wiley & Sons, New York (1986).
87. P. G. Bruce, in *Polymer Electrolyte Reviews-1*; J. MacCallum, and C. Vincent, Eds.; Elsevier: New York (1987), p. 243.
88. R. L. Nafshun, and M. M. Lerner, Unpublished data.
89. J. R. Macdonald, *Impedance Spectroscopy*, John Wiley & Sons, New York (1987), p.14
90. J. R. Macdonald, *Impedance Spectroscopy*, John Wiley & Sons, New York (1987), p.23.
91. P. G. Bruce, in *Polymer Electrolyte Reviews-1*; J. MacCallum, and C. Vincent, Eds.; Elsevier: New York (1987), p. 253.
92. J. R. Macdonald, *Impedance Spectroscopy*, John Wiley & Sons, New York (1987), p.39.

Chapter 2
**Ion Conductivity and Scanning Calorimetry of Poly(ethylene oxide) Complexes of
the Plasticizing Salt $\text{LiSO}_3\text{CF}_2\text{SF}_5$**

Richard L. Nafshun and Michael M. Lerner*

*Department of Chemistry and Center for
Advanced Materials Research
Oregon State University
Corvallis, Oregon 97331-4003, USA*

Nicolas N. Hamel, Paul G. Nixon, and Gary L. Gard*

*Department of Chemistry
Portland State University
Portland, Oregon 97207, USA*

J. Electrochem. Soc., 142, L153 (1995)

2.1 Abstract.

PEO_xLiSO₃CF₂SF₅ complexes show significantly suppressed crystallinity when $x \leq 4$. The 4:1 complex has a conductivity near 10^{-5} at 30°C, comparable to conductivities obtained with PEO complexes of other known plasticizing salts. The role of the anion in plasticizing PEO is discussed by considering the common features of known plasticizers.

2.2 Introduction.

A number of poly(ethylene oxide) (PEO) - salt complexes that are electrochemically stable and exhibit ionic conductivities exceeding 10^{-4} at or below 80 °C have been studied for use as electrolytes in all-solid-state electrochemical cells. Ionic conductivity through polymer-based electrolytes is known to occur principally through an amorphous component of the polymer-salt complex [1]. The goal of enhancing conductivity near ambient temperature therefore means developing polymer-based complexes where crystallization is suppressed at or above the operating temperature. Among the methods of suppressing crystallization examined to date are the use of copolymers, polymer gels, and other plasticizers. The latter method will be especially attractive if the plasticizer is a non-volatile ionic compound so that an all-solid-state electrolyte--without any liquid or volatile component--is obtained.

To date, only a limited number of salts have been demonstrated to suppress crystallization in PEO. Two such salts, lithium bis(trifluoromethanesulfonyl)imide, $\text{LiN}(\text{SO}_2\text{CF}_3)_2$, and lithium tris(trifluoromethanesulfonyl)methide, $\text{LiC}(\text{SO}_2\text{CF}_3)_3$, have been known since 1990 [2-4]. Recently, a report indicates a similar effect using lithium salts of dianions $[(\text{CF}_3\text{SO}_2)_2\text{CR}]\text{C}_6\text{H}_4^{2-}$, $\text{R} = \text{CO}$ or SO_2 , where the dianions are formed from the distribution of chloride in terephthaloyl chloride or benzene-1,3-disulfonyl chloride with $\text{CF}_3\text{SO}_2\text{CH}_2$.[5]. These salt-plasticized complexes are very promising materials as they are readily prepared in anhydrous form, are electrochemically stable, and exhibit ambient temperature conductivities that are amongst the highest obtained for PEO-based

electrolytes. Little is known, however, about the specific interaction that results in the disruption of crystallinity in these complexes. Additional examples of salt-plasticized complexes may be even more promising as electrolytes, and may help to clarify the underlying reasons for this phenomenon and lead to the rational design of additional plasticizers.

We here demonstrate, by thermal and electrical measurements, the plasticizing action of a novel pentafluorothiomethane sulfonate salt, $\text{LiSO}_3\text{CF}_2\text{SF}_3$. At appropriate stoichiometries, PEO complexes are produced that show a marked reduction in crystallinity and correspondingly high ionic conductivity near ambient temperature.

2.3 Experimental.

The synthesis of $\text{LiSO}_3\text{CF}_2\text{SF}_3$ from perfluorovinyl sulfur pentafluoride ($\text{SF}_3\text{CF}=\text{CF}_2$) and sulfur trioxide has been reported [6] and will be described in detail elsewhere [7]. The polymer-salt complexes were subsequently prepared by co-dissolution of the desired stoichiometry of salt and PEO (Aldrich, molecular weight = 5×10^6 D) in acetonitrile. To assure that no residual water or solvent remained in the samples, the complexes were again thoroughly dried under vacuum at 80 °C, and thereafter maintained under an inert atmosphere. Stoichiometries are indicated as $\text{PEO}_x\text{LiSO}_3\text{CF}_2\text{SF}_3$, where x (16, 8, 4, or 2) reflects the mole ratio of etheric oxygen to Li.

Bulk ionic conductivities were measured between -40 °C and 100 °C on ½ inch diameter pressed pellets (approx. thickness = 1 mm). A Solartron 1260 impedance

analyzer and heater/refrigerator under computer control were employed for impedance measurements. Pellets were first annealed at 100 °C for several hours, quenched to -40 °C, then equilibrated for 90 minutes at each temperature. The hysteresis of sample measurements under heating/cooling cycles was minimal, and does not effect the observed trends. Thermal analyses were recorded using a Shimadzu DSC-50, with 15 - 25 mg samples loaded into hermetically-sealed aluminum pans under inert atmosphere. Samples were melted at 100 °C and then quenched to -100 °C prior to data collection. Thermal transitions were recorded at 10 °C / min between -100 °C and 100 °C.

2.4 Results and Discussion.

The thermal stability of $\text{MSO}_3\text{CF}_2\text{SF}_3$ salts up to 250 - 300 °C has been determined: [8] the Li analog is stable up to approximately 280 °C under an inert atmosphere [7]. As with the imide and methide salts, the high thermal stability is significant because it allows for complete dehydration and removal of residual free acid impurity by heating *in vacuo* well above 100 °C. Infrared spectra of dried powder were free of absorption peaks in the -OH (s) region.

Arrhenius plots of conductivity data for the $\text{PEO}_x\text{LiSO}_3\text{CF}_2\text{SF}_3$ complexes are shown in *Figure 2.1*. The thermal effect on conductivity for $x = 16, 8$, and 4 is similar above 50 °C, with conductivities highest at lower salt concentration. The highest salt concentration studied, the 2:1 complex, shows a lower conductivity in this region and throughout the temperatures examined. This result is common for polymer electrolytes,

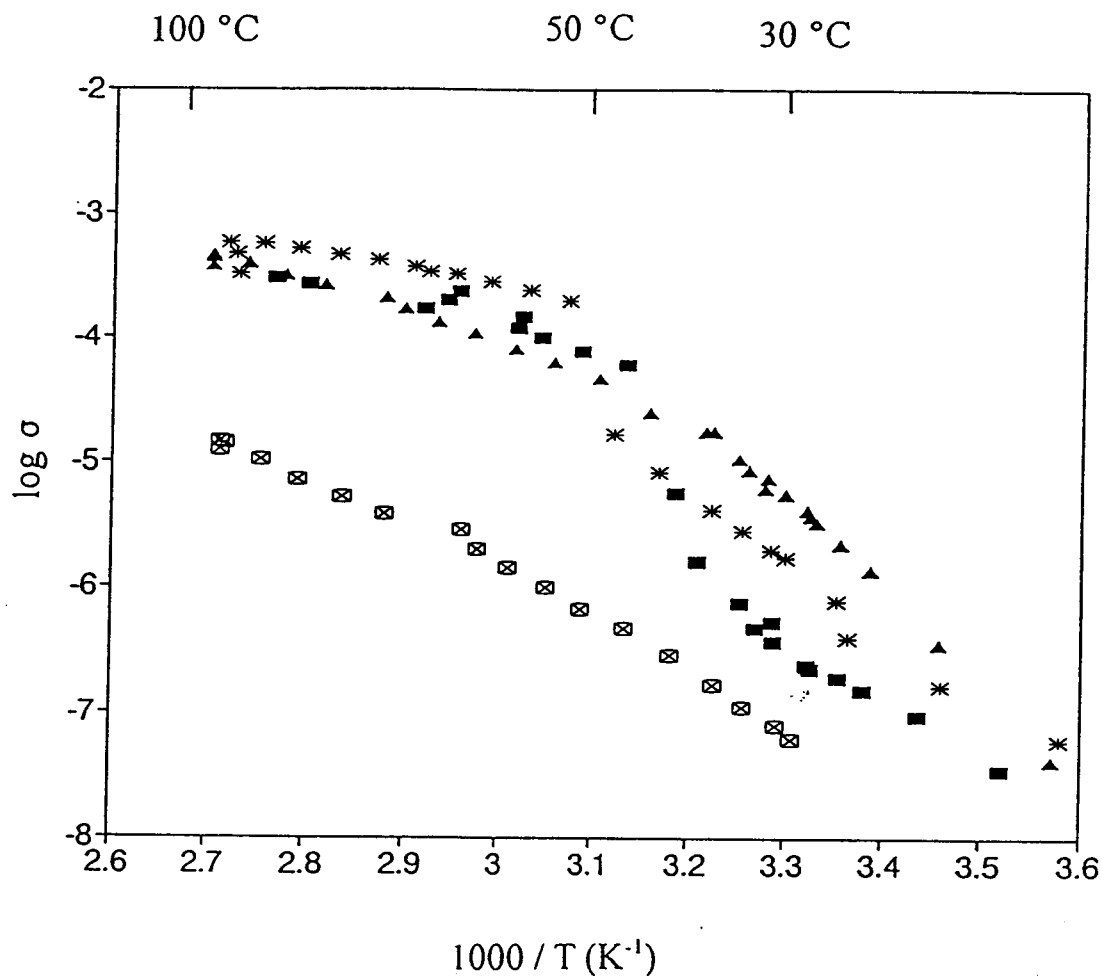


Figure 2.1 Arrhenius plots of impedance data for $PEO_xLiSO_3CF_2SF_6$, between -40 and 100 °C; (*) $x = 16$, (■) $x = 8$, (▲) $x = 4$, and (⊠) $x = 2$.

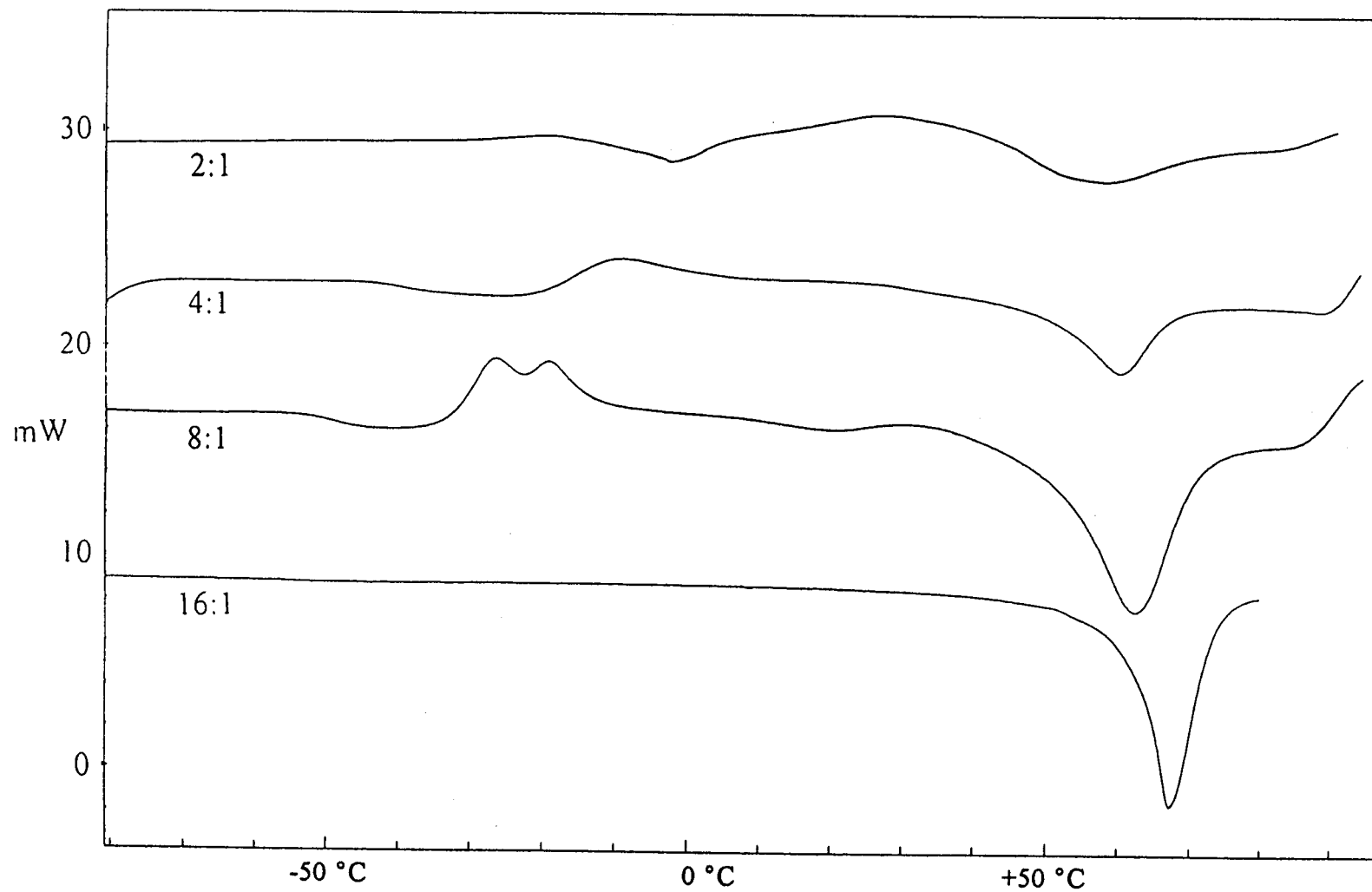


Figure 2.2 Differential scanning calorimetry traces for PEO_xLiSO₃CF₂SF₃ complexes. Samples were run at 10 °C / min under an inert atmosphere.

Table 2.1: Thermal data for PEO_xLiSO₃CF₂SF₅ complexes

x	T _m / °C	T _g / °C	ΔH _m (J / g)
16	67	-52	-78
8	62	-47	-60
4	60	-35	-21
2	58	~-10	-16

and has been ascribed to either (1) ion aggregation, which decreases the number of charge carriers and their mobility, or (2) an increase in the glass transition of the complexes due to strong polymer - ion interactions. The ionic conductivity in amorphous polymer - salt complexes has been described by the Vogel-Tamman-Fulcher relation:

$$\sigma = (A / T^{\frac{1}{2}}) \exp(-B / (T - T_o)) \quad (1)$$

where B is a pseudo-activation energy term and T_o is related to the glass transition temperature. The slopes of the plots obtained above 50 °C do increase slightly with salt concentration, which can therefore be related to an increase in either B or T_o . The thermal data below do indicate that glass transitions increase significantly at higher salt content. The large difference in the magnitude of conductivity for $x = 2$, however, suggests that ion aggregation is the principle cause of the lower conductivity in this complex.

Below 50 °C, there is a significant change in the electrical response of the complexes. A sharp decrease in conductivity is observed for the complexes with $x = 16$ and 8, with an onset at approximately 50 °C and 45 °C, respectively. The complexes with $x = 4$ and 2 do not show this break, and the 4:1 complex show a correspondingly higher conductivity in this temperature range. At 30 °C, the conductivity of this complex is approximately $10^{-5} \text{ S cm}^{-1}$, about 150 times greater than for the 16:1 complex.

Thermal evaluation of the complexes (*Figure 2.2 and Table 2.1*) show that the melting endotherm is significantly reduced at higher salt concentrations, and shifts towards lower temperature. These results coincide with the conductivity data and confirm the

plasticizing effect of the salt. As with other polymer-salt complexes, and increase in glass transition temperature at higher salt content is indicated by the tabulated data, and should partially account for the ordering of conductivities above the melting transition.

The plasticizing effect of $\text{LiSO}_3\text{CF}_2\text{SF}_5$ appears to lie in a reduction, but not complete elimination, of the crystallinity of the complexes obtained. This is different from the imide salt, which is reported to completely suppress crystallization when $x > 6$ [4]. Apart from the thermal data presented here and elsewhere for the imide salt, visible inspection of these complexes make clear this difference. Unlike the translucent imide complexes, the scattering of microcrystallites in $\text{PEO}_x\text{LiSO}_3\text{CF}_2\text{SF}_5$ complexes results in an opaque material.

The origin of the plasticizing effect for this salt and the others remains uncertain, and the limited number of examples do not yet allow for a definitive statement. A starting point lies in finding the common features of these anions. The known plasticizing salts all contain relatively large and highly stable anions that contain strong electron-withdrawing substituents. Several studies on SF_5 -containing compounds, including ^{13}C NMR data [9], dipole moments and ionization constants [10], and isotope exchange rates [11] indicate that the electronegativity of SF_5 exceeds that of CF_3 . The high stability of these anions leads to a degree of dissociation of these anions in polar solvents. The large size of all these anions is notable (and a desired by-product is that this should increase the transport number for Li^+). The possibility that the crystallization of these complexes is simply slowed by the low rate of anionic diffusion is unlikely. We have monitored the conductivity of the 4:1 complex for 30 days at ambient temperature and found that a

change of only 0.2 log units, indicating that the crystalline content has not increased significantly. Long-term studies on the imide salt also show little change in crystallinity after one month [12]. On the other hand, larger anions such as $\text{CF}_3(\text{CF}_2)_7\text{SO}_3^-$ can quickly form crystalline complexes under similar conditions.

The relative flexibility and low symmetry of the imide anion, and associated potential for disordered arrangement, may also limit crystallization. The difference in flexibility and symmetry between trifluoromethanesulfonate (which forms highly crystalline complexes) and pentafluorothiomesanesulfonate (dubbed the SF_5 -triflate anion) is not large, but might be sufficient to cause increased disorder. The structures obtained in recent diffraction studies on $\text{PEO}_3\text{LiSO}_3\text{CF}_3$ indicate that the triflate anions orient around the helical polymer chains and direct the chain packing. The shape and nature of these anions (SF_5 -triflate, imide, methide, ect.) should effect the manner and regularity of the packing of the helicies and thereby play a significant role in lattice stability [13].

A third commonality in plasticizing salts had been the unusual environment of the central atom. The N or C in imide or methide are coordinatively unsaturated and stabilized by bonding to highly electronegative groups (which for the methide requires a sterically-demanding coordination). In this regard, the SF_5 -triflate anion, does not appear similar. The carbon is formally saturated and in an environment more similar to that in trifluoromethanesulfonate than in the methide anion.

2.5 References

1. *Polymer Electrolyte Reviews* - 1; J. MacCallum, and C. Vincent, Eds; Elsevier: New York, (1987).
2. M. Armand, W. Gorecki, and R. Andreani, *Proc. of 2nd Int. Symp. on Polymer Electrolytes*, B. Scrosati, Ed. Elsevier: London, 1989, pp. 99-105.
3. L. Dominey, V. Koch, and T. Blacley, *Electrochim. Acta*, **37**, 1551 (1992).
4. D. Benrabah, D. Baril, J. Sanchez, M. Armand, and G. Gard, *J. Chem. Soc. Far. Trans.*, **89**, 355 (1992).
5. D. Benrabah, J. Sanchez, D. Deroo, and M. Armand, *Sol. St. Ionics*, **70/71**, 157 (1994).
6. N. Hamel, S. Ullrich, G. Gard, R. Nafshun, Z. Zhang, and M. Lerner, 207th Natl. ACS meeting, San Diego, ACS symp., 1994.
7. G. Gard, N. Hamel, and P. Nixon, to be submitted.
8. G. Gard, A. Waterfeld, R. Mews, J. Mahtasham, and R. Winter, *Inorg. Chem.*, **29**, 4588 (1990).
9. J. Canselier, J. Boyer, V. Castro, D. Peyton, J. Mohtasham, F. Behr, and G. Gard, *Magn. Res. in Chem.*, in press.
10. W. Sheppard, *J. Am. Chem. Soc.*, **84**, 3072 (1962).
11. R. Banks, M. Barlow, R. Haszeldine, and W. Morton, *J. C. S. Perkin Trans.*, **1**, 1266 (1974).
12. A. Vallee, S. Besner, and J. Prud'homme, *Electrochim. Acta*, **37**, 1579 (1992).
13. P. Lightfoot, M. Mahta, and P. Bruce, *Science*, **262**, 883 (1993).

Chapter 3
Lithium Salts of SF₆, alkylsulfonic Acids: Synthesis, Characterization, and Conductivity

Richard L. Nafshun and Michael M. Lerner*

*Department of Chemistry and Center for
Advanced Materials Research
Oregon State University
Corvallis, Oregon 97331-4003, USA*

Nicolas N. Hamel, Paul G. Nixon, and Gary L. Gard*

*Department of Chemistry
Portland State University
Portland, OR 97207*

3.1 Abstract.

The lithium sulfonates, $\text{SF}_3\text{CFHSO}_3\text{Li}$ (1) and $\text{SF}_3\text{CF}_2\text{SO}_3\text{Li}$ (2), were prepared by reaction of the corresponding sulfonyl fluorides $\text{SF}_3\text{CFXSO}_2\text{F}$ ($\text{X} = \text{H}$ or F) with lithium hydroxide. The product identities were confirmed by IR, NMR, MS, and elemental analysis and thermal stabilities determined via DSC and TGA. The poly(ethylene oxide) - salt complexes, $\text{PEO}_x\text{LiSO}_3\text{CFHSF}_3$ (3), were prepared for $x = 2$ to 16 (where $x = \text{O} / \text{Li}$ mole ratio) and bulk conductivities measured between 40 and 120 °C. Unlike the $\text{PEO}_x\text{LiSO}_3\text{CF}_2\text{SF}_3$ (4) complexes, thermal and conductivity measurements do not indicate a plasticizing effect for these complexes; these observations are discussed in terms of hydrogen bonding between $\text{SF}_3\text{CFHSO}_3^-$ anions.

3.2 Introduction.

A number of poly(ethylene oxide) (PEO) - salt complexes that exhibit electrochemical stability and high ionic conductivity have been investigated for use as solid polymer electrolytes (SPE's) in solid state electrochemical cells. Ionic conductivity through SPE's is known to occur by means of an amorphous component of the polymer - salt complex [1]. Enhanced conductivity at ambient temperatures in polymer - salt complexes can be achieved by the inclusion of plasticizers that suppress crystallinity at or above the operating temperature. Several compounds, $\text{LiN}(\text{SO}_2\text{CF}_3)_2$, $\text{LiC}(\text{SO}_2\text{CF}_3)_3$, and $\text{SF}_3\text{CF}_2\text{SO}_3\text{Li}$ have been found to suppress crystallinity in PEO - salt complexes and exhibit ionic conductivities exceeding $10^{-4} \text{ S cm}^{-1}$ at or below 80°C [2-6]. New plasticizing compounds such as the lithium salt of the dianion $[(\text{CF}_3\text{SO}_2)_2\text{CR}]\text{C}_6\text{H}_4^{2-}$, where $\text{R} = \text{CO}$ or SO_2 , have also shown suppressed crystallinity and high ionic conductivity when complexed with PEO to form SPE's [7].

This paper reports on the synthesis and characterization of two new lithium salts that potentially, when complexed with PEO, would be excellent candidates as solid state ion conductors; previously the conductivity of complexes containing $\text{SF}_3\text{CF}_2\text{SO}_3\text{Li}$ was published [6]. The pentafluorosulfur containing lithium sulfonates, $\text{SF}_3\text{CFHSO}_3\text{Li}$ (1), and $\text{SF}_3\text{CF}_2\text{SO}_3\text{Li}$ (2), were synthesized by the reaction of the corresponding sulfonyl fluorides, $\text{SF}_3\text{CFXSO}_2\text{F}$ ($\text{X} = \text{H}$ and F), with lithium hydroxide. In this work the conductivity of PEO - salt complexes of 1 were determined and these results are compared to the PEO - salt complexes of 2 [6].

3.3 Experimental.

3.3.1 Materials

The sulfonyl fluorides, $\text{SF}_3\text{CFHSO}_2\text{F}$ and $\text{SF}_3\text{CF}_2\text{SO}_2\text{F}$ were prepared according to literature methods [9]. Methanol (Aldrich) was distilled to use. Lithium hydroxide monohydrate (reagent grade; Matheson, Coleman and Bell) was used as received. PEO ($M_w = 5 \times 10^6$) was obtained from Aldrich Chemical Company. Acetonitrile (reagent grade) was obtained from Mallinckrodt Chemical Company.

3.3.2 General Methods

NMR spectra were recorded with a Varian EM-390 spectrometer operating at 90 MHz for ^1H samples and 84.67 MHz for ^{19}F analyses, and with a Bruker AMX-400 spectrometer operating at 100.6 MHz for ^{13}C analyses; $(\text{CH}_3)_4\text{Si}$ and CFCl_3 were used as reference standards. IR spectra were obtained between potassium bromide plates using a Nicolet 20-DX spectrometer. Mass spectra were recorded with a Finnigan MAT 8230 system operating at 30 eV. Elemental analysis were determined by Beller Mikroanalytisches Laboratorium, Göttingen, Germany. A Mel-Temp melting point apparatus was used to determine melting points; these values were reported without correction.

Differential scanning calorimetry (DSC) was performed with 20 - 25 mg samples loaded in hermetically-sealed Al pans in a Shimadzu DSC-50. Samples were heated to 150 °C, quenched below -100 °C, then heated at 10 °C / min from -100 °C to 150 °C. Thermal gravimetric analyses (TGA) utilized a Shimadzu TGA-50. Salt samples (15 - 20 mg) were loaded into a Pt pan, and heated from 30 °C to 450 °C at 10 °C / min under N₂ flow (50 mL / min).

3.3.3 Synthesis of SF₅CFHSO₃Li (1)

To a 100 mL three-necked flask containing a Teflon stirring bar and fitted with an additional funnel, a reflux condenser and a thermometer, 40 mL of anhydrous methanol and 1.84 g (43.9 mmol) of LiOH•H₂O were added. The flask was cooled in an ice bath and 4.58 g (18.9 mmol) of SF₅CFHSO₂F was added with stirring at such a rate that the temperature was maintained below 20 °C. The turbid mixture was stirred at room temperature for 16 h, then heated to reflux for 4 h. The mixture was cooled in an ice bath and filtered to remove the precipitate. The solvent was removed under vacuum from the filtrate to give 4.48 g of crude product. The crude product was dissolved in THF and filtered followed by removal of residual THF under vacuum. The resulting paste was titrated with hexane and dried under vacuum for 2 d to give 4.12 g (16.7 mmol) of product for a yield of 88%; m.p. 295 °C sintering, 315 °C darkening.

The infrared spectrum of (1) exhibited the following bands (cm^{-1}): 3001 (vw); 1321 (s); 1296 (vs); 1228 (vs); 1135 (m); 1083 (m); 917 (sh); 881 (sh); 857 (vs); 828 (m); 732 (m); 678 (w); 646 (m); 603 (m); 567 (w).

^1H NMR (CD_3CN , $(\text{CH}_3)_4\text{Si}$ ext.): 615 ppm (d, p, $J_{\text{H-F}(\text{eq})} = 5.6$ Hz).

^{19}F NMR (CD_3CN , CFCl_3 ext.): (AB4), $\phi_A = 75.0$ ppm (9 lines, rel. int. = 1.0); $\phi_B = 51.8$ ppm (d, m, rel. int. = 4.0); $J_{AB} = 153.8$ Hz. $\text{CFH} = -155.5$ ppm (d, m, rel. int. = 1.1); $J_{\text{F-H}} = 44.1$ Hz.

^{13}C NMR (CD_3CH , $(\text{CH}_3)_4\text{Si}$ int.): 115.1 ppm (d, d, p); $J_{\text{C-F}} = 267.3$ Hz, $J_{\text{C-H}} = 178.7$ Hz, $J_{\text{C-F}(\text{eq})} = 17.2$ Hz.

Analysis: Calc. for $\text{CHF}_6\text{S}_2\text{O}_3\text{Li}$: C, 4.48; H, 0.41; F, 46.3; S, 26.06%. Found: C, 5.03; H, 0.53; F, 45.5; S, 26.74%.

3.3.4 Preparation of $\text{PEO}_x\text{LiSO}_3\text{CFHSF}_5$ (3)

$\text{LiSO}_3\text{CFHSF}_5$ was thoroughly dried under vacuum at 120°C for 48 h to remove residual water or solvent. (PEO) - salt complexes were prepared by co-dissolution of the desired stoichiometry of salt and PEO in acetonitrile. Complexes were dried *in vacuo* for 48 h and maintained under inert atmosphere. Stoichiometries are described by $\text{PEO}_x\text{LiSO}_3\text{CFHSF}_5$, where x reflects the mole ratio of $\text{C}_2\text{H}_4\text{O}$ to Li.

3.3.5 Characterization of $\text{PEO}_x\text{LiSO}_3\text{CFHSF}_5$ (3)

Bulk ionic conductivities were measured on ½ inch pressed pellets of the complexes in a hermetically-sealed cell using a Solartron 1260 impedance analyzer. Samples were heated to 100 °C and then quenched below -30 °C prior to data collection. Responses were measured from 10 MHz to 0.1 Hz between -30 °C and 100 °C. Bulk conductivities were derived from the high-frequency touchdown of Nyquist plots and the known cell geometry.

3.3.6 Synthesis of $\text{SF}_5\text{CF}_2\text{SO}_3\text{Li}$ (2)

To a 100 mL three-necked flask containing a Teflon stirring bar and fitted with an additional funnel, and a reflux condenser, 40 mL of water and 1.13 g (26.9 mmol) of $\text{LiOH}\cdot\text{H}_2\text{O}$ were added. Over a 20 min period 3.49 g (13.4 mmol) of $\text{SF}_5\text{CF}_2\text{SO}_2\text{F}$ was added with stirring. The mixture was heated at reflux for 2 d until the lower phase was no longer present. The cloudy solution was then heated to reflux at 100 °C for 4 h, cooled, and filtered. The solvent was removed by rotary evaporation; drying *in vacuo* for 10 days gave 1.72 g (6.5 mmol) of product for a yield of 49%; m.p. 270 °C sintering, stable to greater than 350 °C.

The infrared spectrum of (2) exhibited the following bands (cm^{-1}): 1310 (vs); 1246 (vs); 1194 (s); 1140 (s); 1088 (s); 967 (w); 905 (sh); 880 (vs); 840 (vs); 676 (m); 628 (w); 597 (m); 574 (w); 542 (w).

^{19}F NMR (CD_3CN , CFCl_3 ext.): (AB4), $\phi_A = 68.4$ ppm (9 lines, rel. int. = 1.0); $\phi_B = 45.0$ ppm (d, m, rel. int. = 4.1); $J_{AB} = 149.6$ Hz. $\text{CF}_2 = -88.7$ ppm (d, p, rel. int. = 1.9); $J_{\text{F-F(ax)}} = 4.9$ Hz, $J_{\text{F-F(eq)}} = 14.1$ Hz

^{13}C NMR (CD_3CN , $(\text{CH}_3)_4\text{Si}$ int.): 124.2 ppm (t, p); $J_{\text{C-F}} = 334.2$ Hz, $J_{\text{C-F(eq)}} = 21.4$ Hz.

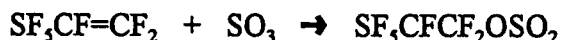
MS (m/z): FAB-; 785 ($2\text{M} \cdot \text{SF}_5\text{CF}_2\text{SO}_3$), 547 ($2\text{M} \cdot \text{F}$), 521 ($\text{SF}_5\text{CF}_2\text{SO}_3$) 2Li , 283 ($\text{M} \cdot \text{F}$), 264 (M), 257 ($\text{SF}_5\text{CF}_2\text{SO}_3$), 149 (CF_3SO_3), 130 (CF_2SO_3), 127 (SF_5), 80 (SO_3).

Analysis: Calc. for $\text{CF}_7\text{S}_2\text{O}_3\text{Li} \cdot \text{H}_2\text{O}$: C, 4.26; H, 0.71; F, 47.1; S, 22.73%. Found: C, 4.31; H, 0.55; F, 46.3; S, 23.6%.

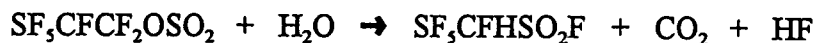
3.4 Results and Discussion.

The SF_5 -fluoroalkyl sulfonate salts, $\text{SF}_5\text{CFXSO}_3\text{Li}$ (X = H or F) were prepared by the following steps:

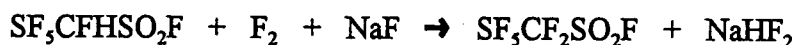
i) reacting perfluorovinyl sulfur pentafluoride, $\text{SF}_5\text{CF}=\text{CF}_2$, with distilled sulfur trioxide. The reaction is carried out in a modified Carius tube under pressure and with mild heating (up to 110 °C) to produce $\text{SF}_5\text{CFCF}_2\text{OSO}_2$ [8,9].



ii) reacting the β -sultone with water at temperatures between 45 - 60 °C to produce $\text{SF}_5\text{CFHSO}_2\text{F}$ [9].



iii) fluorinating $\text{SF}_3\text{CFHSO}_2\text{F}$ to produce $\text{SF}_3\text{CF}_2\text{SO}_2\text{F}$.



The subsequent reaction of the two sulfonyl fluorides, $\text{SF}_3\text{CFHSO}_2\text{F}$ and $\text{SF}_3\text{CF}_2\text{SO}_2\text{F}$, with lithium hydroxide resulted in the corresponding lithium sulfonates 1 and 2.



(1) $\text{X} = \text{H}$

(2) $\text{X} = \text{F}$

The resulting lithium salts were white powdery compounds, thermally stable well above 100 °C. DSC/TGA data (Figures 3.1 and 3.2) indicate main decomposition events at ~310 °C and 270 °C for salts 1 and 2 respectively, and confirm the absence of water (which is evident as a mass loss below 100 °C in the TGA data for samples exposed briefly to air).

The lithium sulfonates were characterized by infrared spectroscopy as well as ^1H , ^{13}C , and ^{19}F NMR spectroscopy. The IR spectrum contained the characteristic S-F stretch of the SF_3 group at 857 and 880 cm^{-1} , respectively for 1 and 2. One of the S-F deformation modes occurs at 597 cm^{-1} for 2 and at 602 cm^{-1} for 1; similar values for SF_3CFH - and SF_3CF_2 -containing sulfonyl fluorides, sulfonate salts, and sulfonic acids have

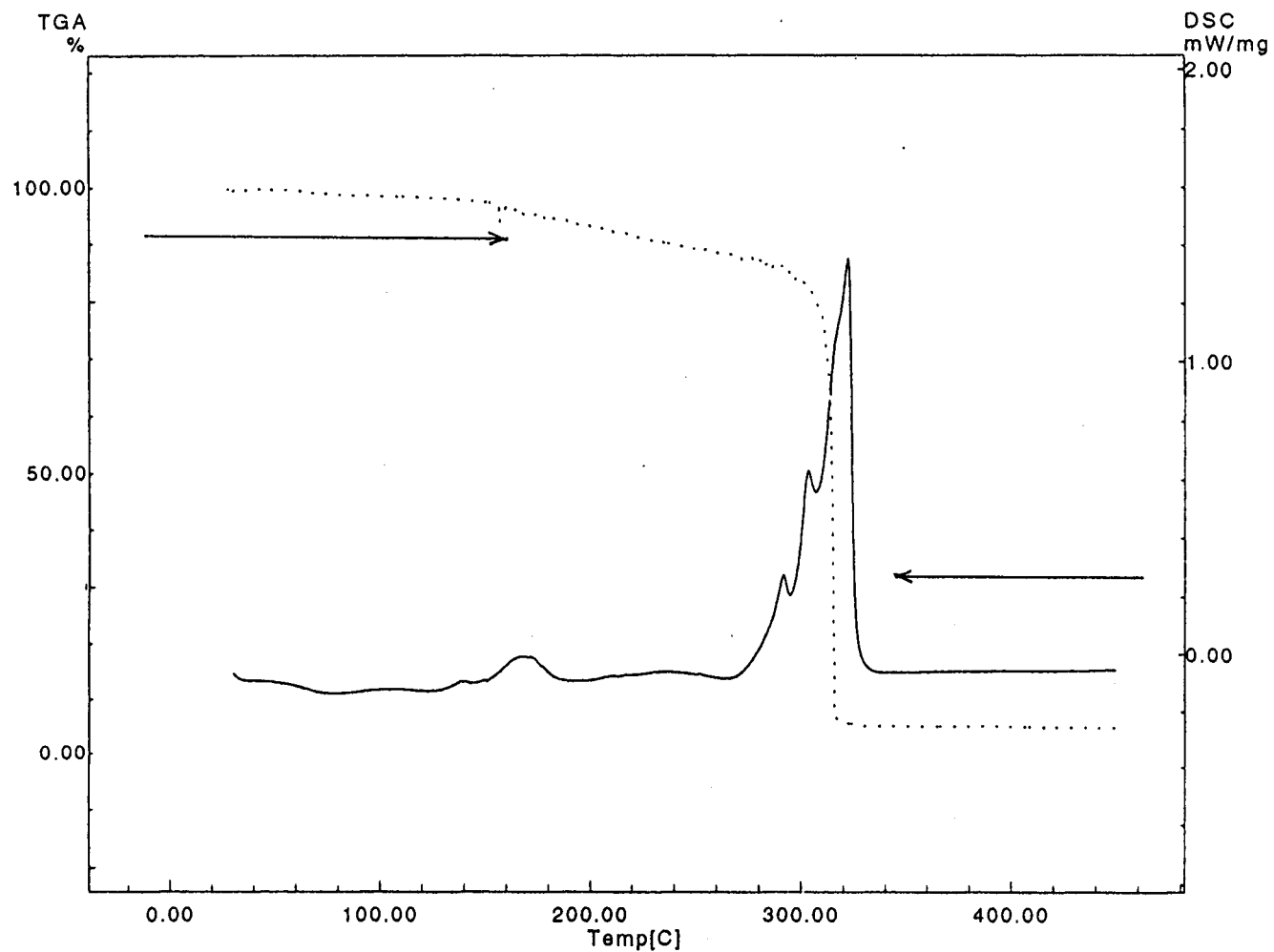


Figure 3.1 DSC and TGA traces for $\text{LiSO}_3\text{CHFSF}_5$

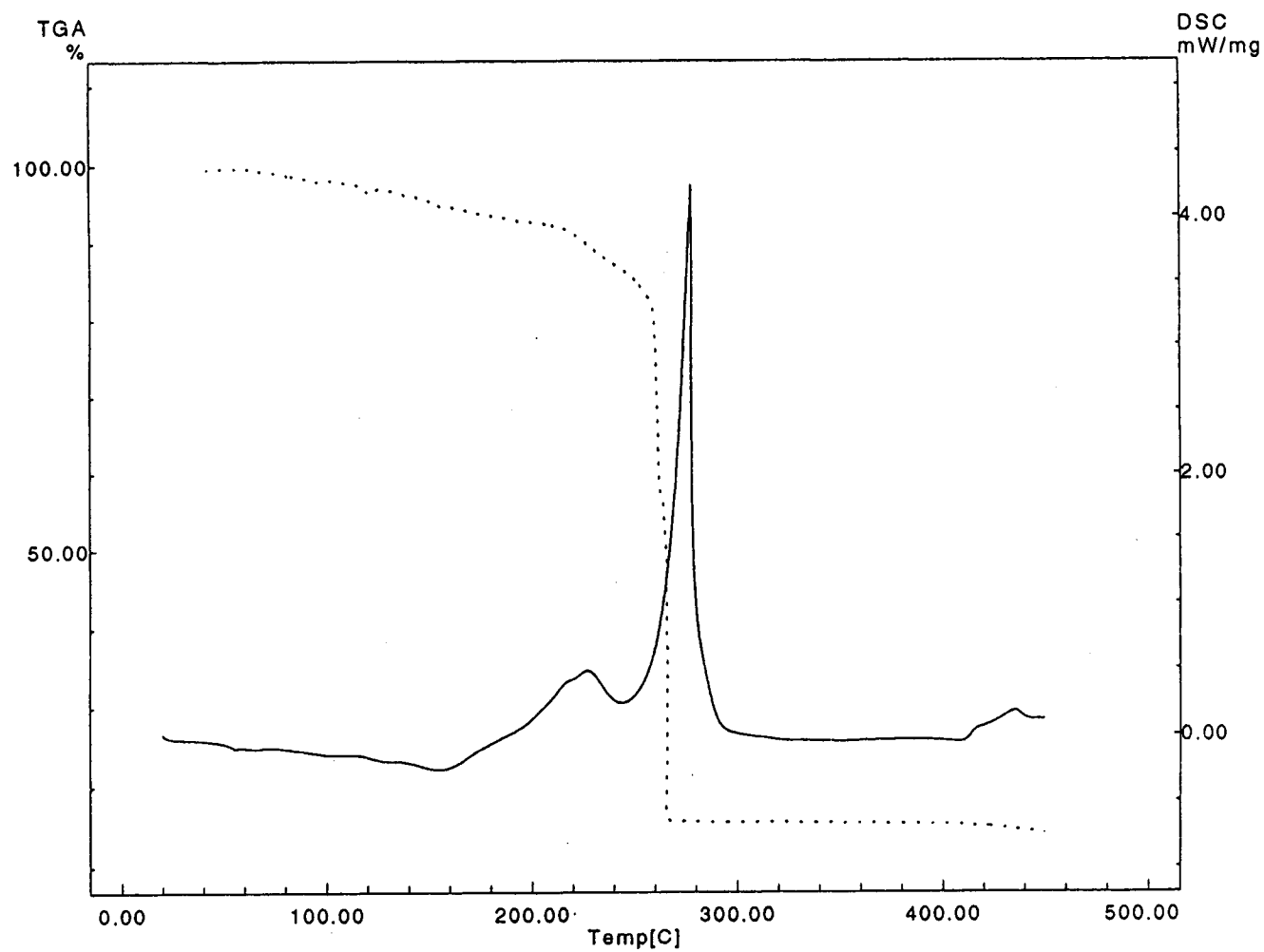


Figure 3.2 DSC and TGA traces for $\text{LiSO}_3\text{CF}_2\text{SF}_6$

been reported and range from 832 - 914 cm^{-1} (S-F stretch) and 586 - 598 cm^{-1} (S-F deformation) [10,11]. The asymmetric and symmetric S=O stretching modes appear at 1310 and 1088 cm^{-1} for **2** and at 1296 and 1083 cm^{-1} for both compounds. These absorption bands agree well with reported values [10].

The ^1H NMR spectrum of **1** consists of the CH chemical shift at 6.15 ppm ($J_{\text{H-F(eq)}} = 5.6$ Hz), this value is indicative of an acidic methine proton. Other systems containing a methine proton with similar chemical shifts include: $\text{F}_5\text{SCH}(\text{SO}_2\text{F})\text{C}(\text{O})\text{OCH}_3$ (6.26 ppm), $\text{F}_5\text{SCH}(\text{SO}_2\text{F})\text{C}(\text{O})\text{OCH}(\text{CH}_3)_2$ (6.4 ppm), and $\text{F}_5\text{SCH}(\text{SO}_2\text{F})\text{C}(\text{O})\text{OC}(\text{CH}_3)_3$ (5.88 ppm) [12-14]. The acidic nature of the methine proton in $\text{F}_5\text{SCH}(\text{SO}_2\text{F})\text{C}(\text{O})\text{OR}$ (where R = CH_3 and $\text{CH}(\text{CH}_3)_2$) has also been demonstrated by forming the corresponding salts with NH_3 and $\text{N}(\text{CH}_2\text{CH}_3)_3$ [15].

The ^{19}F NMR spectra of both **1** and **2** show an AB_4 pattern for the SF_5 grouping. For the AB_4 patterns of the SF_5 grouping in **1** and **2** the equatorial fluorine resonances were observed as doublets and the axial fluorine resonances as a nine-line pattern of multiplets. Both compounds exhibit fine structure in the AB_4 pattern due to second-order effects. The ^{19}F NMR chemical shifts for equatorial and axial fluorines in the SF_5 grouping occurs at 51.8 and 75.0 ppm, respectively, for compound **1** and at 45.0 and 68.4 ppm respectively for compound **2**. Increased shielding of the SF_5 equatorial and axial fluorines upon replacement of hydrogen by fluorine on the adjacent carbon is observed.

Compounds of similar structure, $\text{SF}_5\text{CX}_2\text{SO}_2\text{F}$ and $(\text{SF}_5\text{CX}_2\text{SO}_3)_2\text{Ca}$ where X = H and/or F, show a similar progression of increased shielding of the fluorines in the SF_5 grouping [10,11]. The CF resonance for **1** occurs as a doublet of multiplets ($J_{\text{F-H}} = 44.1$ Hz) at -

155.5 ppm. Compound **2** exhibits CF_2 resonance as a doublet of pentets ($J_{\text{F-F(ax)}} = 4.9$ and $J_{\text{F-F(eq)}} = 14.1$ Hz) at -88.7 ppm.

Chemical shifts in the ^{13}C NMR spectra of **1** and **2** occur at 115.1 and 124.2 ppm, respectively, these chemical shifts agree well with reported values for other SF_5 -fluoroalkyl sulfonate acids/salts [10,16]. The coupling constants $J_{\text{C-F}}$ and $J_{\text{C-F(eq)}}$ found for **1** are 267.3 and 17.2 Hz, respectively. The coupling constant $J_{\text{C-H}}$ for compound **1** was found to be 178.7 Hz. Compound **2** exhibited coupling constants $J_{\text{C-F}}$ and $J_{\text{C-F(eq)}}$ of 334.2 and 21.4 Hz, respectively.

Two strong endotherms are observed (Figure 3.3) for the complexes of $\text{PEO}_x\text{LiSO}_3\text{CFHSF}_5$ (**3**), at 50 - 70 °C and ~0 °C, with the lower temperature event observed principally with $x = 8$ to 3. The appearance of a second, lower endotherm at higher salt contents has also been seen in other PEO - based complexes [4]. The Arrhenius plot (Figure 3.4) for **3** indicate that bulk ionic conductivities are similar to those of other PEO - based electrolytes [17], and are less than $10^{-7} \text{ S cm}^{-1}$ at ambient temperature for all prepared stoichiometries. Breaks in the Arrhenius curves for the 16:1 and 8:1 complexes at ~70 °C and ~50 °C, respectively, are consistent with the phase transitions recorded at these temperatures: impedances were too large to obtain data near 0 °C for these complexes.

The calorimetric and thermal data for **3** stand in marked contrast to those obtained for PEO - complexes prepared from salt **2**. In the latter series of complexes, a plasticizing effect is observed by following the following facts: (i) the exotherm at 50 °C - 70 °C is

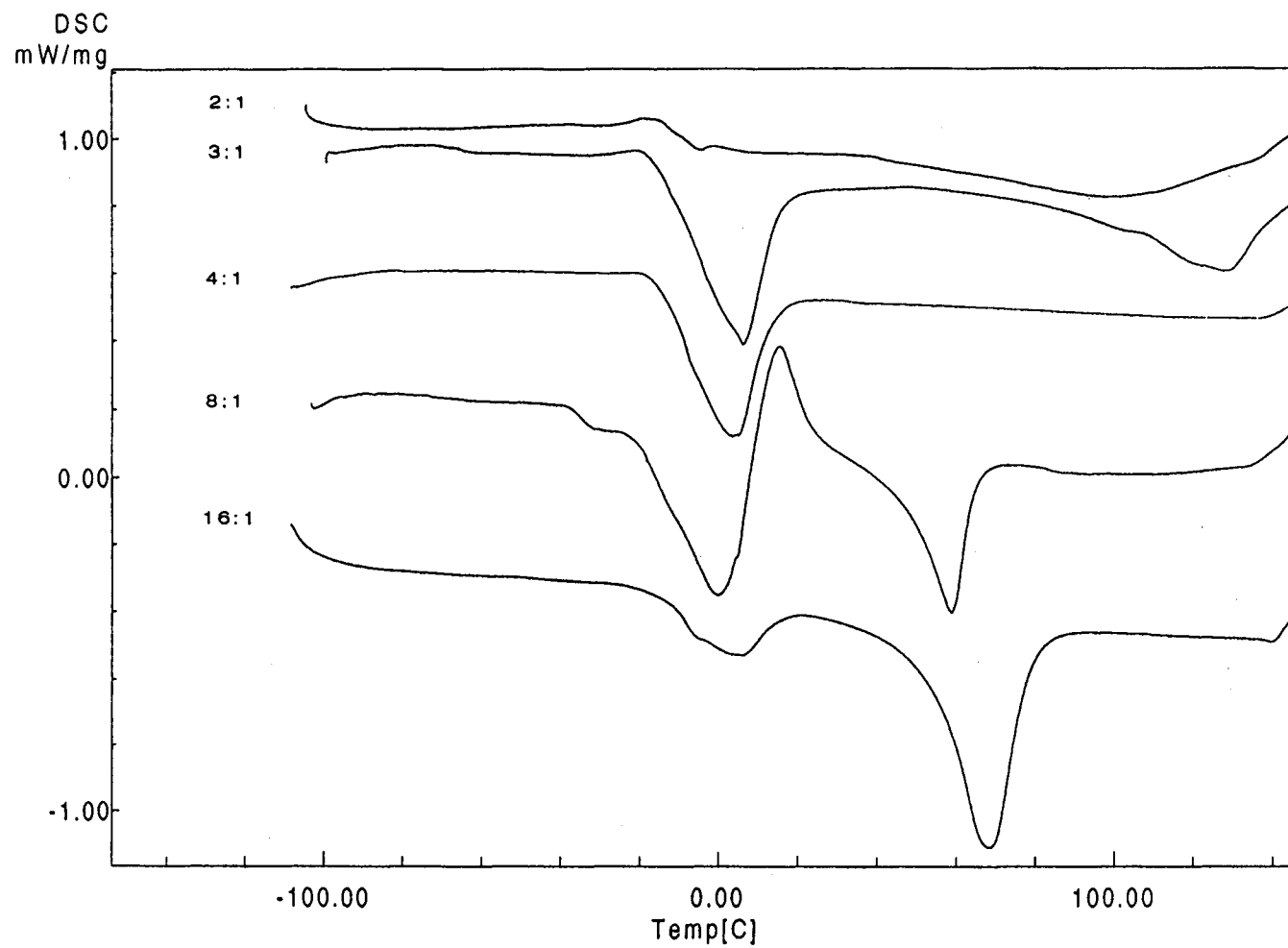


Figure 3.3 DSC traces for PEO_xLiSO₃CHFSF₆ complexes

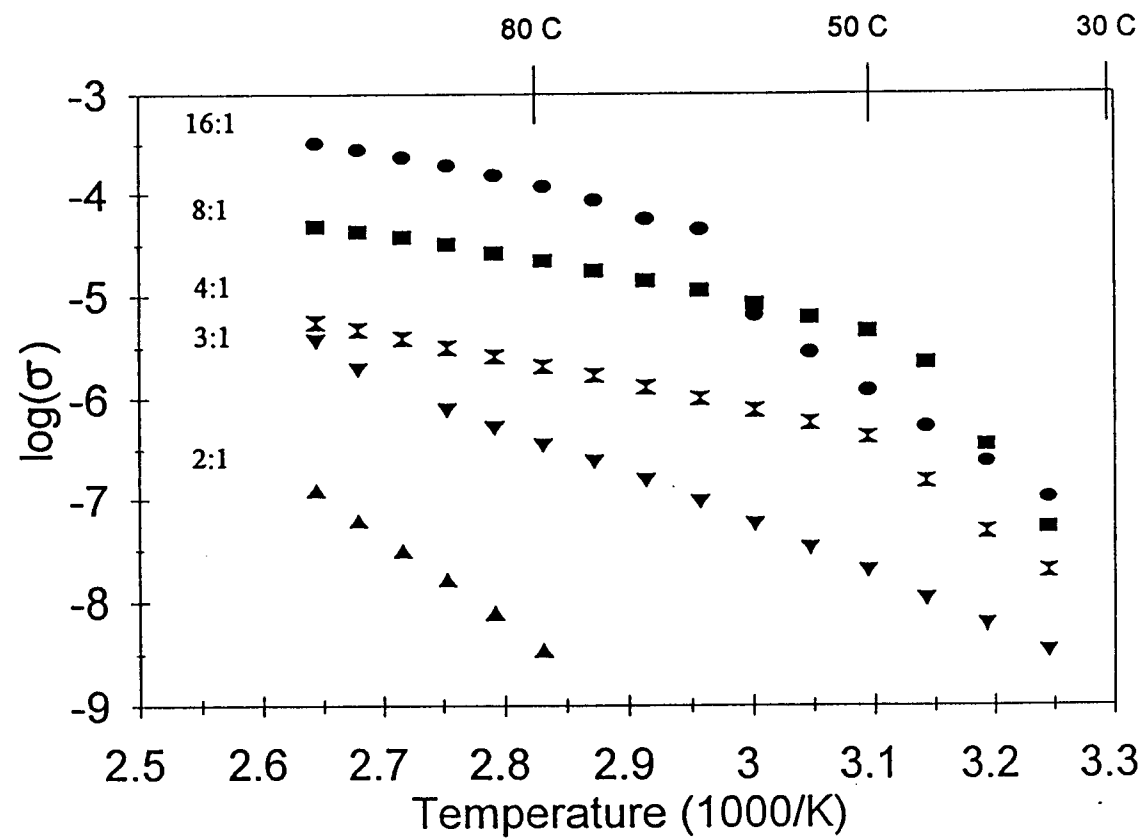


Figure 3.4 Arrhenius plots for PEO_xLiSO₃CHFSF₅ complexes

greatly diminished, but no significant new endotherms arise with increasing salt content, and (ii) high ionic conductivities ($>10^{-5}$ S cm $^{-1}$) can be obtained at ambient temperature. Both of these sets of data are reproducible, and the thermal and impedance data are consistent, yet it is surprising that such closely related salts can display very different behavior in the PEO matrix. The change is related to the formation of a crystalline phase at ~ 0 °C at appropriate stoichiometries for complexes of PEO with salt 1 but not with salt 2.

A model to explain these observations must focus on the different chemistry of the two anions. In particular, it appears that the anion 1 is capable of hydrogen bonding. Evidence for this includes the proton chemical shift and the reactivity of similar compounds with bases. In these complexes, it seems likely that hydrogen bonding would arise between the methine acidic proton and other sulfonate groups.

The role of hydrogen bonding in directing the crystallization of a polymer - salt complex is not understood--it may be conjectured that the assembly and ordering of [PEO $_x$ Li $^+$] helical units, observed in structural studies on similar complexes [18], is facilitated by hydrogen bonding between the anions.

3.5 Acknowledgments.

M.M.L. acknowledges the supporting grant (DMR-9157005) from the National Science Foundation.

3.6 References

1. J. MacCallum and C. Vincent (eds.), *Polymer Electrolyte Reviews - 1*, Elsevier, New York, 1987.
2. M. Armand, W. Gorecki, and R. Andreani, in B. Scrosati (ed.), *Proc. of 2nd Int. Symp. on Polymer Electrolytes*, Elsevier, London, 1989, pp. 99-105.
3. L. Dominey, V. Koch, and T. Blacley, *Electrochim. Acta*, **37**, 1551 (1992).
4. D. Benrabah, D. Baril, J. Sanchez, M. Armand, and G. Gard, *J. Chem. Soc. Far. Trans.*, **89**, 355 (1992).
5. A. Vallee, S. Besner, and J. Prud'homme, *Electrochim. Acta*, **37**, 1579 (1992).
6. R. Nafshun, M. Lerner, N. Hamel, P. Nixon, and G. Gard, *J. Electrochem. Soc.*, **142**, L153 (1995).
7. D. Benrabah, J. Sanchez, D. Deroo, and M. Armand, *Sol. St. Ionics*, **70/71**, 157 (1994).
8. J. Mohtasham, R. Terjeson, and G. Gard in *Inorganic Syntheses: Volume 29*, R. Grimes (ed.), John Wiley & Sons, Inc; New York, 1992, pp. 33-38.
9. J. Canich, M. Ludvig, G. Gard, and J. Shreeve, *Inorg. Chem.*, **23**, 4403 (1984).
10. G. Gard, A. Waterfeld, R. Mews, J. Mohtasham, and R. Winter, *Inorg. Chem.*, **29**, 4588 (1990).
11. (a) W. Shepard, *J. Amer. Chem. Soc.*, **62**, 3072 (1962). (b) J. Thrasher, J. Nielson, S. Bott, D. McClure, S. Morris, and J. Atwood, *Inorg. Chem.*, **27**, 570 (1988). (c) G. Gard, and C. Woolf, *J. Fluorine Chem.*, **1**, 487 (1971/1972). (d) J. Canich, M. Luvig, W. Paudler, G. Gard, and J. Shreeve, *Inorg. Chem.*, **24**, 3668 (1985). (e) J. Hansen, and P. Savu, U.S. Patent 5, 159, 105 (1992).
12. R. Winter, and G. Gard, *Inorg. Chem.*, **29**, 2386 (1990).
13. R. Winter, and G. Gard, *Inorg. Chem.*, **27**, 4329 (1988).
14. R. Winter, and G. Gard, *J. Fluorine Chem.*, **52**, 57 (1991).

15. R. Winter, G. Gard, R. Mews, and M. Notlemeyer, *J. Fluorine Chem.*, **60**, 109 (1993).
16. J. Canselier, J. Boyer, V. Castro, G. Gard, J. Mohtasham, D. Peyton, and F. Behr, *Magn. Reson. Chem.*, **33**, 506 (1995).
17. M. Armand in *Polymer Electrolyte Reviews - 1*, Elsevier, New York, 1987.
18. P. Lightfoot, M. Mehta, and P. Bruce, *Science*, **262**, 883 (1993).

Chapter 4
Lithium Salts of Bis(Perfluoroalkyl)sulfonic Acids: Synthesis, Characterization and Conductivity Studies

Richard L. Nafshun and Michael M. Lerner*

*Department of Chemistry and Center for
Advanced Materials Research
Oregon State University
Corvallis, Oregon 97331-4003, USA*

Steven A. Ullrich and Gary L. Gard*

*Department of Chemistry
Portland State University
Portland, Oregon 97207, USA*

4.1 Abstract.

Lithium salts of bis(perfluoroalkyl)sulfonic acids, $(\text{CF}_2)_n(\text{SO}_2\text{OLi})_2 \cdot w\text{H}_2\text{O}$, where $n = 1-4$ (1-4), w = the number of waters of hydration, and $\text{O}(\text{CF}_2\text{CF}_2\text{SO}_2\text{OLi})_2$, **5**, were prepared by double decomposition and ion exchange methods. Infrared, NMR, and mass spectral data support the assigned structures. Thermal measurements indicate that these salts can be prepared free of acid and water impurities; the salts are stable up to 224°C for the smallest anion, and above 400°C for the largest anion. Impedance analyses were used to provide the bulk ionic conductivities of some poly(ethylene oxide) - salt complexes. Of these salts, **5** was found to have the highest conductivity: σ is about $5 \times 10^{-6} (\Omega \text{ cm})^{-1}$ at 100°C .

4.2 Introduction.

High interest in rechargeable solid state lithium batteries [1] has led to a search for lithium salts that will serve as lithium charge carriers in the polymer electrolyte portion of such batteries.

Bannister, Ward, Davies, and McIntyre have recommended that the dilithium salts of perfluoroalkyl disulfonic acids might be good candidates for high conductivity in polymer electrolyte work [2]. These salts contain large anions and bear a 2^- charge; they can be expected to diffuse more slowly than the triflate ion, resulting in a decrease in the anionic current and thereby limiting the extent of irreversible polarization in PEO-salt electrolytes. Also, Li ion transport numbers for highly-conducting polymer electrolytes are generally less than 0.5, so there is much room for improvement in this area. In general, however, the high lattice stabilization energies of simple salts of type Li_2An or Li_3An will result in limited solubility or insolubility in polyethers. Another concern is the lesser oxidative stability of some highly charged anions. The bis-sulfonate salts, however, should be oxidatively robust and relatively soluble in polyethers due to a low charge/volume ratio.

The following salts $\text{LiO}_3\text{S}(\text{CF}_2)_n\text{SO}_3\text{Li} \cdot w\text{H}_2\text{O}$, where $n = 1, 2, 3, 4$ and the ether salt $\text{O}(\text{CF}_2\text{CF}_2\text{SO}_3\text{Li})_2$ were prepared and characterized. All compounds, except $\text{CF}_2(\text{SO}_3\text{Li})_2 \cdot 3/2\text{H}_2\text{O}$, were then tested for conductivity in poly(ethylene oxide), PEO, at a ratio of 8 oxygens from the PEO to one lithium from the salt; the ether salt was further tested at ratios of 16:1, 32:1, and 64:1.

4.3 Experimental.

4.3.1 Materials

The following chemicals were obtained from the 3M Company: $[\text{CF}_2(\text{SO}_2\text{O})_2]\text{Ba}$, $(\text{CF}_2\text{SO}_2\text{OK})_2$, $\text{CF}_2(\text{CF}_2\text{SO}_2\text{OK})_2$, $[(\text{CF}_2\text{CF}_2\text{SO}_2\text{O})_2]\text{Ca}$, and $[\text{O}(\text{CF}_2\text{CF}_2\text{SO}_2\text{O})_2]\text{Ca}$. These samples were used without further purification. The $\text{LiOH}\cdot\text{H}_2\text{O}$ was obtained from Matheson, Coleman and Bell. The $\text{Li}_2\text{SO}_4\cdot\text{H}_2\text{O}$ and acetonitrile came from Mallinckrodt Chemical Company. The Amberlite IR-120 polystyrene sulfonate ion exchange resin was a Rohm and Haas product. The poly(ethylene oxide) used to make the polymer - salt complexes came from Aldrich Chemical Company ($M_w = 5 \times 10^6$).

4.3.2 General Procedures

A Nicolet 20-DX spectrometer was used to obtain infrared spectra. Solid samples were pelletized with KBr for analysis.

Nuclear magnetic resonance spectra were obtained from two instruments. A Varian EM-390 spectrometer was used at 84.7 Mhz for some of the ^{19}F NMR analyses. A Bruker AMX-400 instrument operating at 376.5 Mhz for ^{19}F samples and at 100.6 Mhz for ^{13}C samples was used for the rest of the NMR work. A D_2O lock was used instead of an internal standard because these compounds are appreciably soluble in water. Downfield is taken as the positive direction for the reporting of fluorine resonance values.

A Mel-Temp melting point apparatus served for the determination of decomposition points for the salts; these decomposition points were reported without correction. A Vacuum Atmospheres Corporation Dri-Lab HE-43-2 was used for the manipulation of moisture sensitive materials. Nitrogen gas, dried under heated molecular sieve, was used as the dry box atmosphere. Moisture was kept below 10 ppm, the point at which titanium tetrachloride begins to fume in moist air [3].

The mass spectrometric work was accomplished using either a Varian MAT CH5 or a Finnigan MAT 8230 system operating at 70 eV. The fast atom bombardment technique was employed in both positive and negative modes; samples were dissolved in glycerin prior to analysis. These analyses were performed at the Institute for Inorganic and Physical Chemistry at the University of Bremen, in Bremen, Germany.

Elemental analyses were performed by Beller Microanalytical Laboratory in Göttingen, Germany.

Differential scanning calorimetry was performed with 20 - 25 mg samples loaded in hermetically-sealed Al pans in the Shimadzu DSC-50. Salt samples were heated at 10 °C / min from 30 °C to 750 °C. Thermogravimetric analyses utilized the Shimadzu TGA-50. Salt samples (15 - 20 mg) were loaded into a Pt pan, and heated from 30 °C to 750 °C at 10 °C / min under N₂ flow (50 mL / min).

4.3.3 Synthesis of $\text{CF}_2(\text{SO}_2\text{OLi})_2 \cdot 3/2\text{H}_2\text{O}$ (1)

A 7.78 g (0.0224 moles) sample of $\text{Ba}[(\text{OSO}_2\text{C}_2\text{F}_5)_2]$ was digested with 2.85 g (0.0223 moles) $\text{Li}_2\text{SO}_4 \cdot \text{H}_2\text{O}$ in 650 mL of water. The resulting mixture was allowed to digest for four days, then filtered through an ASTM 10-15M fritted glass filter. The cloudy filtrate became clear on further filtration using Whatman #42 filter paper. The solution was then concentrated through evaporation on a rotary evaporator to a small volume, and dried in the frozen state under vacuum. Weight of product: 4.29 g; yield: 76.3 %. This sample started to turn gray at 224 °C.

The infrared spectrum showed bands (cm^{-1}) at 3522 (w), 3473 (w), 1631 (w), 1497 (w), 1434 (w), 1286 (st,shldr), 1265 (st), 1223 (st), 1117 (w), 1085 (w), 1072 (m), 1055 (w), 1039 (m), 955 (w), 938 (w), 711 (w, shldr), 698 (m), 620 (w,shldr), 610 (st), 568 (w), 545 (w). MS (m/z) (FAB)⁺: 455 ($2\text{M} \cdot \text{Li}$)⁺, 323 ($\text{M} \cdot \text{C}_3\text{H}_8\text{O}_3 \cdot \text{Li}$)⁺, 231 ($\text{M} \cdot \text{Li}$)⁺, 201 $\text{SO}_2\text{CF}_2\text{SO}_2\text{OLi}^+$, 111 CFSO_3^+ , 33 CH_2F^+ , 31 CF^+ ; (FAB)⁻: 665 ($3\text{M} \cdot \text{Li}$)⁻, 469 ($2\text{M} \cdot 3\text{Li}$)⁻, 457-454 ($2\text{M} \cdot \text{Li}$)⁻, 443/441/440 ($2\text{M} \cdot \text{Li}$)⁻, 423 ($\text{M} \cdot \text{LiOSO}_2\text{CFSO}_2\text{OH}$)⁻, 311 ($\text{M} \cdot \text{SO}_3\text{Li}$)⁻, 304 ($\text{M} \cdot \text{SO}_3$)⁻, 233/231 ($\text{CF}_2(\text{SO}_3\text{H})_2 \cdot \text{F}$)⁻, 219/217/216 $\text{SO}_3\text{CF}_2\text{SO}_3\text{Li}^-$, 211 $\text{HSO}_3\text{CF}_2\text{SO}_3^-$, 199 $\text{LiOSO}_2\text{CFSO}_2\text{OH}^-$, 81 HSO_3^- . Analysis: Calc. for $\text{CF}_2(\text{SO}_3\text{Li})_2 \cdot 3/2\text{H}_2\text{O}$: C, 4.78; H, 1.20; F, 15.1%. Found: C, 5.71; H, 1.39; F, 15.2%.

4.3.4 Synthesis of $(\text{CF}_2\text{SO}_2\text{OLi})_2 \cdot 2\text{H}_2\text{O}$ (2)

An 11.31 g (0.0334 moles) sample of $(\text{KOSO}_2\text{CF}_2)_2$ was passed through two columns (140 mL total volume) of acid form Amberlite IR-120, having resin capacity 288 meq H^+ , to assure quantitative conversion to the corresponding acid. The total residence time was 2 h; the rinse with three bed volumes of water (400 mL) took 1.5 h. The effluent and rinse solution mixture was neutralized with a $\text{LiOH} \cdot \text{H}_2\text{O}$ solution until the pH was 6.4. The total solution volume was then brought to under 20 mL, and dried under vacuum. Yield: 8.47 g, or 86.5%. A previously prepared sample of the salt turned brown at 269 °C.

The infrared spectrum exhibited bands (cm^{-1}) at: 3571 (w,shldr), 3522 (w), 3409 (w,br), 1638 (w), 1427 (w), 1300 (st,shldr), 1272 (st,shldr), 1152 (st), 1137 (m,shldr), 1081 (m), 1056 (st), 845 (w), 654 (w,shldr), 626 (m), 561 (m), 526 (w). MS (m/z) $(\text{FAB})^+$: 281 $(\text{M} \cdot \text{Li})^+$, 155 $\text{CF}_2\text{CF}_2\text{SOLi}^+$, 111 CF_2SO_3^+ , 101 $\text{CF}_2\text{CF}_2\text{H}^+$, 33 CH_2F^+ , 31 CF^+ ; $(\text{FAB})^-$: 543/541/540 $(2\text{m-Li})^-$, 369/368/367 $(2\text{M-Li-CF}_2\text{CF}_2\text{SO}_3\text{H})^-$, 361 $(\text{M} \cdot \text{SO}_3\text{Li})^-$, 269-266 $(\text{M-Li})^-$, 261 $(\text{M} \cdot \text{H-2Li})^-$, 183/181 $\text{CF}_2\text{CF}_2\text{SO}_3\text{H}^-$, 177 $\text{SCF}_2\text{CF}_2\text{SO}_2^-$, 163/161 $\text{CF}_2\text{CF}_2\text{SO}_3^-$, 81 HSO_3^- , 80 SO_3^- , $\text{C}_2\text{F}_2\text{H}_2\text{O}^-$, 19 F^- . Analysis: Calc. for $(\text{CF}_2\text{SO}_3\text{Li})_2 \cdot 2\text{H}_2\text{O}$: C, 7.75; H, 1.30; F, 24.5%. Found: C, 8.36; H, 1.39; F, 24.2%.

4.3.5 Synthesis of $\text{CF}_2(\text{CF}_2\text{SO}_2\text{OLi})_2 \cdot 2\text{H}_2\text{O}$ (3)

A 4.10 g (0.0106 moles) portion of $\text{CF}_2(\text{CF}_2\text{SO}_2\text{OK})_2$ was dissolved in 60 mL of water and passed through 70 mL of acid form Amberlite IR-120 ion exchange resin having

capacity 144 meq H^+ . The column was rinsed with 200mL deionized water; residence and rinsing times together amounted to 1.5 h. A 0.92 g portion of $LiOH \cdot H_2O$ and small additions of lithium hydroxide solution were used to bring the pH of the combined solution of effluent and rinsings to 8.1. The solution was reduced in volume to less than 25mL, and freeze dried imder vacuum. The white powder weighed 3.41 g, representing a 89.7% yield. This powder turns gray at $295^\circ C$.

Infrared bands (cm^{-1}) were found at: 3592(w), 3508(w), 1638(m), 1317(st, shldr), 1305 (st, shldr), 1248(st, br), 1175(m), 1161(m), 1148(m), 1100(m), 1063(st), 1046(m,shldr), 1012 (m), 987(w), 780(w), 712(w), 666(st,br), 607(w), 584(w), 569(w), 546(w), 532(w), 482(w), 461(w). MS (m/z) (FAB) $^+$: 155 $CF_2CF_2SOLi^+$, 111 $CFSO_3^+$, 101 $CF_2CF_2H^+$, 33 CH_2F^+ , 32 CHF^+ , 31 CF^+ ; (FAB) $^-$: 643-640 (2M-Li) $^-$, 555 $(M \cdot CF_2CF_2CF_2SO_3H)^-$, 343 $(M \cdot F)^-$, 319-316 (M-Li) $^-$, 279 $OSCF_2CF_2CF_2SO_3H^-$, 233/231 $CF_2CF_2CF_2SO_3H^-$ 232/230 $CF_2CF_2CF_2SO_3^-$, 211 $CF_2CFCF_2SO_3^-$, 130 $CF_2SO_3^-$, 80 SO_3^- , $C_2F_2H_2O^-$. Analysis: Calc. for $CF_2(CF_2CO_3Li)_2 \cdot 2H_2O$: C, 10.01; H, 1.12; F, 31.7%. Found: C. 9.74; H, 0.99; F, 30.1%.

4.3.6 Synthesis Of $(CF_2CF_2SO_2OLi)_2 \cdot 3/2H_2O$ (4)

A 5.53 g portion of Ca $[(OSO_2CF_2CF_2)_2]$ (0.0139 moles) was converted into acid form by dissolving it in 60 mL of water and passing it through 70 mL of acid form Amberlite IR-120 ion exchange resin having 144 meq H^+ resin capacity. The resin was then washed with approximately 200mL of water; residence and washing together

amounted to 1.5h. The combined effluent and rinse solutions were then neutralized with $\text{LiOH}\cdot\text{H}_2\text{O}$ to give a resulting solution of pH 7.0. This solution was then reduced in volume to less than 25mL by evaporation, and freeze-dried under vacuum. a 4.83 g sample of white powder resulted, representing a yield of 95.8%. A portion of the powder turned dark when heated to 312°C .

The infrared spectrum exhibited the following bands (cm^{-1}): 3634 (w,shldr), 3501 (m), 3459 (m,br), 1666 (w,shldr), 1631 (m), 1518 (w), 1427 (w), 1270 (st), 1253 (st,shldr), 1187 (m), 1164 (m), 1124 (st), 1044 (st), 865 (w), 736, (w), 730 (w), 679 (m), 619 (m), 588 (w), 559 (w), 539 (w), 493 (w), 471 (w), MS (m/z) (FAB)⁺: 155 $\text{CF}_2\text{CF}_2\text{SOLi}^+$, 111 CF_2SO_3^+ , 100 CF_2CF_2^+ , 33 CH_2F^+ , 32 CHF^+ , 31 CF^+ ; (FAB)⁻: 741 $(2\text{M-Li})^-$, 393 $(\text{M}\cdot\text{F})^-$, 369-366 $(\text{M-L})^-$, 281 $(\text{CF}_2)_4\text{SO}_3\text{H}^-$, 280 $(\text{CF}_2)_4\text{SO}_3^-$, 263/261 $\text{C}_4\text{F}_7\text{SO}_3^-$, 161 $\text{CF}_2\text{CF}_2\text{SO}_3^-$, 131 C_3F_5^- , 80 SO_3^- , $\text{C}_2\text{F}_2\cdot\text{H}_2\text{O}^-$, 19 F^- . Analysis: Calac. for $(\text{CF}_2\text{CF}_2\text{SO}_3\text{Li})_2\cdot 3/2 \text{H}_2\text{O}$: C, 11.98; H, 0.75; F, 37.9%. Found: C, 12.37; H, 0.84; F, 37.7%.

4.3.7 Synthesis of $\text{O}(\text{CF}_2\text{CF}_2\text{SO}_2\text{OLi})_2$ (5)

A 5.00 g portion (0.0120 moles) of $\text{Ca}[(\text{OSO}_2\text{CF}_2\text{CF}_2)_2\text{O}]$ was dissolved in 20 mL of water and passed through 70 mL of acid form Amberlite IR-120 ion exchange resin having 144 meq H^+ capacity over a period of 1.5 h. The column was then washed with 200mL of water. a solution prepared from the effluent and washings was neutralized with $\text{LiOH}\cdot\text{H}_2\text{O}$ until the solution pH was 7.0. The solution of the ether salt was slowly

concentrated by evaporation at 40°C; the concentrate was then frozen, and allowed to dry under vacuum. a white powder, 2.64 g, was obtained, a yield of 60.8%.

The infrared spectrum of the product showed the following bands (cm^{-1}) : 3508 (m), 3445 (m,br,shldr), 2924 (w), 2854 (w), 1642 (m), 1346 (m,shldr), 1280 (st,shldr), 1244 (st), 1165 (st), 1085 (m), 1068 (m), 1020 (m), 973 (m), 850 (w), 749 (w), 670 (w, shldr), 655(m), 629 (w, shldr) 554 (w), 535 (w), 514 (w), 500 (w), 489 (w), 477 (w), 462 (w). MS (m/z) (FAB)⁺ : 155 $\text{CF}_2\text{CF}_2\text{SOLi}^+$, 111 CF_2SO_3^+ , 101 $\text{CF}_2\text{CF}_2\text{H}^+$, 100 CF_2CF_2^+ , 33 CH_2F^+ 31 CF^+ ; (FAB)⁻ : 773 (2M-Li)⁻, 385-382 (M-Li)⁻, 297 $\text{HOSO}_2(\text{CF}_2)_2\text{O}(\text{CF}_2)_2^-$, 296 $\text{OSO}_2(\text{CF}_2)_2\text{O}(\text{CF}_2)_2^-$, 277 $\text{CF}_2\text{CF}_2\text{O}(\text{CF}_2)_2\text{SO}_3^-$, 177 $\text{OCF}_2\text{CF}_2\text{SO}_3^-$, 161 $\text{CF}_2\text{CF}_2\text{SO}_3^-$, 117 $\text{HOCF}_2\text{CF}_2^-$, 80 SO_3^- , $\text{C}_2\text{F}_2\cdot\text{H}_2\text{O}^-$.

4.3.8 Electrochemical Analysis of Polymer Complexes

4.3.8.1 Preparation of $\text{PEO}_x(\text{LiSO}_3\text{CF}_2\text{CF}_2)_2\text{O}$

The salt was thoroughly dried under vacuum at 120°C for 48 h to remove residual water or solvents. Poly(ethylene oxide) (PEO) -salt complexes were prepared by co-dissolution of salt and PEO at the required stoichiometry in acetonitrile. Complexes were

dried *in vacuo* for 48 h and maintained under an inert atmosphere. Stoichiometries are described by $\text{PEO}_x(\text{LiSO}_3\text{CF}_2\text{CF}_2)_2\text{O}$, where x reflects the mole ratio of ethoxy repeats to Li ion.

4.3.8.2 Characterization of $\text{PEO}_x(\text{LiSO}_3\text{CF}_2\text{CF}_2)_2\text{O}$

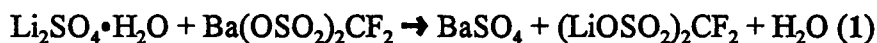
Bulk ionic conductivities were measured on 1/2" pressed pellets of the complexes in a hermetically-sealed cell using the Solartron 1260 impedance analyzer. Samples were heated to 100°C and then quenched below -30°C prior to data collection. Responses were measured from 12MHz between -30°C and 100°C. Bulk conductivities were derived from the high-frequency touchdown of Nyquist plots and known cell geometries.

4.3.8.3 Electrochemical Work With Other Salts

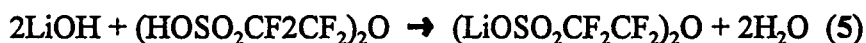
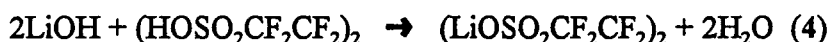
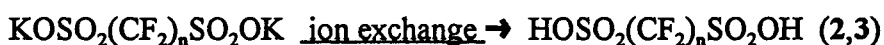
Similar procedures were used for the preparation and characterization of PEO complexes with salts 2, 3, 4.

4.4 Results and Discussion

Two methods were employed for the synthesis of the dilithium salts of the bis(perfluoroalkyl)sulfonic acids. One method involved the reaction of lithium sulfate with the barium salt of the sulfonic acid:



The other method involved the preparation of a sulfonic acid from its corresponding potassium or calcium salt by passing an aqueous solution of the corresponding salt through polystyrene sulfonic acid ion exchange resin. The acid is then neutralized using lithium hydroxide:



None of these compounds had sharp melting points; they all decomposed. An increase in the decomposition point of compounds 1 - 5 was seen: 224°C for 1, 264°C for 2, 295°C for 3, 312°C for 4, and about 450° for 5. The DSC / TGA data provided in Figure 4.1 indicate a single, sharp exothermic decomposition point for $\text{O}(\text{CF}_2\text{CF}_2\text{SO}_2\text{OLi})_2$ at approximately 450°C indicating that the sample is free from volatile impurities such as water or the free acid. The purity of the salt is significant in considering the conductivity data obtained.

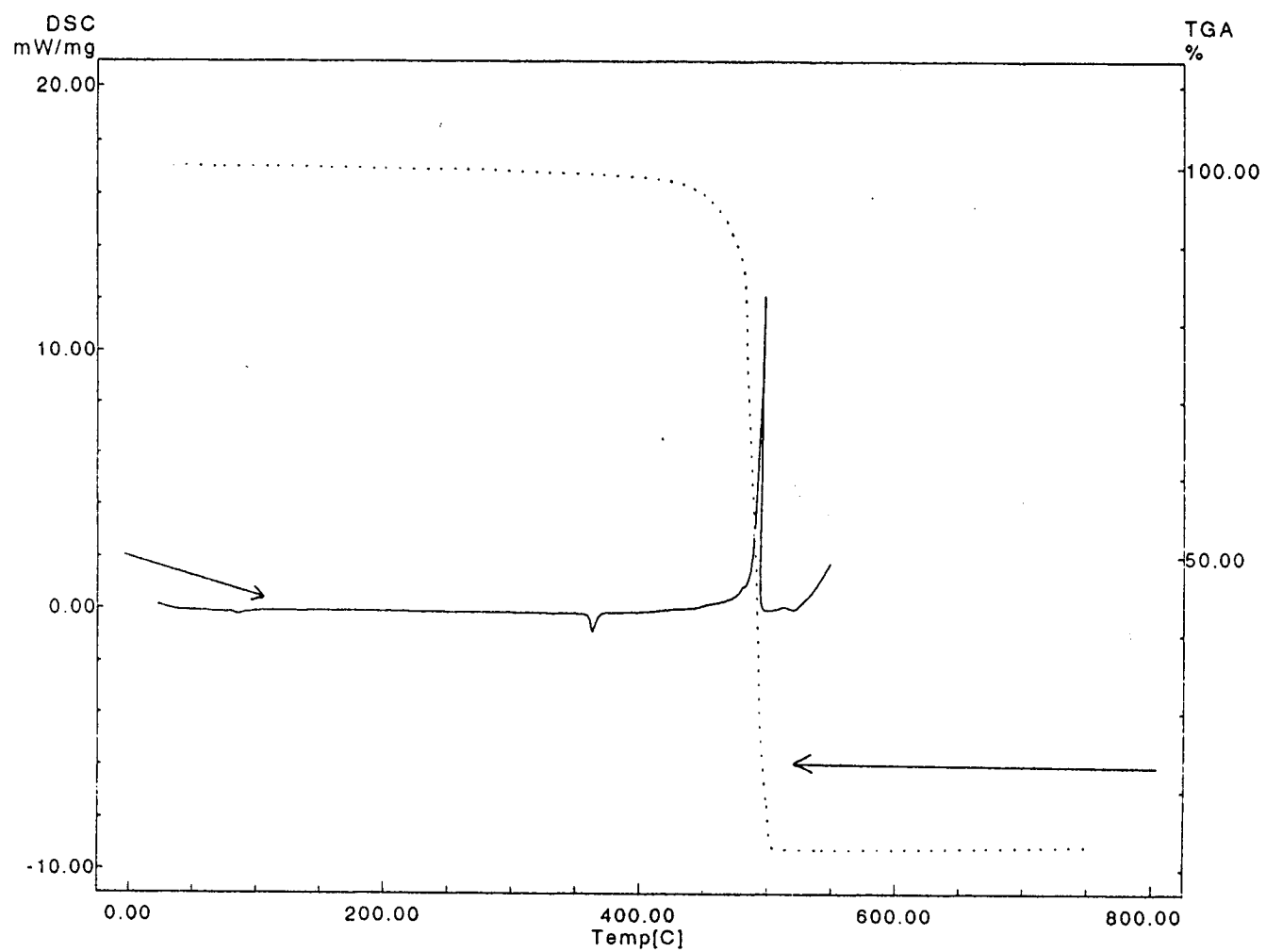


Figure 4.1: TGA and DSC traces for $\text{LiSO}_3\text{CF}_2\text{CF}_2\text{OCF}_2\text{CF}_2\text{SO}_3\text{Li}$

The interpretation of the infrared spectra of these perfluorinated sulfonic acid lithium salts is complicated by the fact that the C-F stretch of the CF_2 group ($1100 - 1300 \text{ cm}^{-1}$) [4-6] appears in the same region of the spectrum as the SO_3 symmetric ($1050 - 1100 \text{ cm}^{-1}$) and asymmetric ($1180 - 1280 \text{ cm}^{-1}$) stretches [4,7,8]. Literature values for these types of compounds would lead us to assign the symmetric SO_3 stretch for our salts to the $1044 - 1072 \text{ cm}^{-1}$ region, the asymmetric stretch to the $1244 - 1265 \text{ cm}^{-1}$ region, and the C-F stretch of CF_2 to the $1117 - 1300 \text{ cm}^{-1}$ region. The C-O-C stretch is usually found at $1060 - 1150 \text{ cm}^{-1}$ vibration for **5** was designated as a C-O-C stretch.

The fast atom bombardment (FAB) technique was applied for the analysis of our samples; it had been used to advantage before in the characterization of perfluoroalkyl sulfonates [9]. Runs producing both positive and negative ions were made.

Cluster ions, some of high molecular weight, are a feature found in FAB mass spectra of perfluoroalkyl sulfonates [10]. For our samples, some of these had high relative intensity; for **1**, negative mode gave: $(2\text{M-Li})^-$ (21.64), $(2\text{M}\bullet\text{Li})^-$ (18.66), $(2\text{M}\bullet 3\text{Li})^-$ (10.62), $(3\text{M-Li})^-$ (1.98), $(3\text{M}\bullet\text{Li})^-$ (1.38). No molecular ions were found in either the positive or negative mode runs.

The ^{19}F NMR spectra of compounds **1-4**, Table 4.1, showed CF_2 resonances that are in line with the literature values for the corresponding acids and potassium or sodium salts [11-13]. The chemical shift value for fluorines $\text{O}_3\text{SCF}_2\text{SO}_3$ is $\varphi = -107 \text{ ppm}$; the range for fluorines $\text{CF}_2\text{CF}_2\text{SO}_3$ is $\varphi = -[114.3-115.3] \text{ ppm}$; and the range for fluorines $\text{CF}_2\text{CF}_2\text{CF}_2$ is $\varphi = -[120-122] \text{ ppm}$. The resonance values for the fluorines in these

Table 4.1: ^{19}F NMR Spectra of Dilithium Perfluoroalkyl Sulfonate Salts

Compound	φ Inner Carbons ^a (ppm)	φ Outer Carbons ^b (ppm)
1		-107 (s)
2		-114.6 (s)
3	-120.3 (m)	-114.3 (m)
4	-122 (m)	-115.3 (m)
	φ CF_2S Carbons ^a (ppm)	φ CF_2O Carbons ^b (ppm)
5	-83.3 (s)	-120.0 (s)

- a. Band center of multiplets; inner carbons attached to carbon only.
 b. Band center of multiplets; outer carbons attached to sulfur.

Table 4.2: ^{13}C NMR Spectra of Dilithium Perfluoroalkyl Sulfonate Salts

Compound	ϕ Inner Carbons ^a (ppm)	ϕ Outer Carbons ^b (ppm)	$^1J_{\text{CF}}$	$^2J_{\text{CF}}$
1		119.0 (t)	310	
2		115.5 (t,t)	288	37.0
3		115.6 (t,t)	292	36.5
	112.7 (t,p)		264	32.3
4		115.2 (m)	291	34
	112.7 (t,p)		269	32
	δ CF_2S Carbons ^a (ppm)	δ CF_2O Carbons ^b (ppm)	$^1J_{\text{CF}}$	$^2J_{\text{CF}}$
5	116.4 (m)		290	31.8
		111.6	290	37.2

- a. Band center of multiplets; inner carbons attached to carbon only.
b. Band center of multiplets; outer carbons attached to sulfur.

lithium salts agree with the literature values for the corresponding acids and the corresponding potassium salts. The fluorine resonances for 1 and 2 were singlets; the resonances for 3 and 4 were unresolved multiplets, as was found to be the case for $\text{CF}_2(\text{CF}_2\text{SO}_2\text{F})_2$ [14].

In Table 4.2, the ^{13}C spectral data for compounds 1 - 5 are presented. the chemical shifts agree with the values reported for the two-, three-, and four-carbon acids and salts [12]. For 1-4, the chemical shift value for carbons CCF_2C is $\delta = 112.7$ ppm, and the range for carbons CF_2S is $\delta = 115.2 - 119$ ppm. The coupling constant range for these compounds is 264-310 Hz for $^1J_{\text{CF}}$ and 32-37 Hz for $^2J_{\text{CF}}$. A Spectrum of 5 showed multiplets for both CCF_2S and CCF_2O carbons.

Two Arrhenius plots, Figures 4.2 and 4.3, are provided to summarize the impedance data. Figure 4.2 contains Arrhenius plots of the data obtained at the stoichiometry $\text{OCH}_2\text{CH}_2 : \text{Li} :: 8 : 1$ for PEO complexes with salts 2 - 4. The response is nearly linear over the temperature range evaluated: the similar slopes of these lines indicate that the activation energies for ionic conduction are all approximately 0.15 eV for these complexes. The curvature evident upon close inspection of the data is associated with VTF behavior that arises from ion conduction through a polymeric matrix [15]. Above 75°C , the conductivities for all these complexes are 2 - 3 orders of magnitude lower than those of PEO complexes with LiCF_3SO_3 or LiClO_4 at similar stoichiometries [16]. Some part of this decrease might be ascribed to the lower diffusion rate of the larger anions, but that will not cause a change of this magnitude. The effect may arise either from changes in the extent of polymer complex crystallinity or slower polymer dynamics

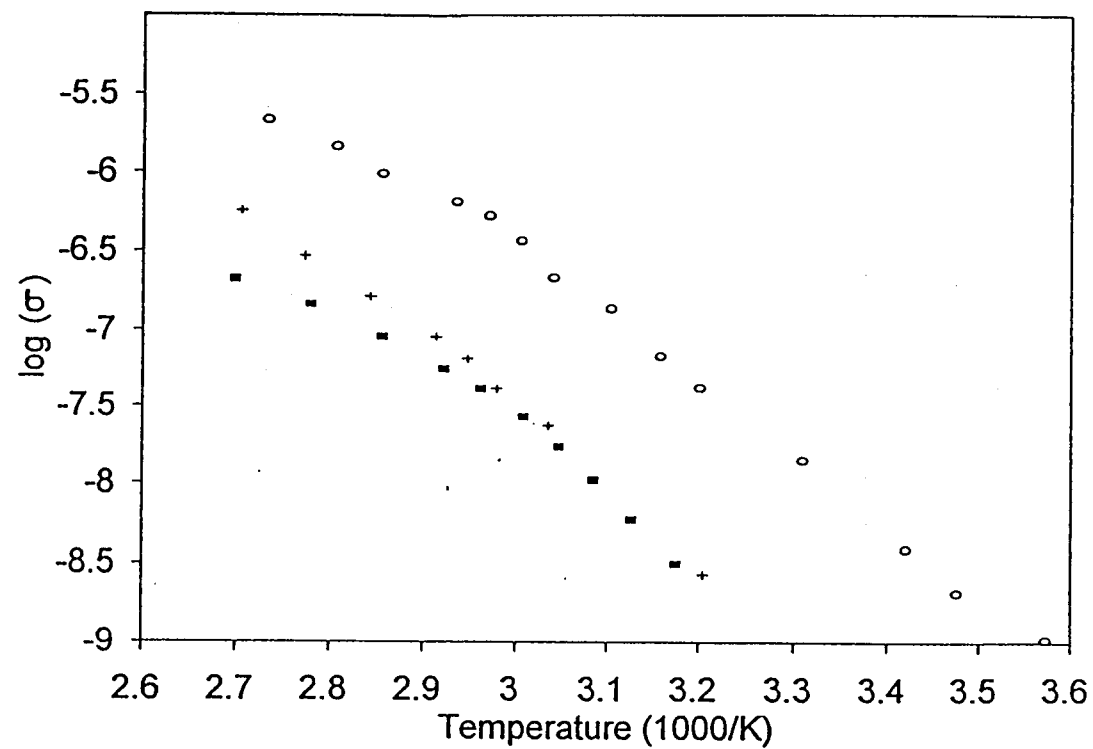


Figure 4.2: Arrhenius plots for $\text{CH}_2\text{CH}_2\text{O}:\text{Li}::8:1$ complexes of salts 2(■), 3(+), and 4(O)

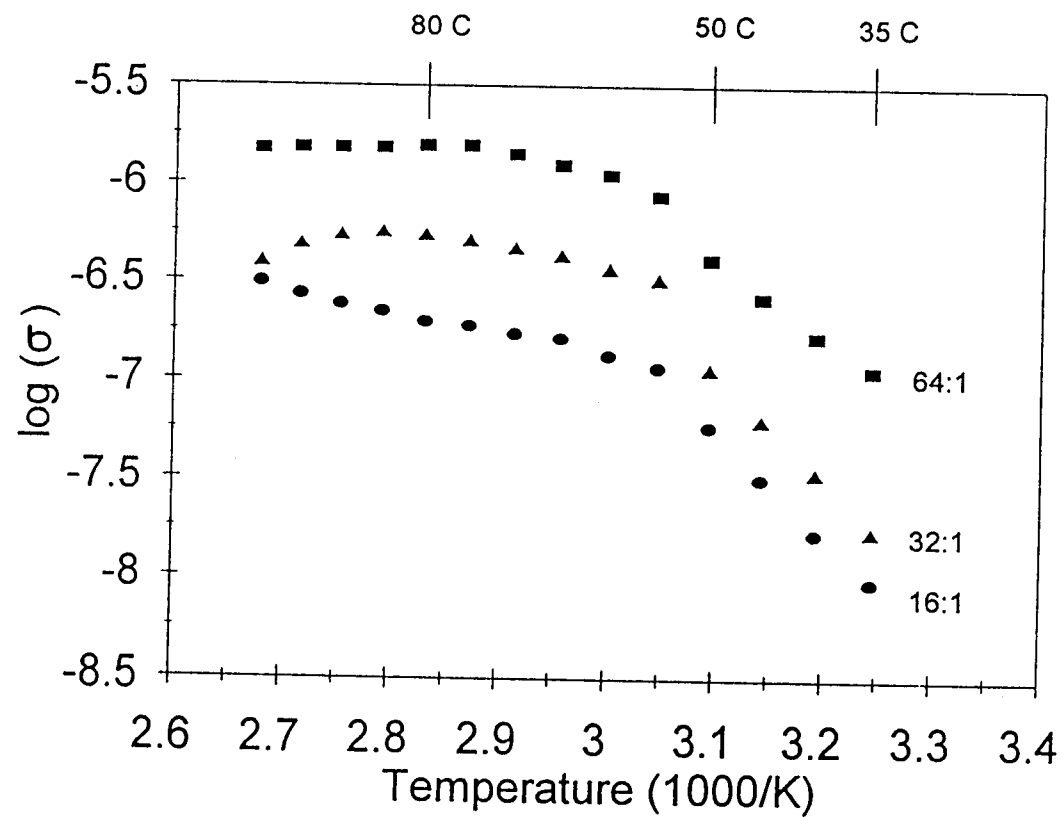


Figure 4.3: Arrhenius plots for PEO complexes with $\text{LiSO}_3\text{CF}_2\text{CF}_2\text{OCF}_2\text{CF}_2\text{SO}_3\text{Li}$ at $\text{CH}_2\text{CH}_2\text{O}:\text{Li}$ mole ratios of 64:1, 32:1, and 16:1

due to association with the more highly charged anions. The conductivity is significantly higher for complexes with 4 than for complexes with the others. Two possible explanations are the increased separation of anionic groups and corresponding decrease in anionic charge density, or a change in the solubility of the salt.

Figure 4.3 shows the effect of stoichiometry on the ionic conductivities of the PEO complexes formed with $\text{O}(\text{CF}_2\text{CF}_2\text{SO}_2\text{OLi})_2$. The conductivities decrease with salt content, and are again significantly lower than those obtained with simple salts such as LiCF_3SO_3 .

4.5 Acknowledgments.

We express our appreciation to Dr Fred Behr of the 3M Company for the gift of the perfluoroalkyl sulfonate salts that were the raw materials for this work.. MML acknowledges a supporting grant from the National Science Foundation (DMR-9322071).

4.6 References

1. B. Scrosati (ed.), Applications of Electroactive Polymers, Chapman and Hall, London, 1993.
2. D.J. Bannister, G.R. Davies, I.M. Ward, J.E. McIntyre, *Polymer Communications* **25**, 1291 (1984).
3. D.F. Shriver and M.A. Drezdson, The Manipulation of Air Sensitive Compounds, Wiley-Interscience, New York, 1986, p. 57.
4. R.J. Willenbring, J. Mohtasham, R. Winter, and G.L. Gard, *Can. J. Chem.* **67**, 2037 (1989).
5. J.K. Brown and K.J. Morgan in Advances in Fluorine Chemistry 4, M. Stacey, J.C. Tatlow, and A.G. Sharpe, (eds.), Butterworth, Washington, 1965.
6. D.G. Weiblen in Fluorine Chemistry II, J.H. Simons (ed.), Academic Press, New York, 1954.
7. R.J. Willenbring, MS Thesis, Portland State University, (1987).
8. G. Socrates, Infrared Characteristic Group Frequencies, Wiley-Interscience: Chichester, 1980.
9. P.A. Lyon, K.B. Tomer, and M.L. Gross, *Anal. Chem.* **57**, 2984 (1985).
10. D.N. Heller, C. Fenselau, J. Yergey, R.J. Cotter, and D. Larkin, *Anal. Chem.* **56**, 2274 (1984).
11. H. Saffarian, P. Ross, F. Behr, and G. Gard, *J. Electrochem. Soc.* **139**, 2391 (1992).
12. R. Herkelmann and P. Sartori, *J. Fluorine. Chem.* **44**, 299 (1989).
13. W. Cen, Z.-X. Dong, T.-J. Huang, D. Su, and J.M. Schreeve, *Inorg. Chem.* **27**, 1376 (1988).
14. E. Hollitzer and P. Sartori, *J. Fluorine Chem.* **35**, 329 (1987).
15. Dale Braden, private communication

16. J. Mohtasham, G. Gard, Portland State University, J. Canselier, Ecole Nationale Supérieure D'Ingenieurs de Genie Chimique, "¹³C NMR Studies of Fluorosultones and Fluorosulfonic Acids", 46th Regional ACS Meeting, La Grande, Oregon, June 1991.
17. M. Ratner, and D. Shriver, *Chem. Rev.* **88**, 109 (1988).
18. M. Armand in Polymer Electrolyte Reviews-I, J. MacCallum, and C. Vincent (eds), Elsevier, New York, 1987.

Chapter 5
Synthesis of $\text{LiCH}(\text{SO}_2\text{CF}_3)_2$ and
Ionic Conductivity of Polyether-Salt Complexes

Richard L. Nafshun and Michael M. Lerner*

*Department of Chemistry and Center for
Advanced Materials Research
Oregon State University
Corvallis, Oregon 97331-4003, USA*

Nelson R. Holcomb, Paul G. Nixon, and Gary L. Gard*

*Department of Chemistry
Portland State University
Portland, Oregon 97207, USA*

J. Electrochem. Soc., 143, 1297 (1996)

5.1 Abstract.

$\text{LiCH}(\text{SO}_2\text{CF}_3)_2$ is prepared by reaction of $\text{CH}_2(\text{CF}_3\text{SO}_2)_2$ with Li_2CO_3 and the product identity confirmed by NMR, IR, and elemental analysis. DSC/TGA data indicate a decomposition temperature near 280 °C under N_2 . $\text{PEO}_x\text{LiCH}(\text{SO}_2\text{CF}_3)_2$ complexes show ionic conductivities as high, or higher than, those derived from other plasticizing salts, with σ near $10^{-4} (\Omega\text{cm})^{-1}$ at 30 °C and $10^{-3} (\Omega\text{cm})^{-1}$ at 80 °C for the $x = 16$ complex. DSC data indicate that the polymer-salt complexes exhibit reduced crystallinity at ambient temperature and show minor crystalline phases at higher salt concentrations. Glass transition temperatures increase with salt content for the complexes. Cyclic voltammetry shows an electrolyte stability window of approximately 4.5 V.

5.2 Introduction.

A number of poly(ethylene oxide) (PEO) - salt complexes are known to be electrochemically stable and exhibit high ionic conductivities, and have therefore been studied for use as solid polymer electrolytes (SPE's) in all-solid-state electrochemical cells.[1-3] Most of these complexes are crystalline, and therefore poor ion conductors near ambient temperature; unfortunately, the addition of liquid plasticizers to improve ionic conductivity can degrade electrolyte performance. In the past 5 years, it has been established that lithium bis-(trifluoromethanesulfonyl)imide, $\text{LiN}(\text{SO}_2\text{CF}_3)_2$ (the "imide" salt), and lithium tris-(trifluoromethanesulfonyl)methide, $\text{LiC}(\text{SO}_2\text{CF}_3)_3$ (the "methide" salt), form complexes with suppressed crystallinities, and consequently higher ionic conductivities, below 80 °C.[4-7] Most recently, interest in ambient temperature SPE's has proceeded along several lines, including studies of (1) new plasticizing anions such as $(\text{CF}_3\text{SO}_2)_2\text{CR}] \text{C}_6\text{H}_4^{2-}$, $\text{R} = \text{CO}$ or SO_2 [8] and $\text{LiSO}_3\text{CF}_2\text{SF}_5$ [9]; (2) plasticizing mixed-salt complexes; [7,10], and (3) "salt-in-polymer" electrolytes.[11]

One disadvantage of the "imide" and "methide" and other plasticizing salts lies in the difficulty of preparation. Previous reports indicate that bis(trifluoromethylsulfonyl)methane, $\text{CH}_2(\text{CF}_3\text{SO}_2)_2$, can be simply converted to alkali-metal salts, $\text{MCH}(\text{CF}_3\text{SO}_2)_2$ in aqueous solution.[12] The properties of the lithium analog are of practical interest if this commercially-available acid reagent can be converted to $\text{LiCH}(\text{SO}_2\text{CF}_3)_2$ in a single step under ambient conditions. We here demonstrate that the salt can be easily prepared in this manner and shows a plasticizing effect in PEO

comparable to that obtained with the “imide” and “methide” salts. The synthesis and characterization of $\text{LiCH}(\text{SO}_2\text{CF}_3)_2$ and electrical and thermal characterization of a series of $\text{PEO}:\text{LiCH}(\text{SO}_2\text{CF}_3)_2$ complexes are examined in detail.

5.3 Experimental.

5.3.1 Preparation of $\text{LiCH}(\text{SO}_2\text{CF}_3)_2$

The acid $\text{CH}_2(\text{CF}_3\text{SO}_2)_2$ was obtained from 3M and purified by sublimation at ambient temperature prior to use. Finely ground Li_2CO_3 (Aldrich, 99.997 %) (0.094 g, 12.7 mmols) were added 34.0 ml (12.3 mmols) of a 10 % aqueous solution of $\text{CH}_2(\text{CF}_3\text{SO}_2)_2$. The reaction mixture was stirred in a 50 ml round-bottom flask containing a magnetic stir bar at room temperature for 72 h. The mixture was suction filtered and the water was removed from the supernatant liquid by rotary evaporation. The crude product was recrystallized from ethanol, then dried *in vacuo* for 24 h to obtain an 80% yield (2.82 g, 9.86 mmols) of $\text{LiCH}(\text{SO}_2\text{CF}_3)_2$.

5.3.2 Characterization of $\text{LiCH}(\text{SO}_2\text{CF}_3)_2$

For $\text{LiCH}^b(\text{SO}_2\text{CF}_3)_2$: ^{19}F NMR (CD_3CN) δ_a - 84.0 (s) ; ^1H NMR (CD_3CN) δ_b 4.1; IR 3083 (w), 1341 (s), 1318 (s), 1197 (s), 1131 (m), 1092 (m), 982 (m), 845 (w), 657 (m), 583 (m) cm^{-1} ; elemental analysis calc. for $\text{LiCH}(\text{SO}_2\text{CF}_3)_2$: C, 12.59; H, 0.35; F, 39.8. Found C, 11.44; H, 0.51; F, 38.1 %. Samples exposure to ambient air, and analyses are lower in C and F weight percent (w/o), and higher in H w/o than calculated for the anhydrous composition.

5.3.3 Preparation of $\text{PEO}_x\text{LiCH}(\text{SO}_2\text{CF}_3)_2$

$\text{LiCH}(\text{SO}_2\text{CF}_3)_2$ was thoroughly dried under vacuum at 120 °C for 48 h to remove residual water or solvents. Poly(ethylene oxide) (PEO) - salt complexes were prepared by co-dissolution of the desired stoichiometry of salt and PEO (Aldrich, $M_w = 5 \times 10^6$) in acetonitrile (Mallinckrodt, reagent). Complexes were dried *in vacuo* for 48 h and maintained under an inert atmosphere. Stoichiometries are described by $\text{PEO}_x\text{LiCH}(\text{SO}_2\text{CF}_3)_2$, where x reflects the mole ratio of $\text{C}_2\text{H}_4\text{O}$ to Li.

5.3.4 Characterization of $\text{PEO}_x\text{LiCH}(\text{SO}_2\text{CF}_3)_2$

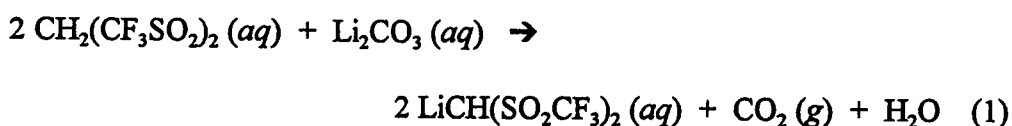
Bulk ionic conductivities were measured on 0.5 in. pressed pellets of the complexes in a hermetically-sealed cell using a Solartron 1260 impedance analyzer.

Samples were heated to 100 °C and then quenched below - 30 °C prior to data collection. Responses were measured from 12 MHz to 0.1 Hz between - 30 °C and 100 °C. Bulk conductivities were derived from the high- frequency touchdown of Nyquist plots and the known cell geometry.

A three-electrode cell configuration with Li metal reference and a thin-film electrolyte was utilized for cyclic voltammetry experiments. Experiments were performed at 20 mV / s between - 0.1 and 5.0 V. Differential scanning calorimetry (DSC) was performed with 20 to 25 mg samples loaded in hermetically-sealed Al pans in a Shimadzu DSC-50Q. Samples were heated to 100 °C, quenched below - 100 °C, then heated at 10 °C / min from - 100 °C to 120 °C. Thermogravimetric analyses (TGA) utilized a Shimadzu TGA-50. Samples (15 to 20 mg) were loaded into a Pt pan, and heated from 30 to 450 °C at 10 °C/min under N₂ flow (50 mL / min).

5.4 Results and Discussion.

The new lithium salt, LiCH(SO₂CF₃)₂, is a stable, colorless solid that is easily prepared in a one-step synthesis from commercial reagents according to the following reaction:



The ^1H and ^{19}F chemical shifts observed (4.1 and - 85.0 ppm, respectively) agree closely with those found for other alkali-metal salts.[12] For example, the potassium salt exhibits singlets in the ^1H spectrum at 3.8 ppm (D_6 -acetone) and in the ^{19}F spectrum at - 81.1 ppm (CD_3CN). The infrared spectrum has characteristic absorption bands for the CH , CF_3 and SO_2 moieties. These results also agree with the values found for other alkali-metal salts.[12]

The TGA/DSC data obtained on the salt (Figure 5.1) show a single, sharp exothermic decomposition with onset at 280 °C, the PEO complexes are stable to approx. 220 °C (Figure 5.2). These thermal stabilities are a significant advantage since high-temperature treatment facilitates the elimination of residual acid or water from the salt or polymer complexes. The salt as prepared is not acidic and does not appear to degrade PEO at ambient temperature.

Arrhenius plots of conductivity data for the series of $\text{PEO}_x\text{LiCH}(\text{SO}_2\text{CF}_3)_2$ complexes (Figure 5.3) are fit to the relation: [13]

$$\sigma = AT^{-1/2}\exp[-B/(T-T_0)] \quad (2)$$

and derived parameters are provided in Table 1. Most noticeable are the large increase in pseudo-activation energy and pre-exponential factor for the complex with $x = 2$.

Conductivities are highest for the $\text{PEO}_{16}\text{LiCH}(\text{SO}_2\text{CF}_3)_2$ complex, approaching $10^{-4} (\Omega\text{cm})^{-1}$ at 30 °C and $10^{-3} (\Omega\text{cm})^{-1}$ at 80 °C, which are as high as, or higher than, those reported for the PEO “imide” and “methide” complexes. A conductivity maximum is

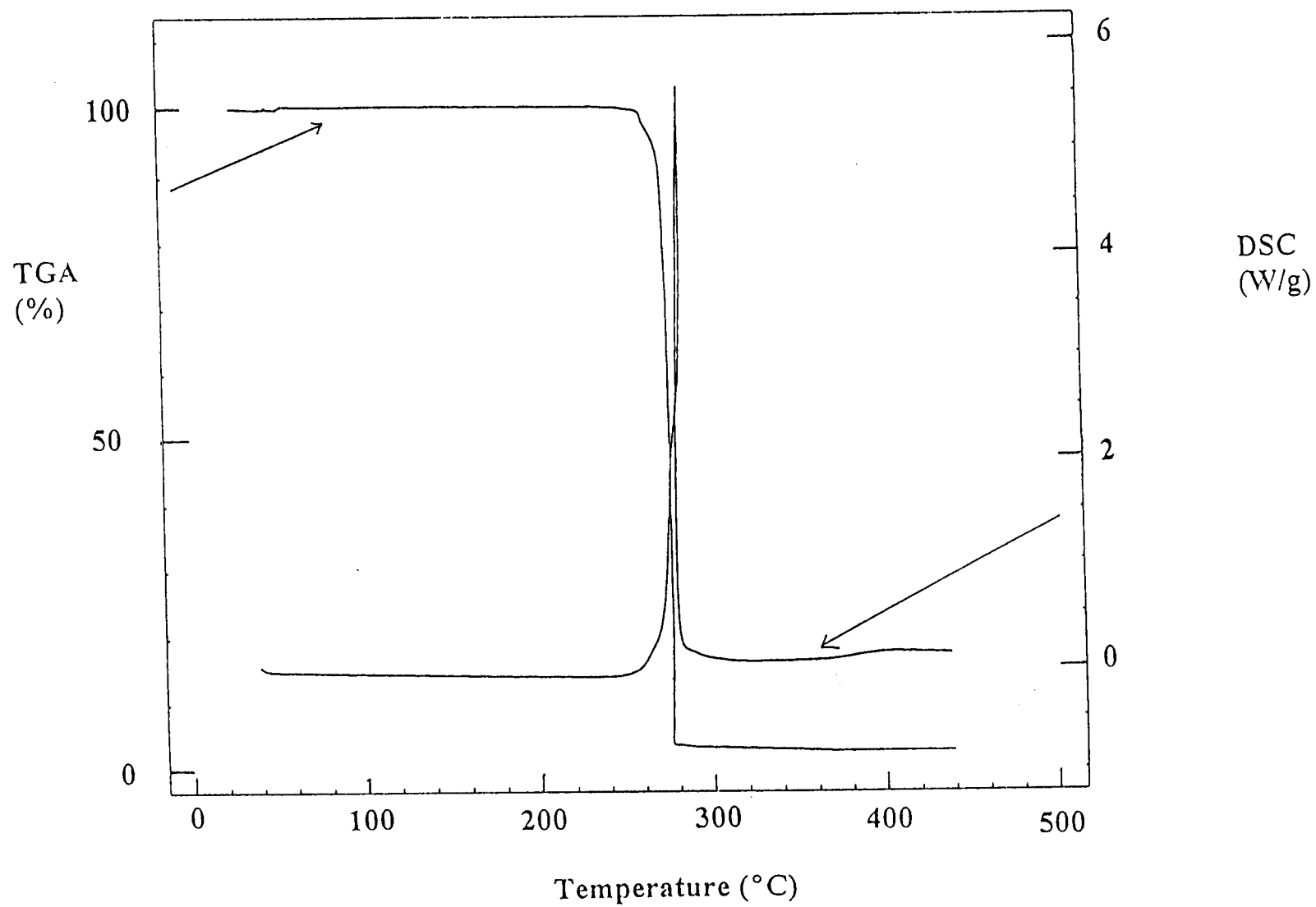


Figure 5.1: DSC and TGA traces for $\text{LiCH}(\text{SO}_2\text{CF}_3)_2$

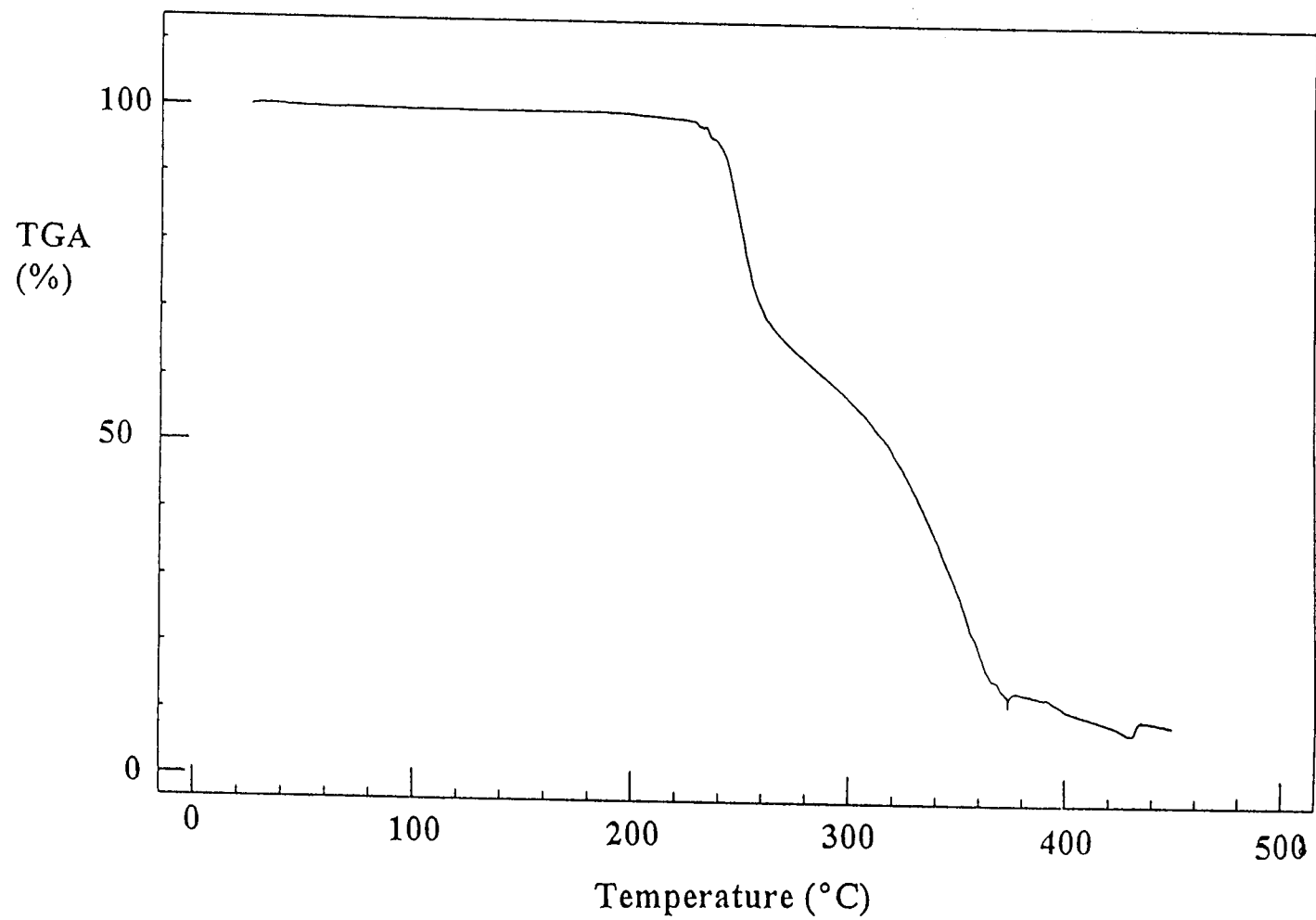


Figure 5.2: TGA trace for $\text{PEO}_8\text{LiCH}(\text{SO}_2\text{CF}_3)_2$

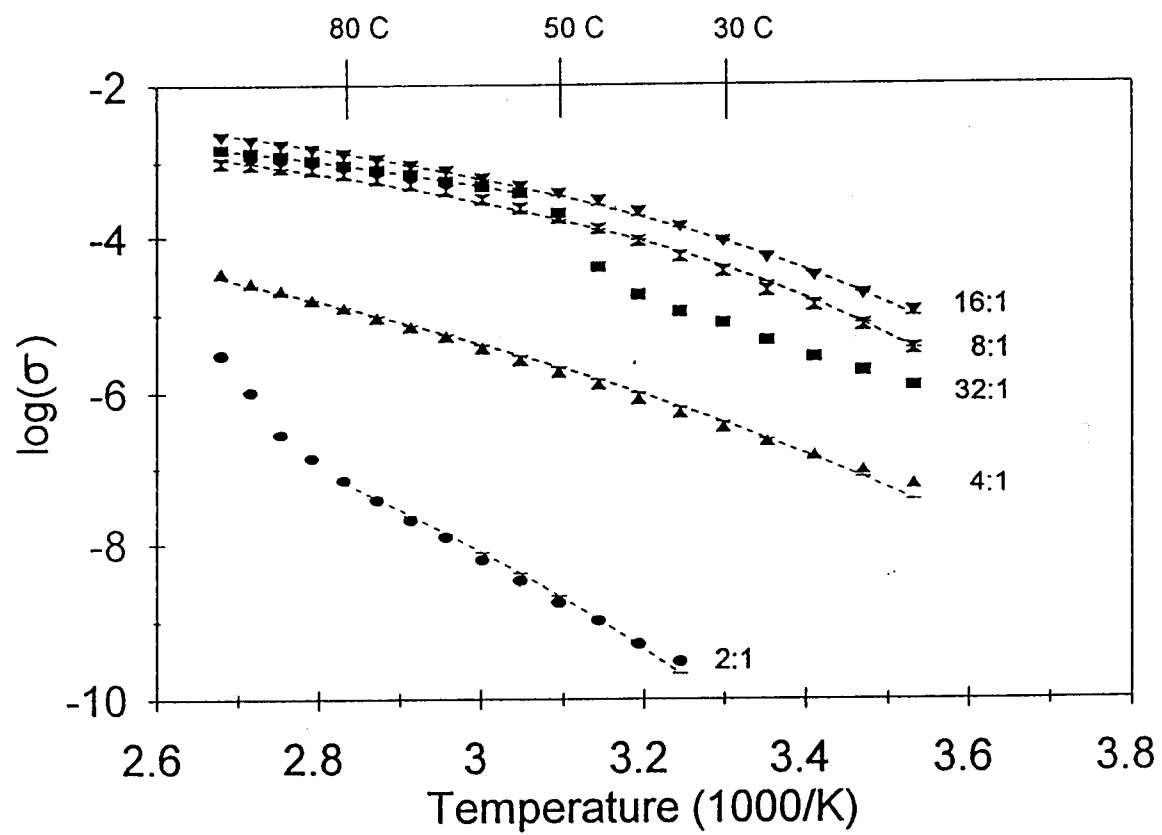


Figure 5.3: Arrhenius plots for PEO_xLiCH(SO₂CF₃)₂ complexes

Table 5.1 A, B, and T_0 parameters derived from Arrhenius plots in Figure 5.2

x	A (Ωcm)⁻¹ K^{1/2}	B K	T₀ K
32	1.15	601	210
16	2.94	650	217
8	0.93	560	225
4	0.71	1325	188
2	14	2800	181

observed at lower temperatures, above 50 °C conductivities are similar for the complexes with $x \geq 8$ (Figure 5.4).

Thermal data (Figure 5.5, Table 5.2) for the series of complexes show a decrease in the temperature and magnitude of the principal melting transition, indicating the plasticizing effect of the salt. The peak decreases in magnitude by about one-half from $x = 32$ to 8, and is too small to measure reliably at higher salt concentrations. Other endothermic peaks are evident at some salt concentrations: a small, sharp peak near 0 °C appears for $x = 8$ and 4, and another small endotherm occurs near 110 °C for the most salt-rich complexes. These peaks indicate the occurrence of minor crystalline phases with higher salt concentrations. Partial phase diagrams for PEO “imide” complexes also indicate crystalline phases at $x = 6, 3$, and 2.[6] The peak here observed at 110 °C also correlates with a break in the Arrhenius plots towards higher conductivities for the complex with $x = 2$: the conductivity increases upon melting of the crystalline phase.

The glass transitions observed for these complexes are larger than for the native PEO, and increase by 20 °C over the range of $x = 32$ to 4. The complex with $x = 4$ has a T_g some 40 °C higher than in PEO. The trend in increasing transition temperatures is similar to those obtained by Vallee, et. al. [6] on the PEO “imide” complexes. The decrease in solid polymer electrolyte conductivity with increasing salt content in polyethers has been ascribed to a decreased ion mobility related to ionic crosslinking at higher salt concentrations.

Cyclic voltammetry for $\text{PEO}_{16}\text{LiCH}(\text{SO}_2\text{CF}_3)_2$ shows the onset of Li metal deposition at - 0.05 V vs. Li and oxidation peaks between 0 and 0.2 V, indicating that

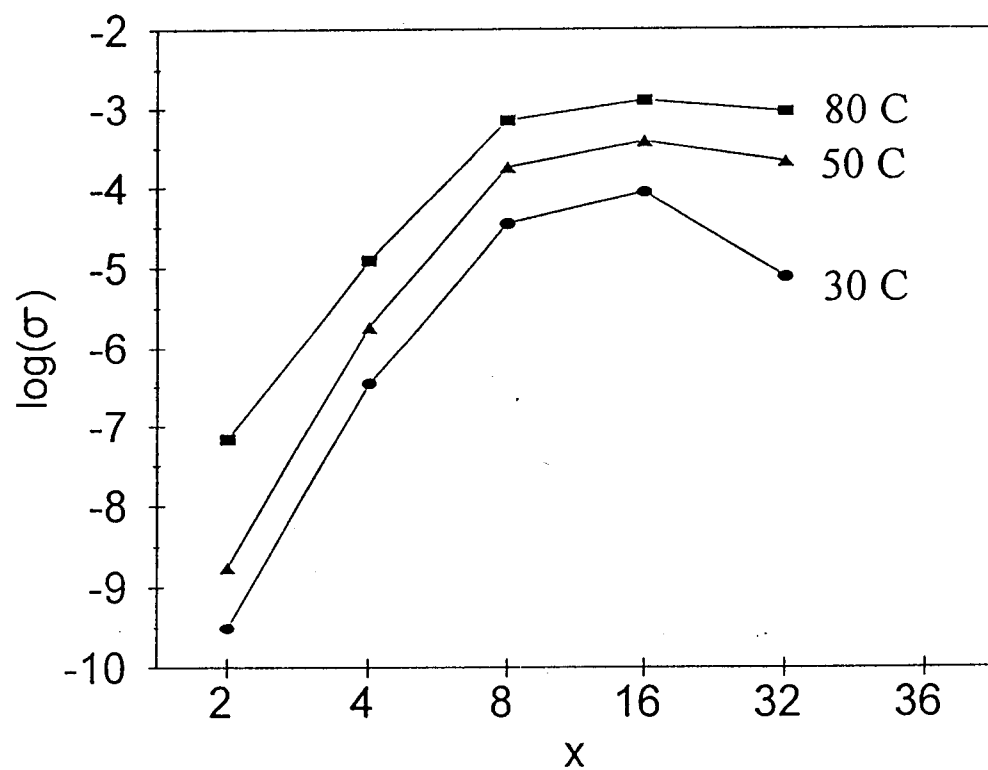


Figure 5.4: $\log \sigma$ versus x for $\text{PEO}_x\text{LiCH}(\text{SO}_2\text{CF}_3)_2$ complexes at 30, 50, and °80

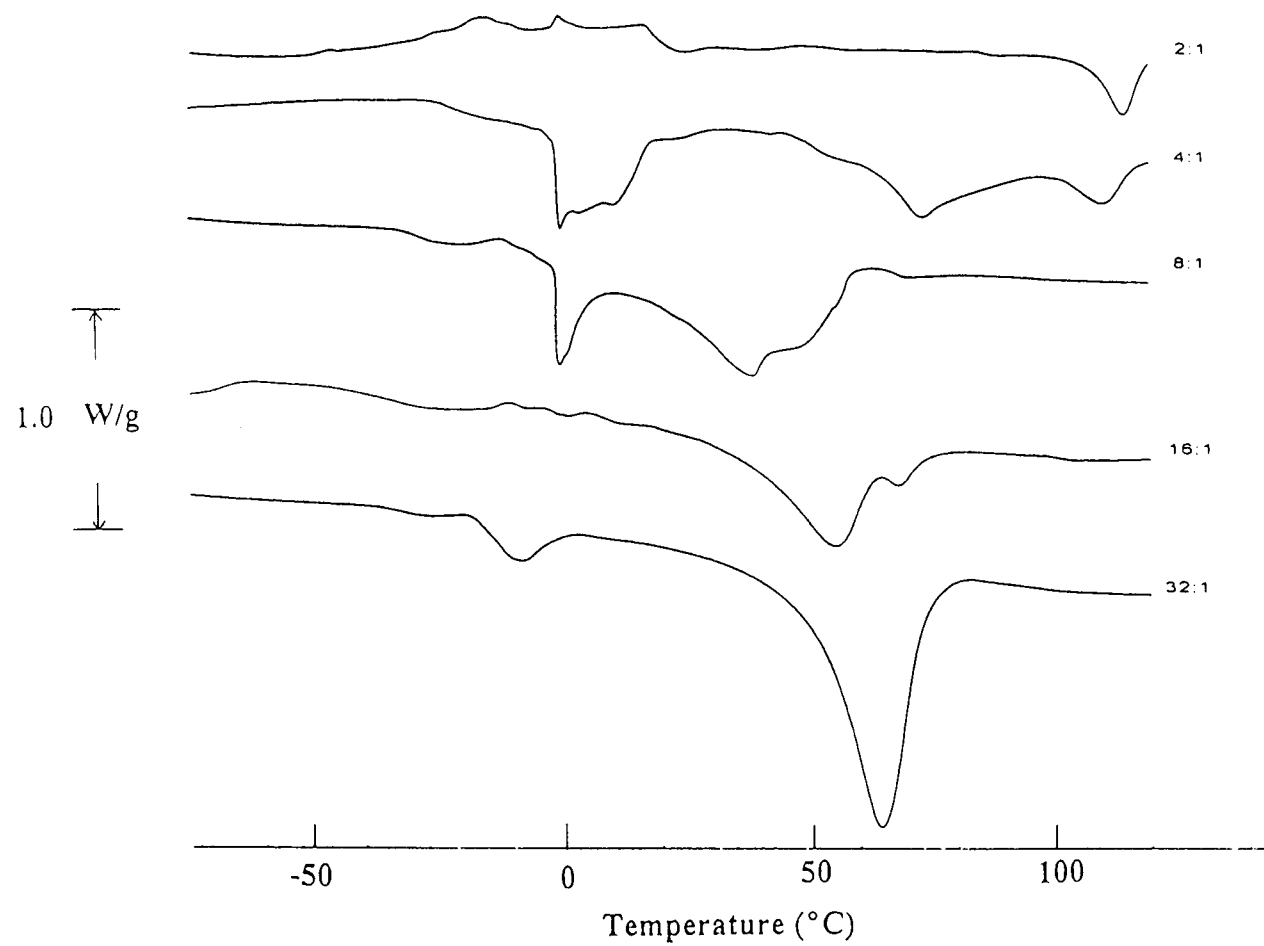


Figure 5.5: DSC traces for $\text{PEO}_x\text{LiCH}(\text{SO}_2\text{CF}_3)_2$ complexes

Table 5.2 Melting transition temperatures, T_m , and enthalpies, ΔH_m , and glass transition temperatures, T_g , and magnitudes, ΔP_g , for $\text{PEO}_x\text{LiCH}(\text{SO}_2\text{CF}_3)_2$ complexes

x	T_m $^{\circ}\text{C}$	ΔH_m J/g	T_g $^{\circ}\text{C}$	ΔP_g W/g
PEO	66	130	- 54	0.02
32	64	100	- 43	0.05
16	55	53	- 34	0.11
8	39	41	- 30	0.11
4	--	--	- 23	0.09

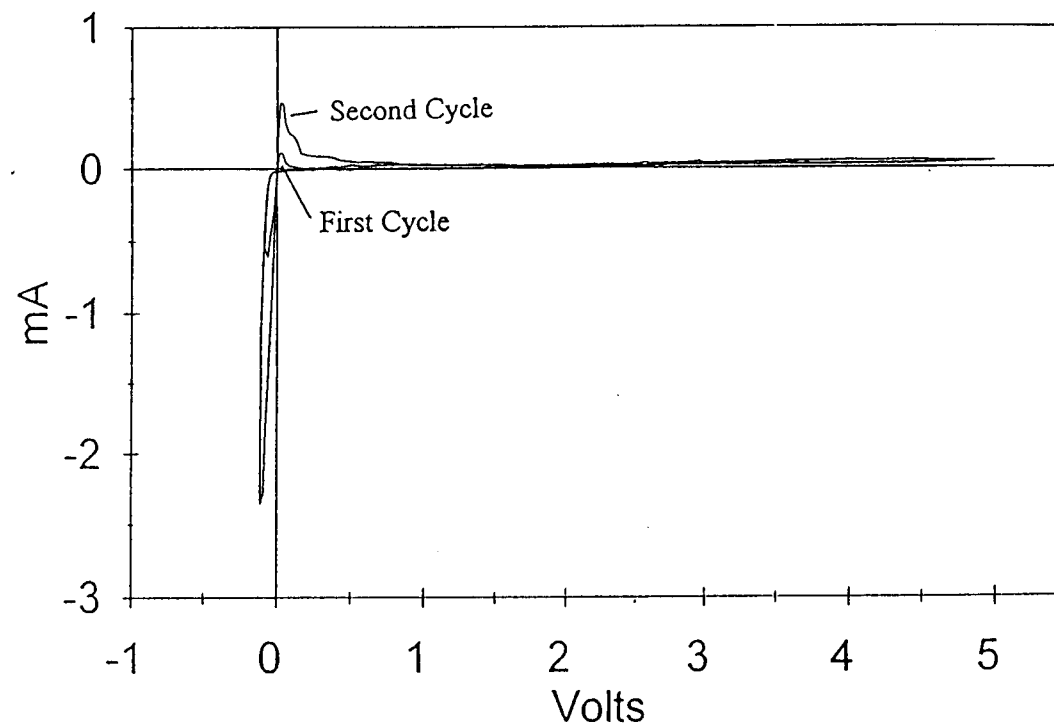


Figure 5.6: Cyclic voltammogram for $\text{PEO}_{16}\text{LiCH}(\text{SO}_2\text{CF}_3)_2$ thin film at 20 mV/s

lithium deposition and stripping occur rapidly and reversibly at the interface. Features associated with oxidative decomposition of the electrolyte are broad and weak, but can be observed in some scans at ~ 4.5 V. The irreversible oxidation is most likely associated with decomposition of the polymer rather than the salt, and a similar electrochemical stability window has been reported for other PEO complexes.[8]

5.5 Acknowledgments.

We are grateful for the receipt of a sample of $(\text{CF}_3\text{SO}_2)\text{CH}_2$ from Fred Behr at 3M. MML acknowledges a supporting grant from the National Science Foundation (DMR-9157005).

5.6 References

1. (a) *Polymer Electrolyte Reviews - 1*; J. MacCallum, and C. Vincent, Eds; Elsevier: New York (1987); (b) *Polymer Electrolyte Reviews - 2*, J. MacCallum, and C. Vincent, Eds; Elsevier Applied Science, Elsevier: New York (1989).
2. M. Ratner and D. Shriver, *Chem. Rev.* **88**, 109 (1988).
3. F. Gray, *Solid Polymer Electrolytes*, VCH: New York (1991).
4. L. Dominey, V. Koch, and T. Blacley, *Electrochim. Acta* **37**, 1551 (1992).
5. M. Armand, W. Gorecki, and R. Andreani, *Proc. of 2nd Int. Symp. on Polymer Electrolytes*, B. Scrosati, Ed. Elsevier: London (1989), pp. 99-105.
6. A. Vallee, S. Besner, and J. Prud'homme, *Electrochim. Acta* **37**, 1579 (1992).
7. D. Benrabah, D. Baril, J. Sanchez, M. Armand, and G. Gard, *J. Chem. Soc. Far. Trans.* **89**, 355 (1992).
8. D. Benrabah, J. Sanchez, D. Deroo, and M. Armand, *Sol. St. Ionics* **70/71**, 157 (1994).
9. (a) R. Nafshun, M. Lerner, N. Hamel, P. Nixon, and G. Gard, *J. Electrochem. Soc.*, in press; (b) N. Hamel, S. Ullrich, G. Gard, R. Nafshun, Z. Zhang, and M. Lerner, *207th Natl. ACS meeting*, San Diego (1994).
10. R. Nafshun and M. Lerner, *ECS National Meeting*, Reno (1995).
11. C. Angell, C. Liu, and E. Sanchez, *Nature* **362**, 137 (1993).
12. D. Desmarteau, W. Pennington, K. Sung, S. Zhu and R. Scott, *Eur. J. Sol. St. Inorg. Chem.* **28**, 905 (1991).
13. M. Armand, J. Chabagno, and M. Dulot in *Fast Ion Transport in Solids*, P. Vashishta, J. Mundy, and G. Shenoy, Eds., North-Holland: Amsterdam (1979), p. 131.

Chapter 6
Conductivity in the Poly(ethylene oxide) Mixed Salt Complexes
 $\text{PEO}_x[\text{LiN}(\text{SO}_2\text{CF}_3)_2]_y[\text{LiSO}_3\text{C}_8\text{F}_{17}]_z$

Richard Nafshun and Michael Lerner*

*Department of Chemistry and Center for
Advanced Materials Research
Oregon State University
Corvallis, Oregon 97331-4003, USA*

J. Electrochem. Soc., 187th Electrochemical Society Meeting,
May 21-26, 1995, Reno, NV, USA

6.1 Abstract.

Poly(ethylene oxide)-salt complexes are known to be good ionic conductors and have been studied for use in all-solid-state electrochemical cells. $\text{LiN}(\text{SO}_2\text{CF}_3)_2$ has been identified as a plasticizing salt, which prevents crystallization of the poly(ethylene oxide) complex, and increases the conductivity throughout the temperature range of -20 through 100 °C. We have investigated a series of poly(ethylene oxide)-salt complexes which contain a mixture or varying concentrations of $\text{LiN}(\text{SO}_2\text{CF}_3)_2$ and $\text{LiSO}_3\text{C}_8\text{F}_{17}$. We here describe the thermal and electrical characterization of a number of new poly(ethylene oxide)-salt complexes. These complexes have up to an order of magnitude greater conductivity than the poly(ethylene oxide)- $\text{LiN}(\text{SO}_3\text{CF}_3)_2$ complex.

6.2 Introduction.

A number of poly(ethylene oxide) (PEO) - salt complexes are known to be electrochemically stable and exhibit high ionic conductivity, and have therefore been studied for use in all-solid-state electrochemical cells [1-5]. $\text{LiN}(\text{SO}_2\text{CF}_3)_2$ has been identified as a plasticizing salt [6,7], suppressing the crystallization of PEO - salt complexes and thereby enhancing ionic conduction at moderate temperatures.

Lithium perfluoroalkylsulfonates show excellent electrochemical stabilities, are highly dissociated in polar solvents, and with larger anions may exhibit high transport numbers for lithium. These are therefore potentially useful electrolyte salts, but form complexes with relatively high melting transitions and therefore low conductivities near ambient temperature [8]. We here investigate by electrical and thermal measurements a series of poly (ethylene oxide) - salt complexes which contain varying concentrations of both $\text{LiN}(\text{SO}_2\text{CF}_3)_2$ and $\text{LiSO}_3\text{C}_8\text{F}_{17}$. These mixed-salt complexes show between one-half and a full order of magnitude higher conductivities than corresponding PEO - $\text{LiN}(\text{SO}_2\text{CF}_3)_2$ complexes.

6.3 Experimental.

6.3.1 Preparation of $\text{PEO}_x[\text{LiN}(\text{SO}_2\text{CF}_3)_2]_y[\text{LiSO}_3\text{C}_8\text{F}_{17}]_z$

The salts $\text{LiN}(\text{SO}_2\text{CF}_3)_2$ and $\text{LiSO}_3\text{C}_8\text{F}_{17}$ were obtained from 3M. To assure that no residual water or solvent remained in the samples, the salts were thoroughly dried under vacuum at a temperature of 120 °C. Poly(ethylene oxide) was obtained from Aldrich ($M_w = 5 \times 10^6$) and dried under vacuum at ambient temperature. The PEO - salt complexes were prepared by co-dissolution of the desired stoichiometry of salts and PEO in acetonitrile (Mallinckrodt). The complexes were then dried under vacuum and maintained under inert atmosphere to prevent water uptake. Stoichiometries are described by $\text{PEO}_x[\text{LiN}(\text{SO}_2\text{CF}_3)_2]_y[\text{LiSO}_3\text{C}_8\text{F}_{17}]_z$, where x reflects the moles of ethoxy repeats.

6.3.2 Characterization of $\text{PEO}_x[\text{LiN}(\text{SO}_2\text{CF}_3)_2]_y[\text{LiSO}_3\text{C}_8\text{F}_{17}]_z$

Bulk ionic conductivities were measured on ½" pressed pellets of the complexes in a hermetically-sealed cell using a Solartron 1260 impedance analyzer. Samples were heated to 100 °C and then quenched below - 30 °C prior to data collection. Responses were measured from 12 MHz to 0.1 Hz between - 30 °C and 100 °C. Bulk conductivities were derived from the high- frequency touchdown of Nyquist plots and the known cell geometry.

Differential scanning calorimetry (DSC) was performed with 20 - 25 mg samples loaded in hermetically-sealed Al pans in a Shimadzu DSC-50. Samples were heated to 100 °C, quenched below - 100 °C, then heated at 10 °C / min from - 100 °C to 120 °C. Thermogravimetric analyses (TGA) utilized a Shimadzu TGA-50. Samples (15 - 20 mg) were loaded into a Pt pan, and heated from 30 - 450 °C at 10 °C/min under N₂ flow (50 mL / min).

6.4 Results and Discussion.

Conductivity data for complexes prepared with equimolar concentrations of LiN(SO₂CF₃)₂ and LiSO₃C₈F₁₇ ($y = z = 1$ in PEO_x[LiN(SO₂CF₃)₂]_y[LiSO₃C₈F₁₇]_z) are plotted in Figure 6.1. At each temperature, a maximum conductivity is obtained at a ratio of ether oxygen to Li [$x/(y + z)$] equal to 8. This concentration dependence is similar to that observed with simple PEO - salt complexes, including PEO_x[LiN(SO₂CF₃)₂], and reflects the competing trends of increasing numbers of charge carriers and decreasing polymer mobility with increasing salt concentration.

As a result of the above observations, subsequent studies focus on complexes with an overall O / Li ratio of 8 (PEO₁₆[LiN(SO₂CF₃)₂]_y[LiSO₃C₈F₁₇]_z; $y + z = 2$): over twenty additional complexes are examined at this ratio with y and z varied. Figure 6.2 displays the conductivities of some of these complexes at 30 °C, 50 °C, and 80 °C as a function of y (the imide concentration). Conductivities are notably higher for the mixed salt complexes relative to either parent complex, with an increase of approximately one-half to

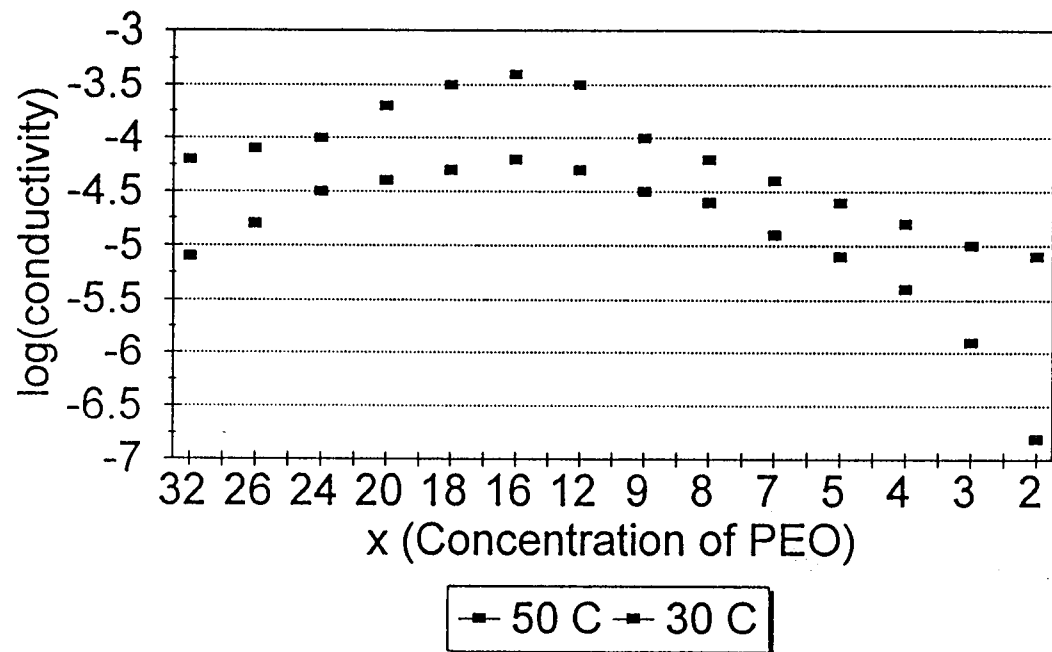


Figure 6.1: $\log \sigma$ versus x for the complexes $\text{PEO}_x[\text{LiN}(\text{SO}_2\text{CF}_3)_2]_1[\text{LiSO}_3\text{C}_8\text{F}_{17}]_1$

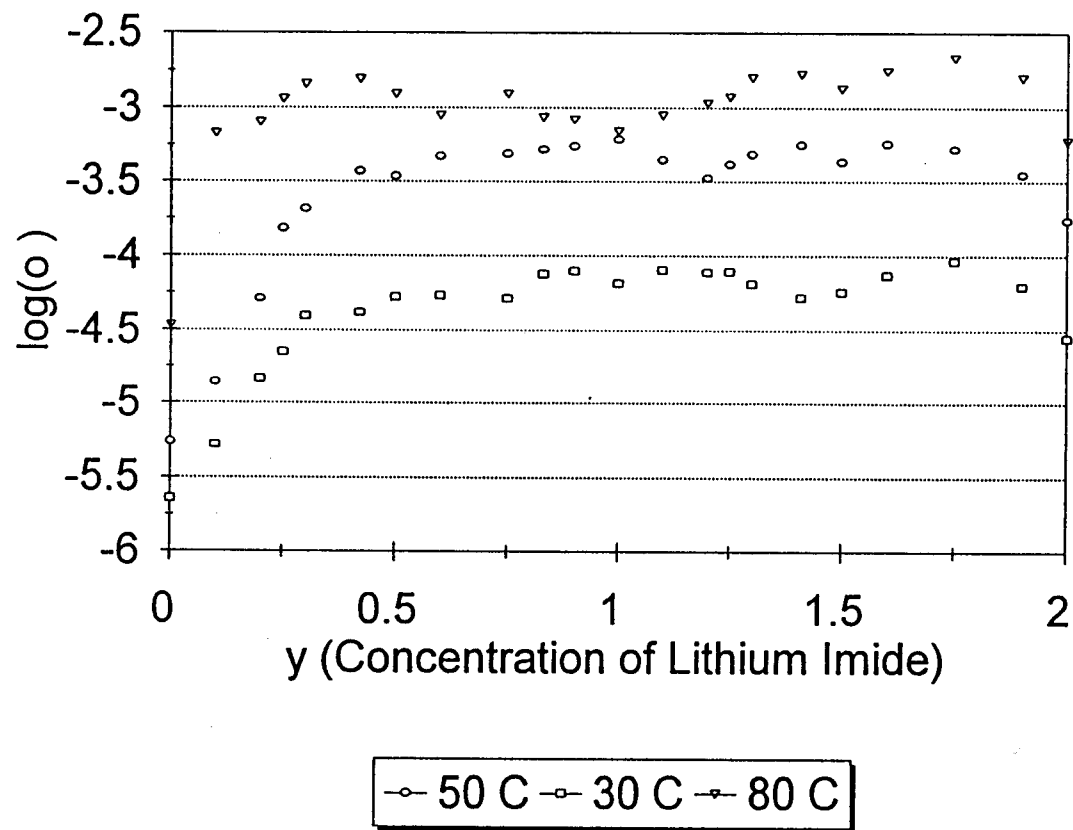


Figure 6.2: $\log \sigma$ versus y for the complexes $\text{PEO}_{16}[\text{LiN}(\text{SO}_2\text{CF}_3)_2]_y[\text{LiSO}_3\text{C}_8\text{F}_{17}]_{1-y}$

a full order of magnitude for a number of salt ratios.

Thermal studies show single, sharp melting transitions for $\text{PEO}_{16}[\text{LiSO}_3\text{C}_8\text{F}_{17}]_2$ and all of the mixed-salt complexes studied. In contrast, the imide salt 8:1 complex is almost entirely amorphous and shows a greatly diminished transition, as has been previously reported.[2] Melting transition temperatures decrease rapidly for the mixed-salt complexes with increasing imide concentration from $y = 0$ to 1 (Figure 6.3). The increase in conductivity with increasing imide concentration from 0 to about 0.5 coincides with the decreasing melting transition temperatures. Glass transition temperatures increase rapidly for the mixed-salt complexes with increasing imide concentration from 1 to 2 (Figure 6.4). The decrease in conductivity with increasing imide concentration from 1.75 to 2 coincides with the increasing glass transition temperatures.

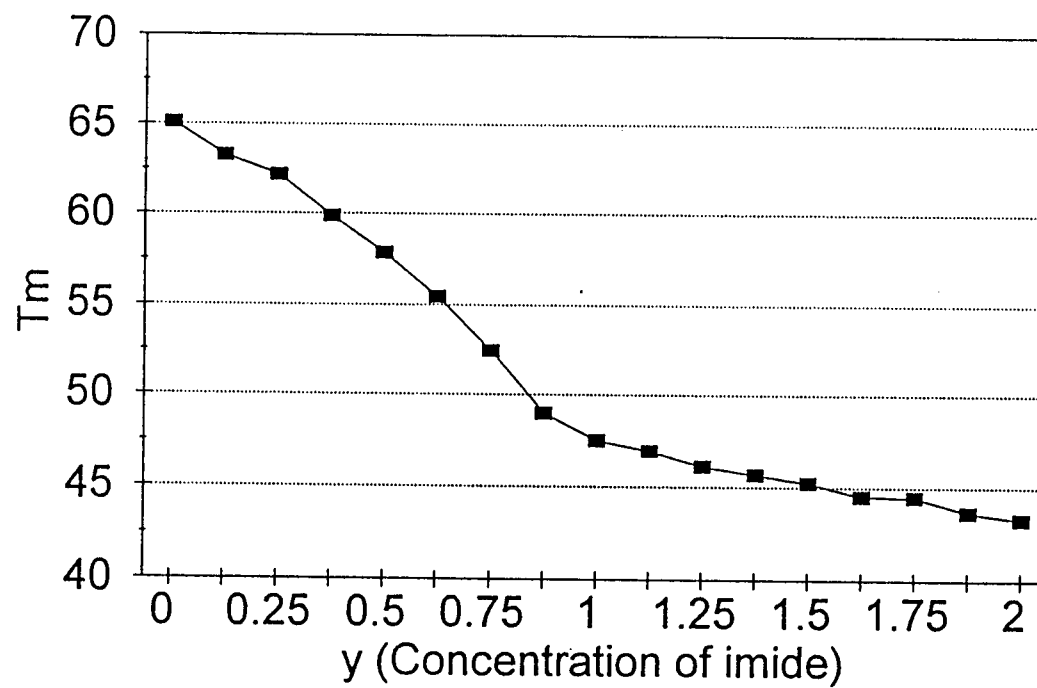


Figure 6.3: T_m versus y for the complexes
 $\text{PEO}_{16}[\text{LiN}(\text{SO}_2\text{CF}_3)_2]_y[\text{LiSO}_3\text{C}_8\text{F}_{17}]_{1-y}$

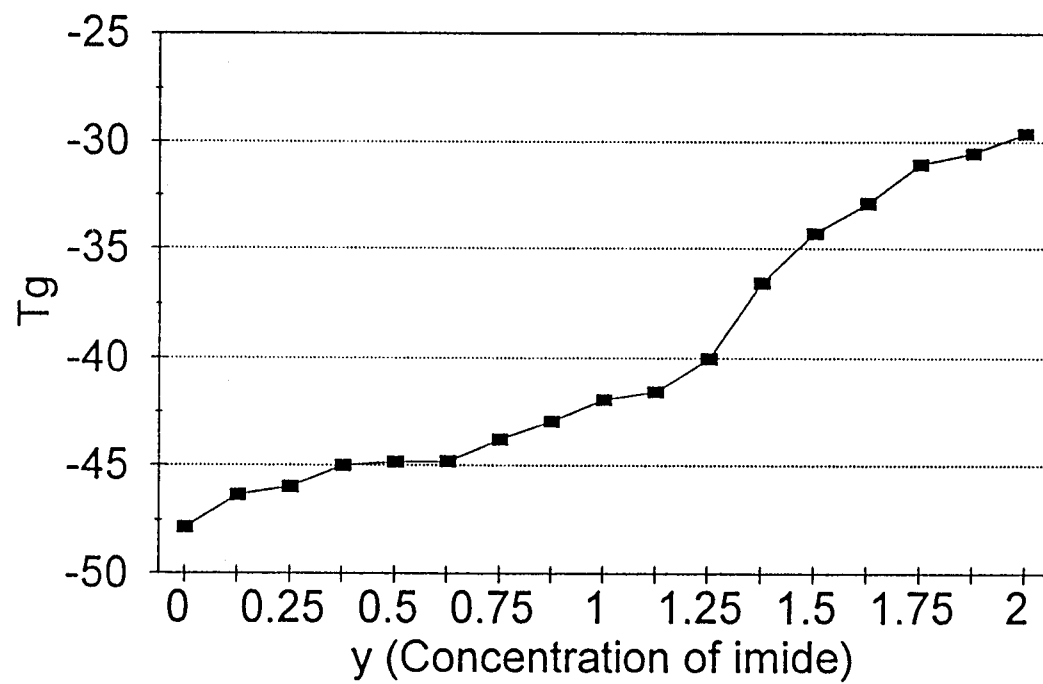


Figure 6.4: T_g versus y for the complexes
 $\text{PEO}_{16}[\text{LiN}(\text{SO}_2\text{CF}_3)_2]_y[\text{LiSO}_3\text{C}_8\text{F}_{17}]_{1-y}$

6.5 References

1. (a) *Polymer Electrolyte Reviews - 1*; J. MacCallum, and C. Vincent, Eds; Elsevier: New York (1987); (b) *Polymer Electrolyte Reviews - 2*, J. MacCallum, and C. Vincent, Eds; Elsevier Applied Science, Elsevier: New York (1989).
2. L. Dominey, V. Koch, and T. Blacley, *Electrochim. Acta* **37**, 1551 (1992).
3. M. Armand, W. Gorecki, and R. Andreani, *Proc. of 2nd Int. Symp. on Polymer Electrolytes*, B. Scrosati, Ed. Elsevier: London (1989), pp. 99-105.
4. D. Benrabah, J. Sanchez, D. Deroo, and M. Armand, *Sol. St. Ionics* **70/71**, 157 (1994).
5. R. Nafshun, M. Lerner, N. Hamel, P. Nixon, and G. Gard, *J. Electrochem. Soc.* **142**, L153 (1995).
6. M. Armand, W. Gorecki, and R. Andreani, *Proc. of 2nd Int. Symp. on Polymer Electrolytes*, B. Scrosati, Ed., London, 1989.
7. D. Benrabah, D. Baril, J. Sanchez, M. Armand, G. Gard, *J. Chem. Soc. Far. Trans.* **89**, 355 (1992).
8. G. Nagasubramanian, D. Shen, S. Surampudi, Q. Wang, and G Prakash, *Electrochim. Acta* **40**, 2277 (1995).

Chapter 7

SUMMARY

This thesis deals with the synthesis and characterization of polymer electrolytes, and a discussion of a novel method for measuring the lithium diffusivities in $[\text{Li}(\text{H}_2\text{O})_2]_x\text{MoO}_3$, and $[\text{Li}(\text{H}_2\text{O})_2]_x\text{PEO}_{0.94}\text{MoO}_3$. The important experimental results are summarized in this chapter.

Poly(ethylene oxide) (PEO), $(\text{CH}_2\text{CH}_2\text{O})_n$, is utilized as a polymer host for polymer electrolytes containing lithium salts. The polymer electrolytes $\text{PEO}_x\text{LiSO}_3\text{CF}_2\text{SF}_5$, and $\text{PEO}_x\text{LiSO}_3\text{CFHSF}_5$, exhibited different thermal and electrical properties. The $\text{PEO}_x\text{LiSO}_3\text{CF}_2\text{SF}_5$ complexes show significantly suppressed crystallinity and the $\text{PEO}_4\text{LiSO}_3\text{CF}_2\text{SF}_5$ complex has a bulk ionic conductivity (σ) near $10^{-5} (\Omega \text{ cm})^{-1}$ at 30 °C. Unlike the $\text{PEO}_x\text{LiSO}_3\text{CF}_2\text{SF}_5$ complexes, a plasticizing effect for the $\text{PEO}_x\text{LiSO}_3\text{CFHSF}_5$ complexes is absent.

In the series of polymer electrolytes $\text{PEO}_x[\text{LiSO}_3(\text{CF}_2)_n\text{SO}_3\text{Li}]$ where $n = 1 - 4$, and $\text{PEO}_x[\text{LiSO}_3\text{CF}_2\text{CF}_2\text{OCF}_2\text{CF}_2\text{SO}_3\text{Li}]$, the $\text{PEO}_{64}\text{LiSO}_3\text{CF}_2\text{CF}_2\text{OCF}_2\text{CF}_2\text{SO}_3\text{Li}$ complex was found to have the highest conductivity: σ is near $5 \times 10^{-6} (\Omega \text{ cm})^{-1}$ at 100 °C.

The polymer electrolytes $\text{PEO}_x\text{LiCH}(\text{SO}_2\text{CF}_3)_2$ show ionic conductivities as high as, or higher than, those derived from other plasticizing salts, with σ reaching $10^{-4} (\Omega \text{ cm})^{-1}$ at 30 °C.

For the equimolar concentration of salts, $\text{PEO}_x[\text{LiN}(\text{SO}_2\text{CF}_3)_2]_y[\text{LiSO}_3\text{C}_8\text{F}_{17}]_z$ ($y = z = 1$), a conductivity maximum of $10^{-4} (\Omega \text{ cm})^{-1}$ at 30°C occurs at $x = 16$. In the compositional range $\text{PEO}_{16}[\text{LiN}(\text{SO}_2\text{CF}_3)_2]_y[\text{LiSO}_3\text{C}_8\text{F}_{17}]_z$ ($y = 2 - z$) a conductivity maximum of $2.5 \times 10^{-3} (\Omega \text{ cm})^{-1}$ at 80°C occurs at $y = 1.75$. Thermal data indicate decreasing melting transition temperatures, and increasing glass transition temperatures, as y increases from 0 to 2.

The modified galvanostatic intermittent titration technique was employed to measure the diffusion of lithium ion in thin films of $[\text{Li}(\text{H}_2\text{O})_2]_x\text{MoO}_3$, and $[\text{Li}(\text{H}_2\text{O})_2]_x\text{PEO}_{0.94}\text{MoO}_3$. The preliminary results indicate that this method is promising and several future experimental considerations are offered.

BIBLIOGRAPHY

- Abraham, K., *J. Power Sources*, 7, 1 (1981).
- Allcock, H., P. Austin, T. Neenan, J. Sisko, P. Blonsky, and D. Shriver, *Macromolecules* 19, 1508 (1986).
- Angell, C., C. Liu, and E. Sanchez, *Nature* 362, 137 (1993).
- Aranda, P., and E. Ruiz-Hitzky, *Chem. Mater.*, 4, 1395 (1992).
- Armand, M., J. Chabagno, and M. Muclot, Second International Meeting on Solid Electrolytes, St. Andrews, Scotland, 20-22 Sept. 1978, Extended Abstract.
- Armand, M., W. Gorecki, and R. Andreani, in *Proceedings of 2nd International Symposium on Polymer Electrolytes*, B. Scorsati, Ed., 105, Elsevier, London, p.99.
- Armand, M., J. Chabagno, and M. Duclot, in *Fast Ion Transport in Solids*; P. Vashista, J. Mundy, and G. Shenoy, Eds; Elsevier North-Holland, Amsterdam, 1979.
- Armand, M., in *Polymer Electrolyte Reviews-1*; J. MacCallum, and C. Vincent, Eds; Elsevier: New York (1987).
- Armand, M. in *Polymer Electrolyte Reviews-2*; J. MacCallum, and C. Vincent, Eds; Elsevier: New York (1989).
- Banks, R., M. Barlow, R. Haszeldine, and W. Morton, *J. C. S. Perkin Trans.*, 1, 1266 (1974).
- Bannister, D., G.R. Davies, I.M. Ward, J.E. McIntyre, *Polymer Communications* 25, 1291 (1984).
- Basu, S., and W. L. Worrell, in: *Fast Ion Transport in Solids*, eds. P. Vashishta, J. N. Mundy, and G. K. Shenoy (North Holland, Amsterdam, 1979) p. 149.
- Benrabah, D., J. Sanchez, and M. Armand, *Electrochim. Acta* 37, 1737 (1992).
- Benrabah, D., D. Baril, J. Sanchez, M. Armand, and G. Gard, *J. Chem. Soc. Far. Trans.* 89, 355 (1992).

Benrabah, D., D. Baril, J. Sanchez, M. Armand, and G. Gard, *J. Chem. Soc. Faraday. Trans.* **89**(2), 355 (1993).

Benrabah, D., J. Sanchez, D. Deroo, and M. Armand, *Solid State Ionics* **70/71**, 157 (1994).

Berthier, C., W. Gorecki, M. Minier, and M. Armand, *Solid State Ionics* **11**, 91 (1983).

Besenhard, J., J. Heydecke, E. Wudy, H. P. Fritz, and W. Foag, *Solid State Ionics*, **8**, 61 (1983).

Blonsky, P., D. Shriver, P. Austin, and H. Allcock, *J. Am. Chem. Soc.* **106**, 6854, (1984).

Blonsky, P., D. Shriver, P. Austin, and H. Allcock, *Solid State Ionics* **18/19**, 258 (1986).

Blonsky, P., D. Shriver, P. Austin, and H. Allcock, *Solid State Ionics* **18/19**, 258 (1989).

Brown, J., and K.J. Morgan in *Advances in Fluorine Chemistry* **4**, M. Stacey, J.C. Tatlow, and A.G. Sharpe, (eds.), Butterworth, Washington, 1965.

Bruce, P., in *Polymer Electrolyte Reviews-1*; J. MacCallum, and C. Vincent, Eds.; Elsevier: New York (1987), p. 243.

Bruce, P., in *Polymer Electrolyte Reviews-1*; J. MacCallum, and C. Vincent, Eds.; Elsevier: New York (1987), p. 253.

Cameron, G., M. Ingram, and K. Sarmouk, *Eur. Polym. J.* **26**, 197 (1990).

Canich, J., M. Ludvig, G. Gard, and J. Shreeve, *Inorg. Chem.*, **23**, 4403 (1984).

Canselier, J., J. Boyer, V. Castro, D. Peyton, J. Mohtasham, F. Behr, and G. Gard, *Magn. Res. in Chem.*, in press.

Canselier, J., J. Boyer, V. Castro, G. Gard, J. Mohtasham, D. Peyton, and F. Behr, *Magn. Reson. Chem.*, **33**, 506 (1995).

Cen, W., Z.-X. Dong, T.-J. Huang, D. Su, and J.M. Schreeve, *Inorg. Chem.* **27**, 1376 (1988).

Desmarteau, D., W. Pennington, K. Sung, S. Zhu and R. Scott, *Eur. J. Sol. St. Inorg. Chem.* **28**, 905 (1991).

Dick, C., G. Ham, *J. Macromol. Sci. Chem.* **A4**, 1301 (1970).

Dominey, L., V. Koch, and T. Blacley, *Electrochim. Acta* **37**, 1551 (1992).

Donoso, P., T. Bonagamba, N. Mello, P. L. Frare, H. Panepucci, G. Gonzalez, M. A. Santa Ana, and E. Benavente in: *XVIII Encontro Nacional de Fisica da Materia Condensada*, Caxambu - MG, 6-10 June, 1995.

Fenton, D., J. Parker, and P. Wright, *Polymer* **14**, 589 (1973).

Fulcher, G., *J. Amer. Ceram. Soc.* **8**, 339 (1925).

Gard, G., P. Nixon, N. Hamel, S. Ullrich, and N. Holcomb, Department of Chemistry, Portland State University.

Gard, G., N. Hamel, and P. Nixon, to be submitted.

Gard, G., A. Waterfeld, R. Mews, J. Mahtasham, and R. Winter, *Inorg. Chem.*, **29**, 4588 (1990).

Goodenough, J., in *Solid State Microbatteries*, Eds.: J. R. Akridge and M. Balkanski, NATO-ASI Series, Ser. B209, Plenum, New York, 1990. P. 213.

Gonzalez, G., M. A. Santa Ana, E. Benavente, P. Donoso, T. Bonagamba, and N. C. Mello, [On line Polymer Electrolyte Conference], (1995).

Gray, F., *Solid Polymer Electrolytes*, VCH Publishers, New York, 1991, p. 35.

Gray, F., *Solid Polymer Electrolytes*, VCH Publishers, New York, 1991, p.97.

Gray, F., *Solid Polymer Electrolytes*, VCH Publishers, New York, 1991, p. 108.

Gray, F., *Solid Polymer Electrolytes*, VCH Publishers, New York, 1991.; *Polymer Electrolyte Reviews-1*; J. MacCallum, and C. Vincent, Eds; Elsevier: New York (1987).

Gray, F. in *Polymer Electrolyte Reviews-1* (J. MacCallum, and C. Vincent, Eds.), Elsevier, London (1987), p. 139.

Gray, F., J. MacCallum, and C. Vincent, *Solid State Ionics* **18/19**, 252 (1986).

- Greenbaum, S., K. Adamic, Y. Pak, M. Wintersgill, and J. Fontanella, *Solid State Ionics* **28-30**, 1042 (1988).
- Hamel, N., S. Ullrich, G. Gard, R. Nafshun, Z. Zhang, and M. Lerner, 207th Natl. ACS meeting, San Diego, ACS symp., 1994.
- Harris, C., D. Shiver, and M. Ratner, *Macromolecules* **19**, 987 (1986).
- Heller, D., C. Fenselau, J. Yergey, R.J. Cotter, and D. Larkin, *Anal. Chem.* **56**, 2274 (1984).
- Herkelmann, R., and P. Sartori, *J. Fluorine. Chem.* **44**, 299 (1989).
- Holcomb, N., P. Nixon, G. Gard, R. Nafshun, and M. Lerner, *J. Electrochem. Soc.* **143**, 1297 (1996).
- Hollitzer, E., and P. Sartori, *J. Fluorine Chem.* **35**, 329 (1987).
- Honders, A., E. W. A. Young, A. H. van Heeren, J. H. W. de Wit, and G. H. J. Broers, *Solid State Ionics*, **9/10**, 375 (1983).
- Honders, A., and G. H. J. Broers, *Solid State Ionics*, **15**, 173 (1985).
- Honders, A., J. M. der Kinderen, A. H. van Heeren, J. H. W. de Wit, and G. H. J. Broers, *Solid State Ionics*, **15**, 265 (1985).
- Julien, C. and G. A. Nazri, *Solid State Ionics*, **69**, 111 (1994).
- Kaplan, M., E. Rietman, R. Cava, L. Holt, and E. Chandross, *Solid State Ionics* **25**, 37 (1987).
- Kaplan, M., E. Rietman, and R. Cava, *Polymer* **30**, 504 (1989).
- Kapustinskii, A., *Quart. Rev. Chem. Soc.* **10**, 283 (1956).
- Kelly, I., J. Owen, and B. Steele, *J. Power Sources* **14**, 13 (1985).
- Kelly, I., J. Owen, and B. Steele, *J. Electroanal. Chem.* **168**, 467 (1984).
- Komarneni, S., *J. Mater. Chem.*, **2**, 1219 (1992).
- Lee, H., X. Yang, J. McBreen, Z. Xu, T. Skotheim, and Y. Okamoto, *J. Electrochem. Soc.* **141**, 886 (1994).

- Lemmon, J., and M. Lerner, *Macromolecules* **25**, 2907 (1992).
- Lemmon, J., J. Wu, and M. M. Lerner, *Mat. Res. Soc. Symp. Proc.*, **351**, 83 (1994).
- Lemmon, J., and M. M. Lerner, *Chem. Mater.*, **6**, 207 (1994).
- Lerner, M., L. Lyons, J. Tonge, and D. Shriver, *Polym. Prepr.* **30**, 435 (1989).
- Lightfoot, P., M. Mehta, and P. Bruce, *Science* **262**, 883 (1993).
- Lyon, P., K.B. Tomer, and M.L. Gross, *Anal. Chem.* **57**, 2984 (1985).
- MacCallum, J., M. Smith, and C. Vincent, *Solid State Ionics* **11**, 307 (1984).
- Macdonald, J., *Impedance Spectroscopy*, John Wiley & Sons, New York (1987), p.14
- Macdonald, J., *Impedance Spectroscopy*, John Wiley & Sons, New York (1987), p.23.
- Macdonald, J., *Impedance Spectroscopy*, John Wiley & Sons, New York (1987), p.39.
- Margalit, N., *J. Electrochem. Soc.*, **121**, 1460 (1974).
- Mendolia, M., and G. Farrington, *High-Conductivity, Solid Polymeric Electrolytes*, in *Materials Chemistry: An Emerging Discipline*; L. Interrante, L. Casper, and A. Ellis, Eds; American Chemical Society: Washington, D.C., 1995, p. 107.
- Messersmith, P., and S. Stupp, *Chem. Mater.*, **7**, 454 (1995).
- Mohtasham, J., G. Gard, Portland State University, J. Canselier, Ecole Nationale Supérieure D'Ingenieurs de Genie Chimique, "¹³C NMR Studies of Fluorosultones and Fluorosulfonic Acids", 46th Regional ACS Meeting, La Grande, Oregon, June 1991.
- Mohtasham, J., R. Terjeson, and G. Gard in *Inorganic Syntheses: Volume 29*, R. Grimes (ed.), John Wiley & Sons, Inc; New York, 1992, pp. 33-38.
- Nafshun, R., M. Lerner, N. Hamel, P. Nixon, and G. Gard, *J. Electrochem. Soc.* **142**, L153 (1995).

Nafshun, R., M. Lerner, N. Holcomb, P. Nixon, and G. Gard, *J. Electrochem. Soc.* **143**, 1297 (1996).

Nafshun, R., and M. Lerner, *ECS National Meeting*, Reno (1995).

Nafshun, R., and M. Lerner, unpublished results.

Nazar, L., H. Wu, and W. Power, *J. Mater. Chem.* **5**(11), 1985 (1995).

Nazri, G., D. MacArthur, J. O'Gara, and R. Aroca, *Mater. Res. Soc. Symp. Proc.* **210**, 163 (1991).

Nazri G., D. MacArthur, and F. Ogara, *Polym. Prepr.* **30**, 430 (1989).

Nazri, G., D. MacArthur, and F. Ogara, *Chem. Mater.* **1**, 370 (1989).

Nicholas, C., D. Wilson, and C. Booth, *Br. Polym. J.* **20**, 289 (1988).

Ohzuku, T., and A. Ueda, *Solid State Ionics*, **69**, 201 (1994).

Oriakhi, C., R. L. Nafshun, and M. M. Lerner, submitted for publication, *Mater. Res. Bulletin*, 6/96.

Paul, J., C. Jegat, and J. Lassegues, *Electrochimica Acta* **37**, 1623 (1992).

Pearson, R., *J. Amer. Chem. Soc.* **85**, 3533 (1963).

Ratner, M. and D. Shriver, *Chem. Rev.* **88**, 109 (1988).

Rivas, B., K. Geckeler, in *Advances in Polymer Science*, v. 102, Springer-Verlag, Berlin (1992), p. 173.

Robitaille, C., and D. Fauteux, *J. Electrochem. Soc.* **133**, 315 (1986).

Saffarian, H., P. Ross, F. Behr, and G. Gard, *J. Electrochem. Soc.* **139**, 2391 (1992).

Sandahl, J., S. Schantz, L. Torell, and R. Frech, *Proceedings of SSI 87 Garmish FRG*, Sep. 6 - 11, 1987.

Schollhorn, R., R. Kuhlmann, and J. O. Besenhard, *Mat. Res. Bull.*, **11**, 83 (1976).

- Scrosati, B., *Mater. Sci. Eng.* **112**, 269 (1992).
- Scrosati, B. (ed.), *Applications of Electroactive Polymers*, Chapman and Hall, London, 1993.
- Sheppard, W., *J. Am. Chem. Soc.*, **84**, 3072 (1962).
- Sloop, S., M. Lerner, T. Stephens, A. Tipton, D. Paull, and J. Stenger-Smith, *J. Appl. Poly. Sci.* **53**, 1563 (1994).
- Shriver, D., and M. Drezzdson, *The Manipulation of Air-Sensitive Compounds*, Second Edition, John Wiley & Sons, New York (1986).
- Shriver, D., S. Clancy, P. Blonsky, and L. Hardy, in *Proceedings of the 6th Risø International Symposium on Metallurgy and Materials Science* (F. Poulsen, N. Hessel Andersen, K. Clausen, S. Skaarup, and O. Sørensen, Eds.), Risø National Laboratory, Roskilde (1984).
- Socrates, G. *Infrared Characteristic Group Frequencies*, Wiley-Interscience: Chichester, 1980.
- Sylla, S., J. Sanchez, and M. Armand, *Electrochim. Acta* **37**, 1699 (1992).
- Tamman, G., and W. Hesse, *Z. Anorg. Allg. Chem.* **156**, 245 (1926).
- Thomas, D., and E. M. McCarron, III, *Mat. Res. Bull.*, **21**, 945 (1986).
- Tonge, J., and D. Shriver, *J. Electrochem. Soc.* **134**, 270 (1987).
- Vallee, A., S. Besner, and J. Prud'homme, *Electrochim. Acta.* **37**, 1579 (1992).
- Vincent C., *Solid St. Chem.* **17**, 145 (1987).
- Vogel, H., *Phys. Z.* **22**, 645 (1921).
- Wantanabe, M., and N. Ogata, in *Polymer Electrolyte Reviews-1*; J. MacCallum, and C. Vincent, Eds; Elsevier: New York (1987), p. 39.
- Weiblen, D. in *Fluorine Chemistry II*, J.H. Simons (ed.), Academic Press, New York, 1954.
- Weston, J., and B. Steele, *Solid State Ionics* **7**, 75 (1982).

- Whittingham, M., *Prog. Solid State Chem.*, **12**, 41 (1978).
- Willenbring, R., MS Thesis, Portland State University, (1987).
- Winter, R., and G. Gard, *Inorg. Chem.*, **27**, 4329 (1988).
- Winter, R., and G. Gard, *Inorg. Chem.*, **29**, 2386 (1990).
- Winter, R., and G. Gard, *J. Fluorine Chem.*, **52**, 57 (1991).
- Winter, R., G. Gard, R. Mews, and M. Notlemeyer, *J. Fluorine Chem.*, **60**, 109 (1993).
- Wintersgill, M., J. Fontanella, Y. Pak, S. Greenbaum, A. Al-Mударis, and A. Chadwick, *Polymer* **30**, 1123 (1989).
- Wu, J., and M. Lerner, *Chem. Mater.*, **5**, 835 (1993).
- 3M, Industrial Chemical Products Division, St. Paul, MN.

APPENDICES

APPENDIX A
A QuickBASIC 4.5 Program to Control the Instrumentation to
Measure the Electrical Properties of a Cell

Richard L. Nafshun and Michael M. Lerner*

Department of Chemistry and Center for
Advanced Materials Research
Oregon State University
Corvallis, Oregon 97331-4003, USA

A1.1 Introduction.

The following program is written in QuickBASIC 4.5. It controls a Sun EC-01 Environmental Chamber, a Schlumberger SI 1206 Impedance/Phase-Gain Analyzer, a custom built relay box, and monitors a thermocouple.

,

'TwoCells.bas

,

'Richard L. Nafshun

'MML Group

'Department of Chemistry

'Oregon State University

'Corvallis, Oregon 97331-4003

,

'(503) 737-3635

,

'Copyright 1993 Richard L. Nafshun

'Portions of this program have been modified from ML Solar

'Mike M. Lerner

,

,

'Open communications with the SI 1260

,

OPEN "COM1:9600,n,8,1,CS2000,DS2000,CD2000" FOR RANDOM AS 1

,

,

'Open communications with the Sun EV Oven

,

OPEN "COM2:2400,n,8,1,cs,ds,cd" FOR RANDOM AS 2

,

,

'Inits

,

DIM f(500), R(500), X(500), rt(50), cyc(50), ot(50), tc(50)

DIM filetot\$(50)

COLOR 15, 1

DEFINT I

iC.R = &H2EC + 1

```

iS.R = &H2EC + 1
ON ERROR GOTO 10000
8 i = 0
k = 0
rt(0) = 25
ikey = 0
tf = 1

```

```

*****

```

```

*****

```

```

'Input Temperatures of Study

```

```

CLS
PRINT " Input measurement temperatures (C) in order. Type (-1) to end"
PRINT
12   k = k + 1
14   PRINT "Temperature Number "; k: INPUT rt(k)
IF rt(k) > 155 OR rt(k) < -60 THEN PRINT "Sorry, out of range.": GOTO 14
IF rt(k) = -1 THEN cycle = k - 1 ELSE GOTO 12
PRINT : CLS : PRINT "Temps (C) are ": PRINT
FOR k = 1 TO cycle: PRINT rt(k): NEXT k
PRINT " Press spacebar to continue"
DO: LOOP UNTIL INKEY$ = " "

```

```

*****

```

```

*****

```

```

'Specify Frequency File

```

```

CLS
PRINT
PRINT "Enter the frequency filename"
INPUT "(Do not use an extension) "; ff$
file$ = ff$ + ".frq"
OPEN file$ FOR INPUT AS #5
INPUT #5, sf

```

```

*****

```

```

*****

```

```

,
'Specify the Output File
,
PRINT "Enter the output filename"
INPUT "(Do not use an extension)"; filename$
PRINT #1, "OP 1,1"
start = TIMER
DO: LOOP WHILE TIMER - start < 2
PRINT #1, "xo 1"
start = TIMER
DO: LOOP WHILE TIMER - start < 2
PRINT #1, "rh 0"
start = TIMER
DO: LOOP WHILE TIMER - start < 2
PRINT #1, "ec 0"
start = TIMER
DO: LOOP WHILE TIMER - start < 2
PRINT #1, "rr 0"
start = TIMER
DO: LOOP WHILE TIMER - start < 2
PRINT #1, "rt 2"
start = TIMER
DO: LOOP WHILE TIMER - start < 2
PRINT #1, "cz 0"
start = TIMER
DO: LOOP WHILE TIMER - start < 2
PRINT #1, "ra 3,0"
,
*****

*****
,
'Specify the Voltage Amplitude
,
PRINT
INPUT "voltage amplitude "; va
PRINT #1, "va "; va
FOR m = 1 TO sf
INPUT #5, f(m)
NEXT m
CLOSE #5
PRINT #1, "sw 0"
PRINT ""

```

```

PRINT "Ready to run the experiment"
PRINT
PRINT "Press the spacebar to continue": DO: LOOP UNTIL INKEY$ = " ": CLS
,
*****

*****
,
'Set the Oven Temperature, Obtain Three Temperatures, and Run
,
FOR i = 1 TO cycle
file$ = filename$ + "a" + LTRIM$(STR$(i)) + "." + LTRIM$(STR$(rt(i)))
filetot$(i) = file$
OPEN file$ FOR OUTPUT AS #3
FOR j = 1 TO 3
ot(j) = 0
NEXT j
rtc$ = LTRIM$(str$(rt(i))) + "C"
PRINT #2, rtc$
start = TIMER
DO: LOOP WHILE TIMER - start < 2
PRINT #2, rtc$: PRINT
PRINT "Setting oven to "; STR$(rt(i)); " C"
IF ABS(rt(i) - rt(i - 1)) > 11 THEN timefac = .1
IF rt(i) < rt(i - 1) THEN timefac = .1 * timefac
start = TIMER
DO
LOCATE 3, 2
PRINT "Time (in seconds) until data aquisition: "; INT(tf * 6000 - (TIMER - start))
LOOP WHILE TIMER - start < tf * 6000
tf = 1
PRINT
FOR j = 1 TO 3
PRINT "Temperature #"; j; " measured as ";
start = TIMER
DO
LOOP WHILE TIMER - start < 30
board% = &H200: gain% = 100: OUT board% + 3, &H90: OUT board% + 2, 1
tresult = 0
FOR sample = 1 TO 10
OUT board% + 3, 5
7020 eoc% = INP(board% + 4) AND 1
IF eoc% <> 1 GOTO 7020

```



```

7040 eoc% = INP(board% + 4) AND 1
IF eoc% <> 0 GOTO 7040
OUT board% + 3, 6: msb% = INP(board%): polarity% = msb% AND 128
OUT board% + 3, 7: lsb% = INP(board%): msb% = (msb% AND 15) * 256
result% = msb% + lsb%
IF polarity% < 128 THEN result% = result% * -1
tresult = tresult + result%
NEXT sample
rr = tresult / 4096000
t = .10086091# + rr * 25727.9437# - 767345.829# * rr ^ 2 + 78025595.81# * rr ^ 3 -
9247486589# * rr ^ 4 + 6.97688E+11 * rr ^ 5 - 2.66192E+13 * rr ^ 6 + 3.94078E+14 *
rr ^ 7
ot(j) = 32! + t
LOCATE (j + 4), 16
PRINT USING "####.#"; ot(j)
start = TIMER
DO: LOOP WHILE TIMER - start < 30
NEXT j
PRINT
PRINT #3, sf, USING "####.#"; ot(1); ot(2); ot(3)
PRINT "Frequency (Hz)"; " R (Ohms)", "X(Ohms)"
PRINT
FOR m = 1 TO sf
PRINT #1, "fr "; f(m)
start = TIMER
DO: LOOP WHILE TIMER - start < 2
PRINT #1, "si "
INPUT #1, f(m), R(m), X(m), g$, g$
PRINT USING "##.##^"; f(m); R(m); X(m)
PRINT #3, USING "##.##^"; f(m); R(m); X(m)
NEXT m
IF ikey = 1 THEN i = i + 1
CLOSE #3

```

```

*****

```

```

'Switch Cells

```

```

GOSUB 50000

```

```

*****

```

```

file$ = filename$ + "b" + LTRIMS$(STR$(i)) + "." + LTRIMS$(STR$(rt(i)))
filetot$(i) = file$
OPEN file$ FOR OUTPUT AS #3
CLS
PRINT
PRINT #3, sf, USING "####.#"; ot(1); ot(2); ot(3)
PRINT "Frequency (Hz)", "R (Ohms)", X(Ohms); ":print"
FOR m = 1 TO sf
PRINT #1, "fr "; f(m)
start = TIMER
DO: LOOP WHILE TIMER - start < 2
PRINT #1, "si "
INPUT #1, f(m), R(m), X(m), g$, g$
PRINT USING "##.##^" "; f(m); R(m); X(m)
PRINT #3, USING "##.##^" "; f(m); R(m); X(m)
NEXT m
IF ikey = 1 THEN i = i + 1
CLOSE #3

```

```

NEXT i
PRINT #2, "OFF"
start = TIMER
DO: LOOP WHILE TIMER - start < 2
PRINT #2, "OFF"
CLS
PRINT "The experiment has concluded."
PRINT ""
PRINT "The following files were constructed:"
FOR i = 1 TO cycle
PRINT filetot$(i)
NEXT i
PRINT "Press the spacebar to continue": DO: LOOP UNTIL INKEY$ = " ": CLS
GOTO 8

```

```

'*****

```

```

'*****

```

```

'On Error

```

,
10000 RESUME NEXT
,

,
'Switch Cells
,

50000

Switch% = 1

LPRINT CHR\$(Switch%)

RETURN
,

APPENDIX B
A QuickBASIC 4.5 Program to Control a EG&G Princeton Applied Research 362
Scanning Potentiostat for Modified Galvanostatic Intermittent Titration Technique
Measurements

Richard L. Nafshun and Michael M. Lerner*

*Department of Chemistry and Center for
Advanced Materials Research
Oregon State University
Corvallis, Oregon 97331-4003, USA*

A2.1 Introduction.

The following program is written in QuickBASIC 4.5. It controls an EG&G Princeton Applied Research 362 Scanning Potentiostat (PAR) for modified galvanostatic intermittent titration technique (MGITT) measurements. A Data Translation DT2801-A Single Board Analog and Digital I/O System is used to send one analog signal and receive two analog signals to and from the PAR. The output potential controls the current the PAR supplies to the sample cell. The two potentials received from the PAR correspond to the current through the sample cell and the observed potential.

**

' MPCB09.BAS [A.K.A. Pulse.bas]

' MPotCon.bas

' Version b0.9.1

' Mini Scanning Potentiostat Control Program

' This program controls the EG&G Scanning Potentiostat Model 362

' The user is asked for the full set of parameters

' This program pulses the 362

' This program applies a specified current and monitors the
' current and the potential

' The user may then plot the potential versus time

' The user is prompted for the pulse time and the current

' April 1, 1994 - April 15, 1994

' MML Group

' Oregon State University

' Department of Chemistry

' Richard L. Nafshun

' Copyright 1994 ZeekSoft

' "Fads Beneath Us"

' ZZZZZZZZZZZZ	EEEEEEEEEEEE	EEEEEEEEEEEE	KK	KKK
' ZZ	EE	EE	KK	KKK
' ZZ	EE	EE	KK	KKK
' ZZ	EEEEEEEE	EEEEEEEE	KKKK	
' ZZ	EE	EE	KK	KKK
' ZZ	EE	EE	KK	KKK

```

' ZZZZZZZZZZZZ EEEEEEEEEEEE EEEEEEEEEEEE KK KKK
'
' SSSSSSSSSSSS OOOOOOOOOOOO FFFFFFFF TTTTTTTTTT
' SS          OO          OO FF          TT
' SS          OO          OO FF          TT
' SSSSSSSSSSSS OO          OO FFFFFFFF TT
'          SS OO          OO FF          TT
'          SS OO          OO FF          TT
' SSSSSSSSSSSS OOOOOOOOOOOO FF          TT
'
'
'

```

' This program was written using QuickBasic 4.5

```

'*****
**

```

```

'*****
**
'*****
**
'

```

' Main Body

MainBody:

```

GOSUB InputFileName
GOSUB InputCurrentRange
GOSUB InputPulseLength
GOSUB InputAfterPulseLength
GOSUB InputPulseTime
GOSUB InputVoltageRange
GOSUB InputCurrentFraction
GOSUB ParametersToScreen
GOSUB ConfirmCurrentRangeSet
GOSUB WriteDataFile
GOSUB WriteToScreen

      GOSUB SendPulseTo362
      GOSUB WaitUntilPulseTime
      GOSUB ReceivePulseFrom362

```

```

GOSUB UpdateScreen
GOSUB UpdateDataFile

GOSUB SendAfterPulseTo362
GOSUB WaitUntilAfterPulseTime
GOSUB ReceiveAfterPulseFrom362
GOSUB UpdateScreen
GOSUB UpdateDataFile
GOSUB WriteFinalScreen
CLOSE #1
END
'
'*****
**
'*****
**

'*****
**
'
' FreshScreen
'
FreshScreen:
CLS
PRINT
PRINT
PRINT "          MML Group PAR Software"
PRINT
PRINT "          Pulsing Program MPCONb9.bas"
PRINT
PRINT "-----"
PRINT
PRINT
PRINT
RETURN
'
'
'*****
**

'*****
**
'

```



```
' Input File Name
```

```
,
```

```
InputFileName:
```

```
GOSUB FreshScreen
```

```
PRINT "      Please enter the filename for this trial; use no extensions."
```

```
PRINT
```

```
INPUT "      The filename of this trial is: ", FileName$
```

```
PRINT
```

```
RETURN
```

```
,
```

```
,
```

```
*****
```

```
**
```

```
*****
```

```
**
```

```
,
```

```
' Input the Current Range (As set on the Scanning Potentiostat.)
```

```
,
```

```
InputCurrentRange:
```

```
GOSUB FreshScreen
```

```
PRINT "      Please enter the current range."
```

```
PRINT
```

```
PRINT "      This current range corresponds to the current range selected"
```

```
PRINT "      on the EG&G Scanning Potentiostat."
```

```
PRINT
```

```
PRINT "      (a) 1 micro Amp"
```

```
PRINT "      (b) 10 micro Amps"
```

```
PRINT "      (c) 100 micro Amps"
```

```
PRINT "      (d) 1 mA"
```

```
PRINT "      (e) 10 mA"
```

```
PRINT "      (f) 100 mA"
```

```
PRINT "      (g) 1 A"
```

```
PRINT
```

```
INPUT "      Please enter the letter that corresponds to your choice: ", CurrentRange$
```

```
CurrentRange = 0
```

```
IF (CurrentRange$ = "a") OR (CurrentRange$ = "A") THEN CurrentRange = .000001 *  
1000
```

```
IF (CurrentRange$ = "b") OR (CurrentRange$ = "B") THEN CurrentRange = .00001 *  
1000
```

```
IF (CurrentRange$ = "c") OR (CurrentRange$ = "C") THEN CurrentRange = .0001 *  
1000
```

```

IF (CurrentRange$ = "d") OR (CurrentRange$ = "D") THEN CurrentRange = .001 *
1000
IF (CurrentRange$ = "e") OR (CurrentRange$ = "E") THEN CurrentRange = .01 * 1000
IF (CurrentRange$ = "f") OR (CurrentRange$ = "F") THEN CurrentRange = .1 * 1000
IF (CurrentRange$ = "g") OR (CurrentRange$ = "G") THEN CurrentRange = 1! * 1000
RETURN
,
,

*****
**

*****
**
,
' Input the Length (in seconds) of the Pulse
,
InputPulseLength:
GOSUB FreshScreen
PRINT "      Enter the length of time for the pulse; in seconds."
PRINT
PRINT
PRINT
PRINT
PRINT
PRINT
INPUT "      The length of the pulse (in seconds) is: ", PulseLength
RETURN
,
,

*****
**

*****
**
,
' Input the number of points per second
,
InputPulseTime:
GOSUB FreshScreen
PRINT "      Enter the number of points to be taken per second."
PRINT

```

```

PRINT
PRINT
PRINT
PRINT
INPUT "      The number of points to be taken per second is: ", PointsPerSecond
TimeBetweenPoints = 1 / PointsPerSecond
RETURN
'
'
'*****
**

'*****
**
'
' Input the Length (in seconds) after the Pulse
'
InputAfterPulseLength:
GOSUB FreshScreen
PRINT "      Enter the length of time after the pulse; in seconds."
PRINT
PRINT
PRINT
PRINT
PRINT
INPUT "      The length of time after the pulse (in seconds) is: ", Length
RETURN
'
'
'*****
**

'*****
**
'
' Input the MINIMUM and MAXIMUM Voltages (in volts) of the Current Segment'

```

InputVoltageRange:

GOSUB FreshScreen

PRINT " Enter the MINIMUM voltage for the segment; in volts."

PRINT

INPUT " The MINIMUM voltage (in volts) is: ", MinVoltage

PRINT

PRINT " Enter the MAXIMUM voltage for the segment; in volts."

PRINT

INPUT " The MAXIMUM voltage (in volts) is: ", MaxVoltage

PRINT

PRINT

RETURN

,

,

**

**

,

' Input the Current

,

InputCurrentFraction:

GOSUB FreshScreen

PRINT " Please enter the current fraction for the segment."

PRINT

PRINT

PRINT " Please enter the current in the fraction"

PRINT " of the current range you have selected."

PRINT

PRINT

PRINT

PRINT " The current you you have selected is "; CurrentRange; "mA."

PRINT

INPUT " The percent of the current range (e.g. 0.2) is: "; PC#

VoltageOut# = PC#

RETURN

,

,

**

```

*****
**
'
' Write the Parameters to the Screen
'
ParametersToScreen:
PRINT
GOSUB FreshScreen
Today$ = DATE$
Clock$ = TIME$
PRINT
PRINT "          "; Today$; "          "; Clock$
PRINT
PRINT " The filename of this trial is "; Filename$; ". "; "dat."
PRINT " The current range is "; CurrentRange; "mA."
PRINT " The pulse length is "; PulseLength; " seconds."
PRINT " The fraction of the current range is "; PC#; "."
PRINT
INPUT " Press 'C' to change these parameters. Press <Enter> to continue.", Chk$
IF (Chk$ = "c") OR (Chk$ = "C") THEN END
RETURN
'
'
*****
**

*****
**
'
' Write "Confirm Current Range Set" message to the screen
'
ConfirmCurrentRangeSet:
GOSUB FreshScreen
PRINT
PRINT
PRINT
PRINT " Please make certain the Current Range on the 362 is set for"; CurrentRange;
"mA."
PRINT
PRINT

```

```

PRINT
INPUT "                Please press <Enter> to continue.", Y$
PRINT
PRINT
PRINT
RETURN
'
'
'*****
**

'*****
**
'
' Write The Data File
'
WriteDataFile:
Today$ = DATES$
Clock$ = TIMES$
DataFile$ = Filename$ + ".prn"
OPEN DataFile$ FOR OUTPUT AS #1
PRINT #1, "Data File:", DataFile$
PRINT #1, "Date = ", Today$
PRINT #1, "Time = ", Clock$
PRINT #1, "CR (mA) = ", CurrentRange
PRINT #1, "CF = ", PC#
PRINT #1, "PL = (s):", PulseLength
PRINT #1, "Pts/s = ", PointsPerSecond
'
'
'*****
**

'*****
**
'
'
'
SendPulseTo362:

BASE.ADDRESS = &H2EC

```

```

COMMAND.REGISTER = BASE.ADDRESS + 1
STATUS.REGISTER = BASE.ADDRESS + 1
DATA.REGISTER = BASE.ADDRESS
COMMAND.WAIT = &H4
WRITE.WAIT = &H2
READ.WAIT = &H5
CSTOP = &HF
CCLEAR = &H1
CERROR = &H2
CDAOUT = &H8
EXT.TRIGGER = &H80

```

```

Offset = 5
Range = 10
FACTOR = 4096

```

```
STATUS = INP(STATUS.REGISTER)
```

```
'    Stop and clear the DT2801.
```

```

OUT COMMAND.REGISTER, CSTOP
TEMP = INP(DATA.REGISTER)
WAIT STATUS.REGISTER, COMMAND.WAIT
OUT COMMAND.REGISTER, CCLEAR
DAC.SELECT = 0

```

```
DAC.RANGE = 4
```

```
Volts# = VoltageOut#
```

```
'    Calculate DAC data value.
```

```

DATA.VALUE# = (Volts# + Offset) * FACTOR
DATA.VALUE# = CINT(DATA.VALUE# / Range)
IF DATA.VALUE# <= (FACTOR - 1) THEN GOTO OutputVoltage
DATA.VALUE# = FACTOR - 1

```

```
'    Calculate and print out rounded DAC output voltage.
```

```
OutputVoltage:
```

```

Volts# = DATA.VALUE# * Range / FACTOR
Volts# = Volts# - Offset

```

' Write WRITE DAC IMMEDIATE command.

WAIT STATUS.REGISTER, COMMAND.WAIT
OUT COMMAND.REGISTER, CDAOUT

' Write DAC SELECT byte.

WAIT STATUS.REGISTER, WRITE.WAIT, WRITE.WAIT
OUT DATA.REGISTER, DAC.SELECT

' Write high and low bytes of DATA.VALUE#.

HIGH = INT(DATA.VALUE# / 256)
LOW = DATA.VALUE# - HIGH * 256
WAIT STATUS.REGISTER, WRITE.WAIT, WRITE.WAIT
OUT DATA.REGISTER, LOW
WAIT STATUS.REGISTER, WRITE.WAIT, WRITE.WAIT
OUT DATA.REGISTER, HIGH

RETURN

'
'

**

**

'
'
'

ReceivePulseFrom362:

'Channel 0

BASE.ADDRESS = &H2EC
COMMAND.REGISTER = BASE.ADDRESS + 1
STATUS.REGISTER = BASE.ADDRESS + 1
DATA.REGISTER = BASE.ADDRESS
COMMAND.WAIT = &H4
WRITE.WAIT = &H2
READ.WAIT = &H5


```

CSTOP = &HF
CCLEAR = &H1
CERROR = &H2
CADIN = &HC
EXT.TRIGGER = &H80

```

```

'   A/D parameter constants.

```

```

PGH(0) = 1: PGH(1) = 2: PGH(2) = 4: PGH(3) = 8
PGL(0) = 1: PGL(1) = 10: PGL(2) = 100: PGL(3) = 500
PGX(0) = 1: PGX(1) = 1: PGX(2) = 1: PGX(3) = 1

```

```

'   Check for legal Status Register.

```

```

STATUS = INP(STATUS.REGISTER)

```

```

'   Stop and clear the DT2801.

```

```

OUT COMMAND.REGISTER, CSTOP
TEMP = INP(DATA.REGISTER)
WAIT STATUS.REGISTER, COMMAND.WAIT
OUT COMMAND.REGISTER, CCLEAR

```

```

FACTOR# = 4096
Gain(0) = PGH(0): Gain(1) = PGH(1)
Gain(2) = PGH(2): Gain(3) = PGH(3)

```

```

Range = 20
Offset = 10

```

```

Number.Channels = 8

```

```

'   Get A/D gain.
Gain.Code = 1

```

```

'   Get A/D channel.

```

```

Channel = 0

```

```

'   Write READ A/D IMMEDIATE command.

```

```

WAIT STATUS.REGISTER, COMMAND.WAIT
OUT COMMAND.REGISTER, CADIN

```

' Write A/D gain byte.

WAIT STATUS.REGISTER, WRITE.WAIT, WRITE.WAIT
OUT DATA.REGISTER, Gain.Code

' Write A/D channel byte.

WAIT STATUS.REGISTER, WRITE.WAIT, WRITE.WAIT
OUT DATA.REGISTER, Channel

' Read two bytes of A/D data from the Data Out Register,
' and combine the two bytes into one word.

WAIT STATUS.REGISTER, READ.WAIT
LOW = INP(DATA.REGISTER)
WAIT STATUS.REGISTER, READ.WAIT
HIGH = INP(DATA.REGISTER)
DATA.VALUE# = HIGH * 256 + LOW

' Calculate and print the A/D reading in volts.

Volts# = ((Range * DATA.VALUE# / FACTOR#) - Offset) / Gain(Gain.Code)
ChannelVoltage# = Volts#

'Channel 1

BASE.ADDRESS = &H2EC
COMMAND.REGISTER = BASE.ADDRESS + 1
STATUS.REGISTER = BASE.ADDRESS + 1
DATA.REGISTER = BASE.ADDRESS
COMMAND.WAIT = &H4
WRITE.WAIT = &H2
READ.WAIT = &H5

CSTOP = &HF
CCLEAR = &H1
CERROR = &H2
CADIN = &HC
EXT.TRIGGER = &H80

' A/D parameter constants.

PGH(0) = 1: PGH(1) = 2: PGH(2) = 4: PGH(3) = 8
 PGL(0) = 1: PGL(1) = 10: PGL(2) = 100: PGL(3) = 500
 PGX(0) = 1: PGX(1) = 1: PGX(2) = 1: PGX(3) = 1

' Check for legal Status Register.

STATUS = INP(STATUS.REGISTER)

' Stop and clear the DT2801.

OUT COMMAND.REGISTER, CSTOP
 TEMP = INP(DATA.REGISTER)
 WAIT STATUS.REGISTER, COMMAND.WAIT
 OUT COMMAND.REGISTER, CCLEAR

FACTOR# = 4096
 Gain(0) = PGH(0): Gain(1) = PGH(1)
 Gain(2) = PGH(2): Gain(3) = PGH(3)

Range = 20
 Offset = 10

Number.Channels = 8

' Get A/D gain.
 Gain.Code = 1

' Get A/D channel.

Channel = 1

' Write READ A/D IMMEDIATE command.

WAIT STATUS.REGISTER, COMMAND.WAIT
 OUT COMMAND.REGISTER, CADIN

' Write A/D gain byte.

WAIT STATUS.REGISTER, WRITE.WAIT, WRITE.WAIT
 OUT DATA.REGISTER, Gain.Code

' Write A/D channel byte.

WAIT STATUS.REGISTER, WRITE.WAIT, WRITE.WAIT
OUT DATA.REGISTER, Channel

' Read two bytes of A/D data from the Data Out Register,
' and combine the two bytes into one word.

WAIT STATUS.REGISTER, READ.WAIT
LOW = INP(DATA.REGISTER)
WAIT STATUS.REGISTER, READ.WAIT
HIGH = INP(DATA.REGISTER)
DATA.VALUE# = HIGH * 256 + LOW

' Calculate and print the A/D reading in volts.

Volts# = ((Range * DATA.VALUE# / FACTOR#) - Offset) / Gain(Gain.Code)
Channel1 Voltage# = Volts#

Ch# = Channel1 Voltage#

RETURN

'
'

**

**

'
'
'

SendAfterPulseTo362:

BASE.ADDRESS = &H2EC
COMMAND.REGISTER = BASE.ADDRESS + 1
STATUS.REGISTER = BASE.ADDRESS + 1
DATA.REGISTER = BASE.ADDRESS
COMMAND.WAIT = &H4
WRITE.WAIT = &H2
READ.WAIT = &H5
CSTOP = &HF
CCLEAR = &H1

```

CERROR = &H2
CDAOUT = &H8
EXT.TRIGGER = &H80

```

```

Offset = 5
Range = 10
FACTOR = 4096

```

```

STATUS = INP(STATUS.REGISTER)

```

```

'   Stop and clear the DT2801.

```

```

OUT COMMAND.REGISTER, CSTOP
TEMP = INP(DATA.REGISTER)
WAIT STATUS.REGISTER, COMMAND.WAIT
OUT COMMAND.REGISTER, CCLEAR
DAC.SELECT = 0

```

```

DAC.RANGE = 4

```

```

Volts# = 0!

```

```

'   Calculate DAC data value.

```

```

DATA.VALUE# = (Volts# + Offset) * FACTOR
DATA.VALUE# = CINT(DATA.VALUE# / Range)
IF DATA.VALUE# <= (FACTOR - 1) THEN GOTO OutputVoltage3
DATA.VALUE# = FACTOR - 1

```

```

'   Calculate and print out rounded DAC output voltage.

```

```

OutputVoltage3:

```

```

Volts# = DATA.VALUE# * Range / FACTOR
Volts# = Volts# - Offset

```

```

'   Write WRITE DAC IMMEDIATE command.

```

```

WAIT STATUS.REGISTER, COMMAND.WAIT
OUT COMMAND.REGISTER, CDAOUT

```

```

'   Write DAC SELECT byte.

```

```
WAIT STATUS.REGISTER, WRITE.WAIT, WRITE.WAIT
OUT DATA.REGISTER, DAC.SELECT
```

```
' Write high and low bytes of DATA.VALUE#.
```

```
HIGH = INT(DATA.VALUE# / 256)
LOW = DATA.VALUE# - HIGH * 256
WAIT STATUS.REGISTER, WRITE.WAIT, WRITE.WAIT
OUT DATA.REGISTER, LOW
WAIT STATUS.REGISTER, WRITE.WAIT, WRITE.WAIT
OUT DATA.REGISTER, HIGH
```

```
RETURN
```

```
,
```

```
,
```

```
*****
```

```
**
```

```
*****
```

```
**
```

```
,
```

```
,
```

```
,
```

```
ReceiveAfterPulseFrom362:
```

```
'Channel 0
```

```
BASE.ADDRESS = &H2EC
COMMAND.REGISTER = BASE.ADDRESS + 1
STATUS.REGISTER = BASE.ADDRESS + 1
DATA.REGISTER = BASE.ADDRESS
COMMAND.WAIT = &H4
WRITE.WAIT = &H2
READ.WAIT = &H5
```

```
CSTOP = &HF
CCLEAR = &H1
CERROR = &H2
CADIN = &HC
EXT.TRIGGER = &H80
```

```
' A/D parameter constants.
```

PGH(0) = 1: PGH(1) = 2: PGH(2) = 4: PGH(3) = 8
 PGL(0) = 1: PGL(1) = 10: PGL(2) = 100: PGL(3) = 500
 PGX(0) = 1: PGX(1) = 1: PGX(2) = 1: PGX(3) = 1

' Check for legal Status Register.

STATUS = INP(STATUS.REGISTER)

' Stop and clear the DT2801.

OUT COMMAND.REGISTER, CSTOP
 TEMP = INP(DATA.REGISTER)
 WAIT STATUS.REGISTER, COMMAND.WAIT
 OUT COMMAND.REGISTER, CCLEAR

FACTOR# = 4096
 Gain(0) = PGH(0): Gain(1) = PGH(1)
 Gain(2) = PGH(2): Gain(3) = PGH(3)

Range = 20
 Offset = 10

Number.Channels = 8

' Get A/D gain.
 Gain.Code = 1

' Get A/D channel.

Channel = 0

' Write READ A/D IMMEDIATE command.

WAIT STATUS.REGISTER, COMMAND.WAIT
 OUT COMMAND.REGISTER, CADIN

' Write A/D gain byte.

WAIT STATUS.REGISTER, WRITE.WAIT, WRITE.WAIT
 OUT DATA.REGISTER, Gain.Code

' Write A/D channel byte.

WAIT STATUS.REGISTER, WRITE.WAIT, WRITE.WAIT
OUT DATA.REGISTER, Channel

' Read two bytes of A/D data from the Data Out Register,
' and combine the two bytes into one word.

WAIT STATUS.REGISTER, READ.WAIT
LOW = INP(DATA.REGISTER)
WAIT STATUS.REGISTER, READ.WAIT
HIGH = INP(DATA.REGISTER)
DATA.VALUE# = HIGH * 256 + LOW

' Calculate and print the A/D reading in volts.

Volts# = ((Range * DATA.VALUE# / FACTOR#) - Offset) / Gain(Gain.Code)
Channel0Voltage# = Volts#

'Channel 1

BASE.ADDRESS = &H2EC
COMMAND.REGISTER = BASE.ADDRESS + 1
STATUS.REGISTER = BASE.ADDRESS + 1
DATA.REGISTER = BASE.ADDRESS
COMMAND.WAIT = &H4
WRITE.WAIT = &H2
READ.WAIT = &H5

CSTOP = &HF
CCLEAR = &H1
CERROR = &H2
CADIN = &HC
EXT.TRIGGER = &H80

' A/D parameter constants.

PGH(0) = 1: PGH(1) = 2: PGH(2) = 4: PGH(3) = 8
PGL(0) = 1: PGL(1) = 10: PGL(2) = 100: PGL(3) = 500
PGX(0) = 1: PGX(1) = 1: PGX(2) = 1: PGX(3) = 1

' Check for legal Status Register.

STATUS = INP(STATUS.REGISTER)

' Stop and clear the DT2801.

OUT COMMAND.REGISTER, CSTOP

TEMP = INP(DATA.REGISTER)

WAIT STATUS.REGISTER, COMMAND.WAIT

OUT COMMAND.REGISTER, CCLEAR

FACTOR# = 4096

Gain(0) = PGH(0): Gain(1) = PGH(1)

Gain(2) = PGH(2): Gain(3) = PGH(3)

Range = 20

Offset = 10

Number.Channels = 8

' Get A/D gain.

Gain.Code = 1

' Get A/D channel.

Channel = 1

' Write READ A/D IMMEDIATE command.

WAIT STATUS.REGISTER, COMMAND.WAIT

OUT COMMAND.REGISTER, CADIN

' Write A/D gain byte.

WAIT STATUS.REGISTER, WRITE.WAIT, WRITE.WAIT
OUT DATA.REGISTER, Gain.Code

' Write A/D channel byte.

WAIT STATUS.REGISTER, WRITE.WAIT, WRITE.WAIT
OUT DATA.REGISTER, Channel

' Read two bytes of A/D data from the Data Out Register,
' and combine the two bytes into one word.

```

WAIT STATUS.REGISTER, READ.WAIT
LOW = INP(DATA.REGISTER)
WAIT STATUS.REGISTER, READ.WAIT
HIGH = INP(DATA.REGISTER)
DATA.VALUE# = HIGH * 256 + LOW

```

```

' Calculate and print the A/D reading in volts.

```

```

Volts# = ((Range * DATA.VALUE# / FACTOR#) - Offset) / Gain(Gain.Code)
ChannellVoltage# = Volts#

```

```

Ch# = ChannellVoltage#

```

```

RETURN

```

```

'

```

```

'

```

```

*****
**

```

```

*****
**

```

```

'

```

```

' Check The Time

```

```

'

```

```

WaitUntilPulseTime:
KEY(1) ON
TotalLength = (PulseLength + Length) * PointsPerSecond
TimeZero = TIMER
OldTime = TIMER
NewTime = TIMER
FOR PointNumber = 0 TO (PulseLength) STEP TimeBetweenPoints
DO WHILE NewTime < OldTime + PointNumber
NewTime = TIMER
ON KEY(1) GOSUB StopProgram
LOOP
GOSUB ReceivePulseFrom362
GOSUB UpdateScreen
GOSUB UpdateDataFile
NEXT PointNumber

```

RETURN

,

**

**

,

' Check The Time

,

WaitUntilAfterPulseTime:

KEY(1) ON

OldTime = TIMER

NewTime = TIMER

FOR PointNumber = 0 TO (Length) STEP TimeBetweenPoints

DO WHILE NewTime < OldTime + PointNumber

NewTime = TIMER

ON KEY(1) GOSUB StopProgram

LOOP

GOSUB ReceiveAfterPulseFrom362

GOSUB UpdateScreen

GOSUB UpdateDataFile

NEXT PointNumber

INPUT " "; WaitUntilReturn\$

RETURN

,

**

**

,

UpdateDataFile:

ElapsedTime = NewTime - TimeZero

PRINT #1, USING "##.###"; ElapsedTime; Channel0Voltage#; Channel1Voltage#

RETURN

```

'
'
*****
**

*****
**
'
' StopProgram
'
StopProgram:
'
'
CLS
PRINT
PRINT "F1 was pressed. The trial was terminated."
KEY(1) OFF
END
'
*****
**

*****
**
'
' WriteFinalScreen: Write Final Stats To The Screen
'
WriteFinalScreen:
'
PRINT
GOSUB FreshScreen
Today$ = DATE$
Clock$ = TIME$
PRINT
PRINT "          Experiment Parameters"
PRINT "          "; Today$, "          "; Clock$
PRINT
PRINT " The file for the trial just completed is "; Filename$, ".PRN"
PRINT
PRINT " Thank you for choosing ZeekSoft."

```

RETURN

,

,

**

*

,

' Write The Plot To The Screen

,

WriteToScreen:

CLS

SCREEN 12

**

' Draw Plot

,

WINDOW (-100, -100)-(100, 100)

LINE (-90, -50)-(90, 90), 3, B

LINE (-90, 90)-(-88, 92), 3

LINE (-88, 92)-(92, 92), 3

LINE (92, 92)-(92, -48), 3

LINE (92, -48)-(90, -50), 3

LINE (90, 90)-(92, 92), 3

LINE (0, -50)-(0, 90), 3

LINE (-45, -50)-(-45, 90), 3

LINE (45, -50)-(45, 90), 3

LINE (-90, 20)-(90, 20), 3

LINE (-90, 55)-(90, 55), 3

LINE (-90, -15)-(90, -15), 3

FOR i = -90 TO 90

LINE (i, 72.5)-(i, 72.5), 3

LINE (i, 37.5)-(i, 37.5), 3

LINE (i, 2.5)-(i, 2.5), 3

LINE (i, -32.5)-(i, -32.5), 3

NEXT i

FOR i = -50 TO 90

LINE (-67.5, i)-(-67.5, i), 3

LINE (-22.5, i)-(-22.5, i), 3

LINE (22.5, i)-(22.5, i), 3

LINE (67.5, i)-(67.5, i), 3

NEXT i

**

' Title

,

LOCATE 1, 8

PRINT "Current File: "; DataFile\$

,

,

,

**

' X-axis Labels

,

LOCATE 24, 5

PRINT "0"

LOCATE 24, 20

PRINT ((Length + PulseLength) / 4)

LOCATE 24, 37

PRINT ((Length + PulseLength) / 2)

LOCATE 24, 55

PRINT ((3 * (Length + PulseLength)) / 4)

LOCATE 25, 36

PRINT "Time (s)"

,

,

**

' Y-axis labels

,

LOCATE 9, 80

PRINT "V"

LOCATE 10, 80

PRINT "o"

LOCATE 11, 80

PRINT "I"

LOCATE 12, 80

PRINT "t"

LOCATE 13, 80

PRINT "s"

Y1 = MinVoltage

Y5 = MaxVoltage

Y3 = (MaxVoltage + MinVoltage) / 2

```

Y2 = (Y1 + Y3) / 2
Y4 = (Y3 + Y5) / 2
LOCATE 2, 1
PRINT USING "##.##"; Y5
LOCATE 7, 1
PRINT USING "##.##"; Y4
LOCATE 13, 1
PRINT USING "##.##"; Y3
LOCATE 18, 1
PRINT USING "##.##"; Y2
LOCATE 23, 1
PRINT USING "##.##"; Y1
*****
**
' Write Statistics
'
LOCATE 28, 58
PRINT "Current = "
LOCATE 27, 5
PRINT "Voltage    = "
LOCATE 27, 58
PRINT "Charge ="
LOCATE 28, 5
PRINT "Elapsed Time ="
RETURN
'
'
*****
**

*****
**
'
' Update The Plot
'
UpdateScreen:
PlotTime = TIMER
ElapsedTime = PlotTime - TimeZero

LOCATE 28, 70
PRINT "    "

```

```

LOCATE 28, 70
PRINT USING "###.###"; Ch#;
PRINT " mA"

```

```

LOCATE 27, 24
PRINT "      "
LOCATE 27, 24
PRINT USING "###.###"; Channel0Voltage#;
PRINT " V"
LOCATE 28, 22
PRINT "      "
LOCATE 28, 22
PRINT USING "#####"; ElapsedTime;
PRINT " s"
LOCATE 27, 69
PRINT "      "
LOCATE 27, 69
PRINT USING "###.###"; CumulCharge#;
PRINT " C"

```

```

*****

```

```

**

```

```

,

```

```

, Write The Data Point
,

```

```

YCoord = (((Channel0Voltage# - MinVoltage) * 140 / (MaxVoltage - MinVoltage))) +
(-50)

```

```

XCoord = ((ElapsedTime * 180 / (Length + PulseLength))) + (-90)

```

```

LINE (XCoord, YCoord)-(XCoord, YCoord + 1), 10

```

```

RETURN
,
,

```

```

*****

```

```

**

```


APPENDIX C
A QuickBASIC 4.5 Program to Control a EG&G Princeton Applied Research 362
Scanning Potentiostat for Cyclic Voltammetry Measurements

Richard L. Nafshun and Michael M. Lerner*

*Department of Chemistry and Center for
Advanced Materials Research
Oregon State University
Corvallis, Oregon 97331-4003, USA*

A3.1 Introduction.

The following program is written in QuickBASIC 4.5. It controls an EG&G Princeton Applied Research 362 Scanning Potentiostat (PAR) for cyclic voltammetry measurements. A Data Translation DT2801-A Single Board Analog and Digital I/O System is used to send one analog signal and receive two analog signals to and from the PAR. The output potential controls the potential the PAR applies to the sample cell. The two potentials received from the PAR correspond to the current through the sample cell and the observed potential.

**

,

' MPCB06.BAS [A.K.A. CV.bas]

,

' MPotCon.bas

' Version b0.6.3

,

' Mini Scanning Potentiostat Control Program

,

' This program controls the EG&G Scanning Potentiostat Model 362

' The user is asked for the full set of parameters

,

' This program controls the 362 for cyclic voltammetry measurements

,

' This program applies a specified potential and monitors the

' current and the potential

,

' The user is prompted for the starting, minimum, and maximum

' potentials

,

' April 1, 1994 - May 27, 1994

' MML Group

' Oregon State University

' Department of Chemistry

,

,

' Richard L. Nafshun

,

,

,

,

' Copyright 1994 ZeekSoft

,

' "Speeding motorcycle, won't you change me?

' In a world of funny changes,

' Speeding motorcycle, won't you change me?

' Speeding motorcycle,

' Of my heart."

,

" This program was written using QuickBasic 4.5

,

```

*****
**
*****
**

*****
**
'
' Main Body
'
MainBody:
GOSUB InputFileName
GOSUB InputCurrentRange
GOSUB InputScanRate
GOSUB InputPotentials
GOSUB VoltageRange

    IF VOne > VStart THEN GOSUB PositiveScan
    IF VOne < VStart THEN GOSUB NegativeScan

GOSUB StartCV
GOSUB UpdateDataFile
GOSUB WriteFinalScreen
CLOSE #1
END
'
*****
**
*****
**

*****
**
'
' FreshScreen
'
FreshScreen:
CLS
PRINT
PRINT
PRINT "          MML Group PAR Software"
PRINT
PRINT "          Cyclic Voltammetry Program MPCONb6.bas"

```

```

PRINT
PRINT "-----"
PRINT
PRINT
PRINT
RETURN
'
'

*****
**

*****
**
'
' Input File Name
'
InputFileName:
GOSUB FreshScreen
PRINT "      Please enter the filename for this trial; use no extensions."
PRINT
INPUT "      The filename of this trial is: ", FileName$
PRINT
RETURN
'
'

*****
**

*****
**
'
' Input the Current Range (As set on the Scanning Potentiostat.)
'
InputCurrentRange:
GOSUB FreshScreen
PRINT "      Please enter the current range."
PRINT
PRINT "      This current range corresponds to the current range selected"
PRINT "      on the EG&G Scanning Potentiostat."
PRINT
PRINT "      (a) 1 micro Amp"
PRINT "      (b) 10 micro Amps"

```

```

PRINT "      (c) 100 micro Amps"
PRINT "      (d) 1 mA"
PRINT "      (e) 10 mA"
PRINT "      (f) 100 mA"
PRINT "      (g) 1 A"
PRINT
INPUT "      Please enter the letter that corresponds to your choice: ", CurrentRange$
CurrentRange = 0
IF (CurrentRange$ = "a") OR (CurrentRange$ = "A") THEN CurrentRange = .000001 *
1000
IF (CurrentRange$ = "b") OR (CurrentRange$ = "B") THEN CurrentRange = .00001 *
1000
IF (CurrentRange$ = "c") OR (CurrentRange$ = "C") THEN CurrentRange = .0001 *
1000
IF (CurrentRange$ = "d") OR (CurrentRange$ = "D") THEN CurrentRange = .001 *
1000
IF (CurrentRange$ = "e") OR (CurrentRange$ = "E") THEN CurrentRange = .01 * 1000
IF (CurrentRange$ = "f") OR (CurrentRange$ = "F") THEN CurrentRange = .1 * 1000
IF (CurrentRange$ = "g") OR (CurrentRange$ = "G") THEN CurrentRange = 1! * 1000
RETURN
'
'
'*****
**

'*****
**
'
' Input the Scan Rate (in mV/S) of the CV
'
InputScanRate:
GOSUB FreshScreen
PRINT "      Enter the scan rate for this trial (in mV/s)."
PRINT
PRINT
PRINT
PRINT
PRINT
PRINT
INPUT "      The scan rate (in mV/s) is: ", ScanRate
RETURN
'
'

```

```
*****
**
```

```
*****
**
```

```
' Input the potentials
```

```
InputPotentials:
```

```
GOSUB FreshScreen
```

```
PRINT " Enter the starting potential, the first turn around potential,"
```

```
PRINT " and the second turn around potential (in volts)."
```

```
PRINT
```

```
PRINT
```

```
INPUT " The starting potential (in Volts) is: ", VStart
```

```
PRINT
```

```
PRINT
```

```
INPUT " The first turn around potential (in Volts) is: ", VOne
```

```
PRINT
```

```
PRINT
```

```
INPUT " The second turn around potential (in Volts) is: ", VTwo
```

```
RETURN
```

```
'
```

```
'
```

```
*****
**
```

```
*****
**
```

```
' Calculate the voltage range for the plot
```

```
'
```

```
VoltageRange:
```

```
MaxVoltage = 10
```

```
FOR i = 9 TO -9 STEP -1
```

```

        IF (VOne < i) AND (VTwo < i) THEN MaxVoltage = i
    NEXT i

    MinVoltage = -10
    FOR i = -9 TO 9
        IF (VOne > i) AND (VTwo > i) THEN MinVoltage = i
    NEXT i

RETURN
'
'
'*****
**

'*****
**
'
' Positive scan
'
PositiveScan:

' Magnitudes of legs (in mV)

Leg1 = (VOne - VStart) * 1000
Leg2 = (VOne - VTwo) * 1000
Leg3 = (VStart - VTwo) * 1000
LegTotal = (Leg1 + Leg2 + Leg3)

ScanTime = LegTotal / ScanRate

ScanPoints = ScanTime * 10

NumberOfPoints = ScanPoints + 1

DIM DataPoint(NumberOfPoints)

DataPoint(1) = VStart

    VoltageOut# = DataPoint(1)
    GOSUB SendTo362
    GOSUB ConfirmCurrentRangeSet

Leg1Points = (Leg1 / ScanRate) * 10

```


VoltageIncrement = (Leg1 / 1000) / Leg1Points

StartPoint = 2

EndPoint = Leg1Points

```
FOR i = StartPoint TO EndPoint
    DataPoint(i) = DataPoint(i - 1) + VoltageIncrement
NEXT i
```

Leg2Points = (Leg2 / ScanRate) * 10

StartPoint = EndPoint + 1

EndPoint = (Leg1Points + Leg2Points)

```
FOR i = StartPoint TO EndPoint
    DataPoint(i) = DataPoint(i - 1) - VoltageIncrement
NEXT i
```

Leg3Points = (Leg3 / ScanRate) * 10

StartPoint = EndPoint + 1

EndPoint = (Leg1Points + Leg2Points + Leg3Points)

```
FOR i = StartPoint TO EndPoint
    DataPoint(i) = DataPoint(i - 1) + VoltageIncrement
NEXT i
```

RETURN

,

,

```
*****
**
```

```
*****
**
```

,

Negative scan

,

NegativeScan:

' Magnitudes of legs (in mV)

Leg1 = (VStart - VOne) * 1000

Leg2 = (VTwo - VOne) * 1000

Leg3 = (VTwo - VStart) * 1000

LegTotal = (Leg1 + Leg2 + Leg3)

ScanTime = LegTotal / ScanRate

ScanPoints = ScanTime * 10

NumberOfPoints = ScanPoints + 1

DIM DataPoint(NumberOfPoints)

DataPoint(1) = VStart

VoltageOut# = DataPoint(1)

GOSUB SendTo362

GOSUB ConfirmCurrentRangeSet

Leg1Points = (Leg1 / ScanRate) * 10

VoltageIncrement = (Leg1 / 1000) / Leg1Points

StartPoint = 2

EndPoint = Leg1Points

FOR i = StartPoint TO EndPoint

 DataPoint(i) = DataPoint(i - 1) - VoltageIncrement

NEXT i

Leg2Points = (Leg2 / ScanRate) * 10

StartPoint = EndPoint + 1

EndPoint = (Leg1Points + Leg2Points)

FOR i = StartPoint TO EndPoint

 DataPoint(i) = DataPoint(i - 1) + VoltageIncrement

NEXT i

Leg3Points = (Leg3 / ScanRate) * 10

StartPoint = EndPoint + 1

EndPoint = (Leg1Points + Leg2Points + Leg3Points)

FOR i = StartPoint TO EndPoint

 DataPoint(i) = DataPoint(i - 1) - VoltageIncrement

NEXT i

RETURN

,

,

**

**!

,

' Start the scan

,

StartCV:

,

,

**

**

,

' Write the Parameters to the Screen

,

ParametersToScreen:

GOSUB FreshScreen

Today\$ = DATES\$

Clock\$ = TIMES\$

PRINT

```

PRINT "          "; Today$; "          "; Clock$
PRINT
PRINT " The filename of this trial is "; Filename$; ". "; "prn."
PRINT " The current range is "; CurrentRange; "mA."
PRINT " The starting potential is "; VStart
PRINT " The first turn around potential is "; VOne
PRINT " The second turn around potential is "; VTwo
PRINT " The collection frequency is 10 Hz."
PRINT
INPUT " Press 'C' to change these parameters. Press <Enter> to continue.", Chk$
IF (Chk$ = "c") OR (Chk$ = "C") THEN END
RETURN
'
'
*****
**

*****
**
'
' Write "Confirm Current Range Set" message to the screen
'
ConfirmCurrentRangeSet:
GOSUB FreshScreen
PRINT
PRINT
PRINT
PRINT " Please make certain the Current Range on the 362 is set for"; CurrentRange;
"mA."
PRINT
PRINT " A potential of "; VStart; "volts is now being applied."
PRINT " You may now power up the 362."
PRINT
INPUT " Please press <Enter> to continue.", Y$
PRINT
PRINT
PRINT
RETURN
'
'

```

```
*****
**
```

```
*****
**
```

```
' Write The Data File
```

```
WriteDataFile:
```

```
Today$ = DATE$
```

```
Clock$ = TIME$
```

```
DataFile$ = Filename$ + ".prn"
```

```
OPEN DataFile$ FOR OUTPUT AS #1
```

```
PRINT #1, "Data File:", DataFile$
```

```
PRINT #1, "Date = ", Today$
```

```
PRINT #1, "Time = ", Clock$
```

```
PRINT #1, "Starting potential is", VStart
```

```
PRINT #1, "V1 is", VOne
```

```
PRINT #1, "V2 is", VTwo
```

```
PRINT #1, "Frequency is 10 Hz."
```

```
*****
**
```

```
*****
**
```

```
SendTo362:
```

```
BASE.ADDRESS = &H2EC
```

```
COMMAND.REGISTER = BASE.ADDRESS + 1
```

```
STATUS.REGISTER = BASE.ADDRESS + 1
```

```
DATA.REGISTER = BASE.ADDRESS
```

```
COMMAND.WAIT = &H4
```

```
WRITE.WAIT = &H2
```

```
READ.WAIT = &H5
```

```
CSTOP = &HF
```

```
CCLEAR = &H1
```

```

CERROR = &H2
CDAOUT = &H8
EXT.TRIGGER = &H80

```

```

Offset = 5
Range = 10
FACTOR = 4096

```

```

STATUS = INP(STATUS.REGISTER)

```

```

'   Stop and clear the DT2801.

```

```

OUT COMMAND.REGISTER, CSTOP
TEMP = INP(DATA.REGISTER)
WAIT STATUS.REGISTER, COMMAND.WAIT
OUT COMMAND.REGISTER, CCLEAR
DAC.SELECT = 0

```

```

DAC.RANGE = 4

```

```

Volts# = VoltageOut#

```

```

'   Calculate DAC data value.

```

```

DATA.VALUE# = (Volts# + Offset) * FACTOR
DATA.VALUE# = CINT(DATA.VALUE# / Range)
IF DATA.VALUE# <= (FACTOR - 1) THEN GOTO OutputVoltage
DATA.VALUE# = FACTOR - 1

```

```

'   Calculate and print out rounded DAC output voltage.

```

```

OutputVoltage:

```

```

Volts# = DATA.VALUE# * Range / FACTOR
Volts# = Volts# - Offset

```

```

'   Write WRITE DAC IMMEDIATE command.

```

```

WAIT STATUS.REGISTER, COMMAND.WAIT
OUT COMMAND.REGISTER, CDAOUT

```

```

'   Write DAC SELECT byte.

```

```
WAIT STATUS.REGISTER, WRITE.WAIT, WRITE.WAIT
OUT DATA.REGISTER, DAC.SELECT
```

```
' Write high and low bytes of DATA.VALUE#.
```

```
HIGH = INT(DATA.VALUE# / 256)
LOW = DATA.VALUE# - HIGH * 256
WAIT STATUS.REGISTER, WRITE.WAIT, WRITE.WAIT
OUT DATA.REGISTER, LOW
WAIT STATUS.REGISTER, WRITE.WAIT, WRITE.WAIT
OUT DATA.REGISTER, HIGH
```

```
RETURN
```

```
'
```

```
'
```

```
*****
**
```

```
*****
**
```

```
'
```

```
'
```

```
'
```

```
ReceivePulseFrom362:
```

```
'Channel 0
```

```
BASE.ADDRESS = &H2EC
COMMAND.REGISTER = BASE.ADDRESS + 1
STATUS.REGISTER = BASE.ADDRESS + 1
DATA.REGISTER = BASE.ADDRESS
COMMAND.WAIT = &H4
WRITE.WAIT = &H2
READ.WAIT = &H5
```

```
CSTOP = &HF
CCLEAR = &H1
CERROR = &H2
CADIN = &HC
EXT.TRIGGER = &H80
```

```
' A/D parameter constants.
```

PGH(0) = 1: PGH(1) = 2: PGH(2) = 4: PGH(3) = 8
 PGL(0) = 1: PGL(1) = 10: PGL(2) = 100: PGL(3) = 500
 PGX(0) = 1: PGX(1) = 1: PGX(2) = 1: PGX(3) = 1

' Check for legal Status Register.

STATUS = INP(STATUS.REGISTER)

' Stop and clear the DT2801.

OUT COMMAND.REGISTER, CSTOP
 TEMP = INP(DATA.REGISTER)
 WAIT STATUS.REGISTER, COMMAND.WAIT
 OUT COMMAND.REGISTER, CCLEAR

FACTOR# = 4096
 Gain(0) = PGH(0): Gain(1) = PGH(1)
 Gain(2) = PGH(2): Gain(3) = PGH(3)

Range = 20
 Offset = 10

Number.Channels = 8

' Get A/D gain.
 Gain.Code = 1

' Get A/D channel.

Channel = 0

' Write READ A/D IMMEDIATE command.

WAIT STATUS.REGISTER, COMMAND.WAIT
 OUT COMMAND.REGISTER, CADIN

' Write A/D gain byte.

WAIT STATUS.REGISTER, WRITE.WAIT, WRITE.WAIT
 OUT DATA.REGISTER, Gain.Code

' Write A/D channel byte.

WAIT STATUS.REGISTER, WRITE.WAIT, WRITE.WAIT
OUT DATA.REGISTER, Channel

' Read two bytes of A/D data from the Data Out Register,
' and combine the two bytes into one word.

WAIT STATUS.REGISTER, READ.WAIT
LOW = INP(DATA.REGISTER)
WAIT STATUS.REGISTER, READ.WAIT
HIGH = INP(DATA.REGISTER)
DATA.VALUE# = HIGH * 256 + LOW

' Calculate and print the A/D reading in volts.

Volts# = ((Range * DATA.VALUE# / FACTOR#) - Offset) / Gain(Gain.Code)
Channel0Voltage# = Volts#

'Channel 1

BASE.ADDRESS = &H2EC
COMMAND.REGISTER = BASE.ADDRESS + 1
STATUS.REGISTER = BASE.ADDRESS + 1
DATA.REGISTER = BASE.ADDRESS
COMMAND.WAIT = &H4
WRITE.WAIT = &H2
READ.WAIT = &H5

CSTOP = &HF
CCLEAR = &H1
CERROR = &H2
CADIN = &HC
EXT.TRIGGER = &H80

' A/D parameter constants.

PGH(0) = 1: PGH(1) = 2: PGH(2) = 4: PGH(3) = 8
PGL(0) = 1: PGL(1) = 10: PGL(2) = 100: PGL(3) = 500
PGX(0) = 1: PGX(1) = 1: PGX(2) = 1: PGX(3) = 1

' Check for legal Status Register.

STATUS = INP(STATUS.REGISTER)

' Stop and clear the DT2801.

OUT COMMAND.REGISTER, CSTOP
 TEMP = INP(DATA.REGISTER)
 WAIT STATUS.REGISTER, COMMAND.WAIT
 OUT COMMAND.REGISTER, CCLEAR

FACTOR# = 4096
 Gain(0) = PGH(0): Gain(1) = PGH(1)
 Gain(2) = PGH(2): Gain(3) = PGH(3)

Range = 20
 Offset = 10

Number.Channels = 8

' Get A/D gain.
 Gain.Code = 1

' Get A/D channel.

Channel = 1

' Write READ A/D IMMEDIATE command.

WAIT STATUS.REGISTER, COMMAND.WAIT
 OUT COMMAND.REGISTER, CADIN

' Write A/D gain byte.

WAIT STATUS.REGISTER, WRITE.WAIT, WRITE.WAIT
 OUT DATA.REGISTER, Gain.Code

' Write A/D channel byte.

WAIT STATUS.REGISTER, WRITE.WAIT, WRITE.WAIT
 OUT DATA.REGISTER, Channel

' Read two bytes of A/D data from the Data Out Register,
 ' and combine the two bytes into one word.

```

WAIT STATUS.REGISTER, READ.WAIT
LOW = INP(DATA.REGISTER)
WAIT STATUS.REGISTER, READ.WAIT
HIGH = INP(DATA.REGISTER)
DATA.VALUE# = HIGH * 256 + LOW

```

```

'   Calculate and print the A/D reading in volts.

```

```

Volts# = ((Range * DATA.VALUE# / FACTOR#) - Offset) / Gain(Gain.Code)
Channel1Voltage# = Volts#

```

```

Ch# = Channel1Voltage#

```

```

RETURN

```

```

'

```

```

'

```

```

!*****
**

```

```

!*****
**

```

```

'

```

```

'

```

```

'

```

```

SendTo362:

```

```

BASE.ADDRESS = &H2EC
COMMAND.REGISTER = BASE.ADDRESS + 1
STATUS.REGISTER = BASE.ADDRESS + 1
DATA.REGISTER = BASE.ADDRESS
COMMAND.WAIT = &H4
WRITE.WAIT = &H2
READ.WAIT = &H5
CSTOP = &HF
CCLEAR = &H1
CERROR = &H2
CDAOUT = &H8
EXT.TRIGGER = &H80

```

```

Offset = 5

```

```

Range = 10

```

FACTOR = 4096

STATUS = INP(STATUS.REGISTER)

' Stop and clear the DT2801.

OUT COMMAND.REGISTER, CSTOP

TEMP = INP(DATA.REGISTER)

WAIT STATUS.REGISTER, COMMAND.WAIT

OUT COMMAND.REGISTER, CCLEAR

DAC.SELECT = 0

DAC.RANGE = 4

Volts# = 0!

' Calculate DAC data value.

DATA.VALUE# = (Volts# + Offset) * FACTOR

DATA.VALUE# = CINT(DATA.VALUE# / Range)

IF DATA.VALUE# <= (FACTOR - 1) THEN GOTO OutputVoltage3

DATA.VALUE# = FACTOR - 1

' Calculate and print out rounded DAC output voltage.

OutputVoltage3:

Volts# = DATA.VALUE# * Range / FACTOR

Volts# = Volts# - Offset

' Write WRITE DAC IMMEDIATE command.

WAIT STATUS.REGISTER, COMMAND.WAIT

OUT COMMAND.REGISTER, CDAOUT

' Write DAC SELECT byte.

WAIT STATUS.REGISTER, WRITE.WAIT, WRITE.WAIT

OUT DATA.REGISTER, DAC.SELECT

' Write high and low bytes of DATA.VALUE#.

```

HIGH = INT(DATA.VALUE# / 256)
LOW = DATA.VALUE# - HIGH * 256
WAIT STATUS.REGISTER, WRITE.WAIT, WRITE.WAIT
OUT DATA.REGISTER, LOW
WAIT STATUS.REGISTER, WRITE.WAIT, WRITE.WAIT
OUT DATA.REGISTER, HIGH

```

```

RETURN

```

```

'
'
'*****
**

```

```

'*****
**
'
'
'

```

```

ReceiveFrom362:

```

```

'Channel 0

```

```

BASE.ADDRESS = &H2EC
COMMAND.REGISTER = BASE.ADDRESS + 1
STATUS.REGISTER = BASE.ADDRESS + 1
DATA.REGISTER = BASE.ADDRESS
COMMAND.WAIT = &H4
WRITE.WAIT = &H2
READ.WAIT = &H5

```

```

CSTOP = &HF
CCLEAR = &H1
CERROR = &H2
CADIN = &HC
EXT.TRIGGER = &H80

```

```

'    A/D parameter constants.

```

```

PGH(0) = 1: PGH(1) = 2: PGH(2) = 4: PGH(3) = 8
PGL(0) = 1: PGL(1) = 10: PGL(2) = 100: PGL(3) = 500
PGX(0) = 1: PGX(1) = 1: PGX(2) = 1: PGX(3) = 1

```

' Check for legal Status Register.

STATUS = INP(STATUS.REGISTER)

' Stop and clear the DT2801.

OUT COMMAND.REGISTER, CSTOP
TEMP = INP(DATA.REGISTER)
WAIT STATUS.REGISTER, COMMAND.WAIT
OUT COMMAND.REGISTER, CCLEAR

FACTOR# = 4096

Gain(0) = PGH(0): Gain(1) = PGH(1)

Gain(2) = PGH(2): Gain(3) = PGH(3)

Range = 20

Offset = 10

Number.Channels = 8

' Get A/D gain.

Gain.Code = 1

' Get A/D channel.

Channel = 0

' Write READ A/D IMMEDIATE command.

WAIT STATUS.REGISTER, COMMAND.WAIT
OUT COMMAND.REGISTER, CADIN

' Write A/D gain byte.

WAIT STATUS.REGISTER, WRITE.WAIT, WRITE.WAIT
OUT DATA.REGISTER, Gain.Code

' Write A/D channel byte.

WAIT STATUS.REGISTER, WRITE.WAIT, WRITE.WAIT
OUT DATA.REGISTER, Channel

' Read two bytes of A/D data from the Data Out Register,

' and combine the two bytes into one word.

```
WAIT STATUS.REGISTER, READ.WAIT
LOW = INP(DATA.REGISTER)
WAIT STATUS.REGISTER, READ.WAIT
HIGH = INP(DATA.REGISTER)
DATA.VALUE# = HIGH * 256 + LOW
```

' Calculate and print the A/D reading in volts.

```
Volts# = ((Range * DATA.VALUE# / FACTOR#) - Offset) / Gain(Gain.Code)
Channel0Voltage# = Volts#
```

'Channel 1

```
BASE.ADDRESS = &H2EC
COMMAND.REGISTER = BASE.ADDRESS + 1
STATUS.REGISTER = BASE.ADDRESS + 1
DATA.REGISTER = BASE.ADDRESS
COMMAND.WAIT = &H4
WRITE.WAIT = &H2
READ.WAIT = &H5
```

```
CSTOP = &HF
CCLEAR = &H1
CERROR = &H2
CADIN = &HC
EXT.TRIGGER = &H80
```

' A/D parameter constants.

```
PGH(0) = 1: PGH(1) = 2: PGH(2) = 4: PGH(3) = 8
PGL(0) = 1: PGL(1) = 10: PGL(2) = 100: PGL(3) = 500
PGX(0) = 1: PGX(1) = 1: PGX(2) = 1: PGX(3) = 1
```

' Check for legal Status Register.

```
STATUS = INP(STATUS.REGISTER)
```

' Stop and clear the DT2801.

```

OUT COMMAND.REGISTER, CSTOP
TEMP = INP(DATA.REGISTER)
WAIT STATUS.REGISTER, COMMAND.WAIT
OUT COMMAND.REGISTER, CCLEAR

```

```

FACTOR# = 4096
Gain(0) = PGH(0): Gain(1) = PGH(1)
Gain(2) = PGH(2): Gain(3) = PGH(3)

```

```

Range = 20
Offset = 10

```

```

Number.Channels = 8

```

```

'   Get A/D gain.
Gain.Code = 1

```

```

'   Get A/D channel.

```

```

Channel = 1

```

```

'   Write READ A/D IMMEDIATE command.

```

```

WAIT STATUS.REGISTER, COMMAND.WAIT
OUT COMMAND.REGISTER, CADIN

```

```

'   Write A/D gain byte.

```

```

WAIT STATUS.REGISTER, WRITE.WAIT, WRITE.WAIT
OUT DATA.REGISTER, Gain.Code

```

```

'   Write A/D channel byte.

```

```

WAIT STATUS.REGISTER, WRITE.WAIT, WRITE.WAIT
OUT DATA.REGISTER, Channel

```

```

'   Read two bytes of A/D data from the Data Out Register,
'   and combine the two bytes into one word.

```

```

WAIT STATUS.REGISTER, READ.WAIT
LOW = INP(DATA.REGISTER)
WAIT STATUS.REGISTER, READ.WAIT
HIGH = INP(DATA.REGISTER)

```


DATA.VALUE# = HIGH * 256 + LOW

' Calculate and print the A/D reading in volts.

Volts# = ((Range * DATA.VALUE# / FACTOR#) - Offset) / Gain(Gain.Code)
Channel1Voltage# = Volts#

Ch# = Channel1Voltage#

RETURN

,

,

**

**

,

,

UpdateDataFile:

ElapsedTime = NewTime - TimeZero

PRINT #1, USING "##.###"; ElapsedTime; Channel0Voltage#; Channel1Voltage#

RETURN

,

,

**

**

,

' StopProgram

,

StopProgram:

,

,

```

CLS
PRINT
PRINT "F1 was pressed. The trial was terminated."
KEY(1) OFF
END
'
'*****
**

'*****
**
'
' WriteFinalscreen: Write Final Stats To The Screen
'
WriteFinalScreen:
'
PRINT
GOSUB FreshScreen
Today$ = DATES$
Clock$ = TIMES$
PRINT
PRINT "                Experiment Parameters"
PRINT "                "; Today$, "                "; Clock$
PRINT
PRINT " The file for the trial just completed is "; Filename$, ".DAT"
PRINT
PRINT " Thank you for choosing ZeekSoft."
RETURN
'
'
'*****
**

'*****
*
'
' Write The Plot To The Screen
'
WriteToScreen:
CLS
SCREEN 12

```

```

*****
**
' Draw Plot
,

WINDOW (-100, -100)-(100, 100)
LINE (-90, -50)-(90, 90), 3, B
LINE (-90, 90)-(-88, 92), 3
LINE (-88, 92)-(92, 92), 3
LINE (92, 92)-(92, -48), 3
LINE (92, -48)-(90, -50), 3
LINE (90, 90)-(92, 92), 3
LINE (0, -50)-(0, 90), 3
LINE (-45, -50)-(-45, 90), 3
LINE (45, -50)-(45, 90), 3
LINE (-90, 20)-(90, 20), 3
LINE (-90, 55)-(90, 55), 3
LINE (-90, -15)-(90, -15), 3
FOR i = -90 TO 90
LINE (i, 72.5)-(i, 72.5), 3
LINE (i, 37.5)-(i, 37.5), 3
LINE (i, 2.5)-(i, 2.5), 3
LINE (i, -32.5)-(i, -32.5), 3
NEXT i
FOR i = -50 TO 90
LINE (-67.5, i)-(-67.5, i), 3
LINE (-22.5, i)-(-22.5, i), 3
LINE (22.5, i)-(22.5, i), 3
LINE (67.5, i)-(67.5, i), 3
NEXT i
*****
**
' Title
,

LOCATE 1, 8
PRINT "Current File: "; DataFile$
,
,
,
*****
**
' X-axis Labels
,

LOCATE 24, 5

```

```

PRINT "0"
LOCATE 24, 20
PRINT ((Length + PulseLength) / 4)
LOCATE 24, 37
PRINT ((Length + PulseLength) / 2)
LOCATE 24, 55
PRINT ((3 * (Length + PulseLength)) / 4)
LOCATE 25, 36
PRINT "Time (s)"
'
'
'*****
**
' Y-axis labels
'
LOCATE 9, 80
PRINT "V"
LOCATE 10, 80
PRINT "o"
LOCATE 11, 80
PRINT "I"
LOCATE 12, 80
PRINT "t"
LOCATE 13, 80
PRINT "s"
Y1 = MinVoltage
Y5 = MaxVoltage
Y3 = (MaxVoltage + MinVoltage) / 2
Y2 = (Y1 + Y3) / 2
Y4 = (Y3 + Y5) / 2
LOCATE 2, 1
PRINT USING "##.##"; Y5
LOCATE 7, 1
PRINT USING "##.##"; Y4
LOCATE 13, 1
PRINT USING "##.##"; Y3
LOCATE 18, 1
PRINT USING "##.##"; Y2
LOCATE 23, 1
PRINT USING "##.##"; Y1
'*****
**
' Write Statistics

```

```

'
LOCATE 28, 58
PRINT "Current = "
LOCATE 27, 5
PRINT "Voltage    = "
LOCATE 27, 58
PRINT "Charge ="
LOCATE 28, 5
PRINT "Elapsed Time ="
RETURN
'
'
*****
**

*****
**
'
' Update The Plot
'
UpdateScreen:
PlotTime = TIMER
ElapsedTime = PlotTime - TimeZero

LOCATE 28, 70
PRINT "      "
LOCATE 28, 70
PRINT USING "#.###"; Ch#;
PRINT " mA"

LOCATE 27, 24
PRINT "      "
LOCATE 27, 24
PRINT USING "##.##"; Channel0Voltage#;
PRINT " V"
LOCATE 28, 22
PRINT "      "
LOCATE 28, 22
PRINT USING "#####"; ElapsedTime;
PRINT " s"
LOCATE 27, 69

```

```

PRINT "      "
LOCATE 27, 69
PRINT USING "##.###"; CumulCharge#;
PRINT " C"

```

```

*****

```

```

**

```

```

'

```

```

' Write The Data Point

```

```

'

```

```

YCoord = (((Channel0Voltage# - MinVoltage) * 140 / (MaxVoltage - MinVoltage))) +
(-50)

```

```

XCoord = ((ElapsedTime * 180 / (Length + PulseLength))) + (-90)

```

```

LINE (XCoord, YCoord)-(XCoord, YCoord + 1), 10

```

```

RETURN

```

```

'

```

```

'

```

```

*****

```

```

**

```